

10 **Design, synthesis and photophysical studies of
dipyrromethene-based materials: insights into
their incorporation in organic photovoltaic
applications**

15 André Bessette^{ab} and Garry S. Hanan^{*a}

Cite this: DOI: 10.1039/c3cs60411j

20 Received 12th November 2013

25 DOI: 10.1039/c3cs60411j

www.rsc.org/csr

This review article presents the most recent developments in the use of materials based on the dipyrromethene (DPM) dye and some of its structurally related azadipyrromethenes (ADPM) for organic photovoltaic applications (OPV). These chromophores and especially their corresponding BF₂-chelated derivatives BODIPY and aza-BODIPY, respectively, are well known for fluorescence-based applications but are relatively new in the photovoltaic research field. This work examines the variety of relevant designs, synthetic methodologies and photophysical studies related to materials that incorporate these porphyrinoid-related dyes in their architecture. The main idea is to inspire readers to explore new avenues in the design of next generation small-molecule and bulk-heterojunction solar cell (BHJSC) OPV materials based on DPM chromophores. The main concepts are briefly explained, along with the main challenges that are to be resolved in order to take full advantage of solar energy.

30 **Introduction**

At the end of 2009, Jacobson and Delucchi published in Scientific American the first plan to power 100% of the planet with energy from renewable sources.¹ In their plan, they calculated that about 30% of the world's continuous power needs of 11.5 TW should be produced by solar power within 20 years. In the same vein, Grätzel was already pointing out in a

^a Département de Chimie, Université de Montréal, Pavillon J.-A. Bombardier, 5155 Decelles Avenue, Montréal, Québec, H3T-2B1, Canada.

E-mail: garry.hanan@umontreal.ca; Fax: +1-514-343-7586; Tel: +1-514-340-5156

^b Saint-Jean Photochimie Inc., 725 Trotter street, Saint-Jean-sur-Richelieu, Québec, J3B 8J8, Canada



André Bessette

André Bessette (Montréal, Canada, 1987) received his BSc in Chemistry (2009) from the Université de Sherbrooke and his MSc (2012) from the Université de Montréal under the guidance of Prof. G. S. Hanan. He is currently a PhD student in the Green Energy Group of Prof. G. S. Hanan, in collaboration with St-Jean Photochemicals Inc. His research interests span a wide range of fields including photoactive and photovoltaic

materials, photophysics, self-assembly, organometallic chemistry and polymeric materials.



Garry S. Hanan

Garry S. Hanan (Winnipeg, Canada, 1966) received his BSc from the University of Winnipeg in 1989. He obtained his Diplôme d'Études Approfondies (1991) and PhD (1995) from the Université Louis Pasteur in Strasbourg, France, under the supervision of Prof. J.-M. Lehn. He was then an Alexander von Humboldt fellow with Prof. M. T. Reetz in Germany and a post-doctoral fellow with Professors V. Balzani and S. Campagna in Italy. In

1998, he joined the faculty of the University of Waterloo and in September 2002, he moved to the Université de Montréal where he is currently professor of chemistry.

1 *Nature* publication of 2001 that covering 0.1% of the Earth's surface with 10% efficiency solar cells would satisfy the world's energy needs for the time at which it was published.² More recently, Armaroli and Balzani presented the idea of an electricity-powered world as a major challenge for the 21st century³ and editorials have also pointed out a path toward competitiveness for solar energy.⁴ Additionally, the SunShot program founded in 2010 by the US Department of Energy with an annual budget of nearly \$300 million aimed to bring down the cost of solar energy to 6 cents per kilowatt-hour by 2020.⁵

10 Considering the well-documented change in climate that the world faces, first generation solar cells based on solid-state junction and often made of silicon are a good start. This is especially true as they have conversion efficiencies currently oscillating around 25% for crystalline Si based cells and of 28% for GaAs thin film cells.⁶ On the other hand, these cells are expensive and energy-intensive in their fabrication process, while their rigid shape limits them to specific applications.²

15 Fortunately, the field of light-harvesting materials is currently undergoing a tremendous growth and a rich variety of other technologies are battling to emerge as "The Paramount One", the principal ones being photoelectrochemical cells based on nanocrystalline junctions and interpenetrating networks, tandem cells for water cleavage by visible light, dye-sensitized solid heterojunctions and extremely thin absorber (ETA) cells, and soft junctions and organic solar cells. In short, we can say that this domain is in full growth.

20 Back in 2009, Brabec studied the economic aspects of organic photovoltaic (OPV) devices in an interesting review.⁷ He concluded that a low-cost technology like OPV could become competitive with other energy sources at an efficiency of around 7% and a lifetime of the module of 7 years. State-of-the-art devices' conversion efficiencies are now at 9.1% for polymer/fullerene organic solar cells in an inverted bulk-heterojunction (BHJ) architecture by the American company Polyera⁸ and at 10.6% for tandem polymeric devices developed by Sumitomo Chemical in collaboration with Pr Yang Yang at UCLA.^{8,9} The latter was a world record which was achieved only a few months after the reported efficiency of 9.8% for oligomer-based (small-molecule) tandem solar cells achieved by the German company Heliatek GmbH.¹⁰ The Nobel laureate Alan J. Heeger also reported recently solution-processed small-molecule BHJ solar cells with 6.7% efficiency.¹¹ Such high conversion efficiencies are very promising for this field, especially as OPV have three major advantages compared with their competing technologies: the flexibility of the material for coating virtually everything as a thin film, the low weight of the device and the low cost of production.

25 Many types of synthons are presently used at the industrial scale in OPV, such as thiophene- and carbazole-based derivatives.⁷ However, the quest for new families of molecules is wide open in order to resolve the few limitations that still hinder good conversion efficiencies on large surface area plastic solar cells, as discussed in a recent review.¹² A good source of inspiration for solar energy conversion are Nature's photosynthetic systems which are still being investigated by the

scientific community.¹³ Porphyrinoid dyes are essential chromophores in the light-harvesting process of natural photosystems; therefore they give good insight to researchers into how to create artificial ones based on them since many decades. The understanding of photophysics and synthetic chemistry related to these derivatives is central to many research groups around the globe. Actually, porphyrinoids have started to attract attention lately for their incorporation in OPV devices.^{14–17} This renaissance is years after the very first example of organic solar cell (OSC) was reported by Tang and Albrecht in 1975, who incorporated chlorophyll-a as the photoactive layer between two electrodes with a power-conversion efficiency of about 0.001%.¹⁸

This review will focus from an OPV point of view on the most recent developments of molecules that incorporate dipyrromethenes (DPM) and some azadipyrromethenes (ADPM) in their structure (Fig. 1). Structurally, DPM and ADPM are half porphyrins and porphyrazines, respectively, but present interesting advantages for OPV. In fact, their photophysical properties are similar to those of porphyrinoids, with many synthetic advantages. First, they avoid the low-yield macrocyclization step and difficult purification of porphyrins, an important point to consider for commercialization. Second, they offer abundant leverage possibilities for fine-tuning of the photophysical properties by variation of the substituents. Third, they present greater versatility of metal coordination geometries allowed by a bidentate motif as compared to the more rigid square planar one of the parent family. This is of great interest from the perspective of developing new OPV materials taking advantage of the metallic center as a way to coarsely tune the energetic levels.

In order to give a good overview of recent advances and possibilities in this specific field of OPV, we propose here to present the variety of synthetic methodologies, photophysical studies and relevant designs based on small molecules or polymeric materials showing the most promising results

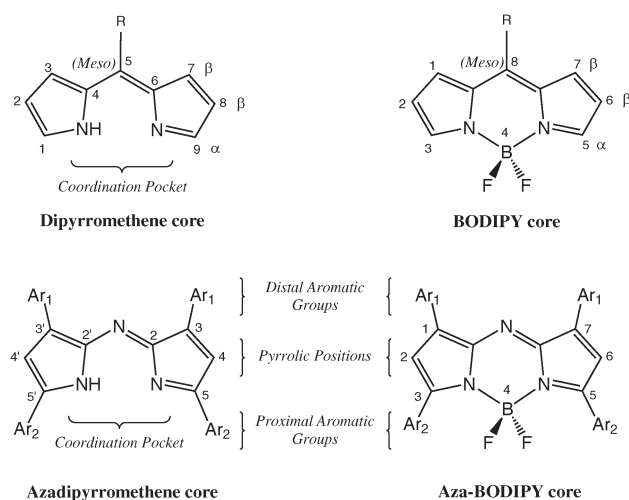


Fig. 1 Core structures of dipyrromethene (DPM) and azadipyrromethene (ADPM).

towards an improvement in the conversion efficiency of solar cells. The review will be presented from a critical point of view in order to inspire readers to explore new avenues in the design of next generation OPV materials based on DPM chromophores. We will introduce a brief explanation of OPV concepts along with the main challenges that are to be resolved.

Specific OPV requirements

1.1. General concepts

An important link exists between photovoltaic devices and their opposite counterparts, light-emitting devices (LED), which convert electricity into light (Fig. 2). This is an important point to consider in the analysis of a specific compound to know if it may be a good prospect for optoelectronic applications since, in some cases, it can be used in both solar cells and LED. Therefore, this energetic interplay of light and electricity will be used in the review to find out if a system is suitable for heterojunction photovoltaic devices.

There are mainly two types of organic-based solar cells currently in use/development. The first one is the heterojunction solar cells, which include planar- and bulk-heterojunction solar cell devices (PHJSC and BHJSC, respectively) and will be the focus of this review. The second one consists of dye-sensitized solar cells (DSSCs), which provide some interesting

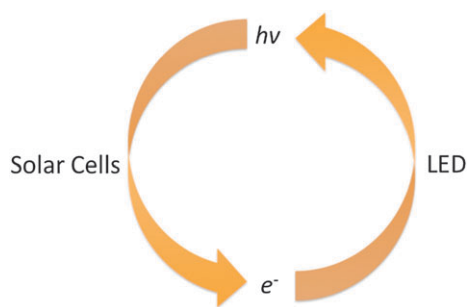


Fig. 2 Energetic interplay of light ($h\nu$) and electricity (e^-) between solar cells and light-emitting diodes (LED).

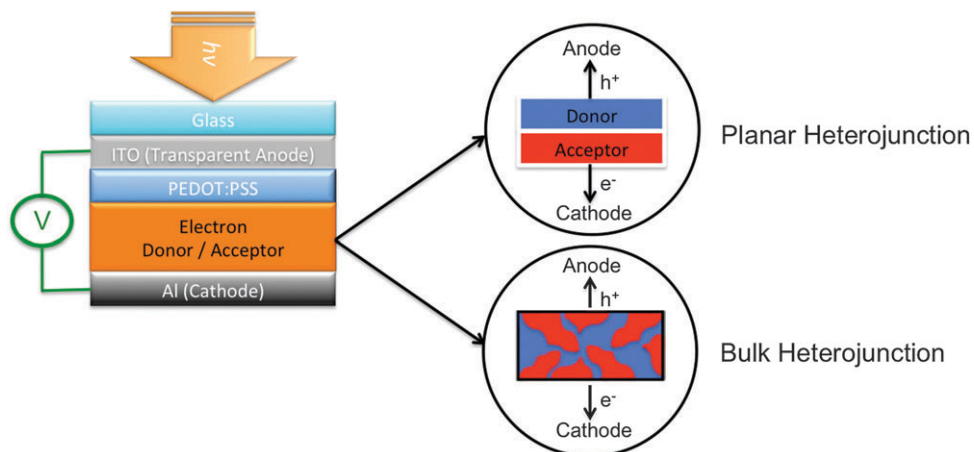


Fig. 3 Schematic diagram of planar- (top) and bulk- (bottom) heterojunction solar cell structures.

molecular architectures incorporating DPM and ADPM that will be evaluated from an OPV point of view. For good reviews on the latter type of solar cells, interested readers should consult the papers published in 2009 by Grätzel on recent advances in the field and in 2011 by Falaras *et al.* on ruthenium-based sensitizers for DSSC.^{19,20}

The general structure of heterojunction solar cells consists of n-type and p-type semiconductor stacks sandwiched between two electrodes, namely an aluminum cathode wired with a transparent indium tin oxide (ITO) anode (Fig. 3). In addition, a PEDOT:PSS layer is interwoven between the heterojunctions and the ITO electrode to improve the surface quality of the latter and for better charge transfer. The composition of the n-type material is based generally on fullerene derivatives, such as PCBM and PC₇₀BM (Fig. 4), which offer an “ideal” low-lying LUMO acting as an electron (e^-) acceptor (A) and charge transporter toward the cathode. The photoactive material acts as the electron donor (D) allowing the hole (h^+) transporter to be based on small-molecules that are vacuum-deposited planar-heterojunctions or on polymers that assemble into nano-domains with fullerene derivatives in the case of BHJSCs.

The working mechanism of D–A heterojunction solar cells involves four distinct events.²¹ First, there is photoexcitation in the donor material leading to the formation of an electron–hole pair, namely an exciton. In the second event, the exciton diffuses to the D–A heterojunction. If the distance it has to travel is longer than the maximum diffusion length ($\max L_D$), this excited state will be quenched, inhibiting any further process. The third step of the mechanism involves the dissociation of the exciton at the D–A interface. In fact, this step is the passage of the excited electron from the lowest unoccupied molecular orbital (LUMO) of the D to that of the A. On the other hand, the hole reintegrates with the highest occupied molecular orbital (HOMO) of the donor. Finally, the fourth step consists of charge transport and collection at the anodic and cathodic electrodes of the geminate pair of charges generated in the previous step. Overall, this process leads to the photogeneration of a current that can be converted into useful work.

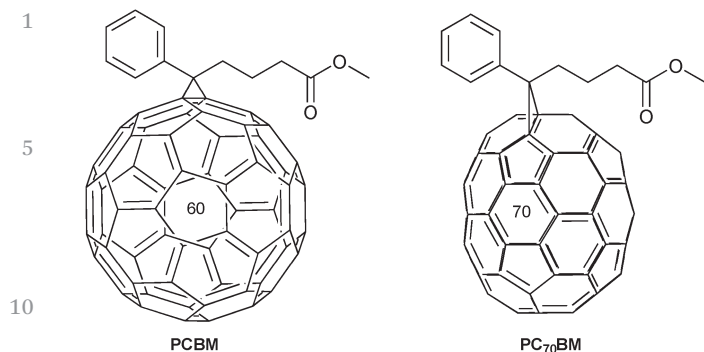


Fig. 4 PCBM and PC₇₀BM chemical structures.

Fig. 5 presents the relative energies of HOMO and LUMO orbitals of both the D and A and the inter-correlated parameters affecting photovoltaic performance. The band-gap (E_g) consists of the energy required to excite an electron from the HOMO to the LUMO of D. Obviously, the source of energy (E) for the excitation is light ($h\nu$) in the case of photovoltaic applications. The built-in potential (V_B) is the gain in voltage generated by the system and is linearly dependent on the open-circuit voltage (V_{OC} , not shown). Finally, the E_d parameter represents the difference between the LUMO orbitals of the D and A. This difference is the downhill driving force for electron transfer to occur and should be about 0.3–0.4 eV to ensure a good exciton dissociation into a pair of charges at the D–A interface.²²

As will be discussed in the following sections, some researchers have begun to integrate dyes as photosensitizers in BHJSCs that act as electron relays (Fig. 5). These additives tend to increase the overall energy conversion of solar cells; in addition they increase the absorption of solar light in the near-infrared (NIR) region. This point is especially important since about 50% radiation intensity of the sunlight range between 700 and 2000 nm and the core solar flux between 600 and 800 nm (Fig. 6).^{23,24}

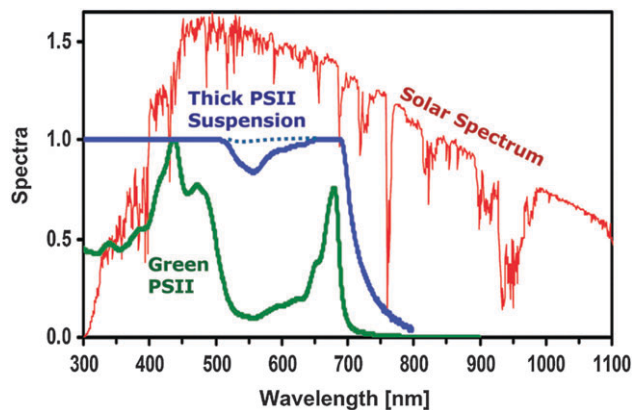


Fig. 6 Solar spectrum (in $W\ m^{-2}\ nm^{-1}$) and absorption spectra of plant PSII.²⁵ (Reprinted with permission from *Acc. Chem. Res.*, 2009, **42**(12), 1861–1870. Copyright © 2009 American Chemical Society.)

In order to determine the power-conversion efficiency (PCE) (η) of the solar cell, current–voltage (J – V) curves under dark and illumination conditions are generated as a direct characterization method. As presented in a very recent review by Mishra and Bäuerle, essential parameters determining the cell performance are shown in Fig. 7: V_{OC} = open-circuit voltage; J_{SC} = short-circuit current density; FF = fill factor; V_{mp} and J_{mp} are voltage and current, respectively, at which the power output of a device reaches its maximum; J_L is the light-generated current.²⁴ Therefore, the equation of η is defined as the ratio of maximum power output (P_{out}) to power input (P_{in}).

1.2. Challenges and parameters to control

The equation for PCE in Fig. 7 provides three key parameters chemists and physicists have to control in order to increase the overall quality of organic solar cells. Reviews concerning small-molecule and polymer based organic solar cell characterization are available for a detailed explanation of the various parameters influencing V_{OC} , J_{SC} and FF in OPV.^{24,26,27} Nevertheless,

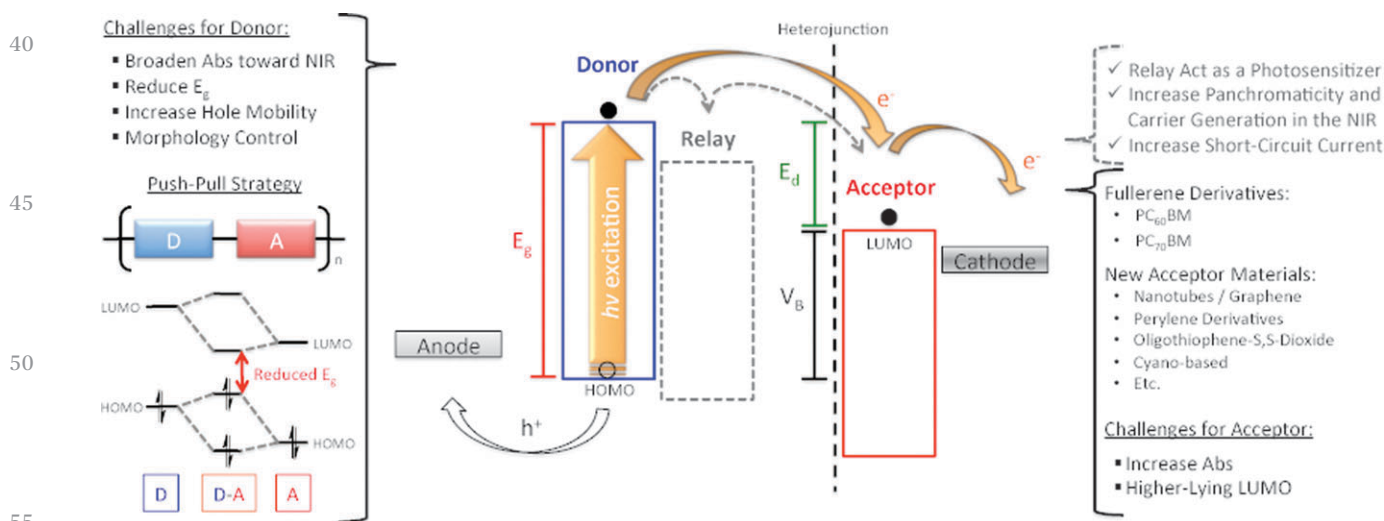
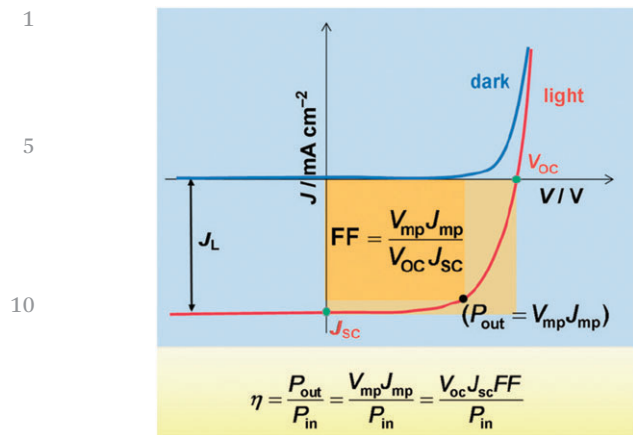


Fig. 5 OPV principles and challenges for the next generation of materials.



15 Fig. 7 Current–voltage (J – V) characteristics of a typical solar cell.²⁴ (Reprinted with permission from *Angew. Chem., Int. Ed.*, 2012, **51**, 2020–2067. Copyright© 2012 WILEY-VCH Verlag GmbH & Co. KGaA, Weinheim.)

20 we can consider that V_{OC} is mainly dependent on the HOMO
level of the donor relative to the LUMO of the acceptor. Therefore,
a good way to increase V_{OC} consists of lowering the HOMO
of the donor. This can be achieved by fine-tuning frontier
orbitals in photoactive donor materials with electron rich
25 (donor) and/or poor (acceptor) groups, judiciously incorporated
in their molecular structure. In BHJSC, this strategy for copoly-
mers is known as the “push-pull” effect. The effects of combin-
ing an electron-rich monomer with an electron-poor monomer
on the resulting molecular orbitals are schematized in Fig. 5
30 (bottom-left). We can see in the scheme that the resulting HOMO
and LUMO are both affected to various extent by copolymeriza-
tion. Consequently, it becomes a major tactic for the reduction
of the band-gap toward absorption of low-energy photons in the
NIR region, a crucial aspect as discussed previously. Recently,
35 Wang reviewed the structures and properties of conjugated D–A
copolymers for SC applications in quite an interesting fashion,
clearly putting in relation parameters to explain how new push-
pull copolymers should be designed.²⁸ Brédas *et al.* also made
a theoretical investigation of the impact of chemical structure
modifications on electronic and optical properties in relevant
40 OPV D–A copolymers.²⁹ In small-molecule/oligomer photoactive
materials, the same concept is used to create an assortment of
D–A, D–A–D or A–D–A architectures.²⁴

For J_{SC} , the maximum photocurrent obtained depends strongly
45 on the number of photons that can be used by the solar cell,
until saturation effects are initiated. The photocurrent also
depends on the surface area of the cell, which explains why
standardization of the testing conditions is necessary to
compare two different cells. Among other parameters affect-
ing J_{SC} , a mention of device thickness, absorption coverage
50 and especially charge transport properties of organic semi-
conductors is required.

Describing the overall quality of the solar cell, FF relies on
the proportion of charge carriers that reach the electrodes
55 instead of recombining. Similar to the V_{OC} , the HOMO/LUMO
levels of D and A materials need to be optimized in order
to optimize the FF. Molar absorption of the photoactive layer also

needs to be high in order to reach a high external quantum
1 efficiency (EQE) without having a thickness that hinders charge
transport toward the electrodes.

In the case of BHJSC, active layer morphology and quality of
phase separation, *i.e.* a balanced repartition of the D and A
2 nano-domains, are essential for high PCE. The role of these
parameters has been extensively reviewed lately.^{30,31} The main
parameters to consider for a suitable morphology are material
composition, selection of solvent, annealing conditions and the
use of additives. On the other hand, the phase separation and
more general ordering in the solid state rely intrinsically on the
molecular structure. Therefore, careful engineering of the
photoactive material is fundamental to a successful device.

1.3. Commercial considerations and new avenues envisaged

The OPV field has grown exponentially in the last two decades
(Fig. 8 and 9), pushed forward by both academic and industrial

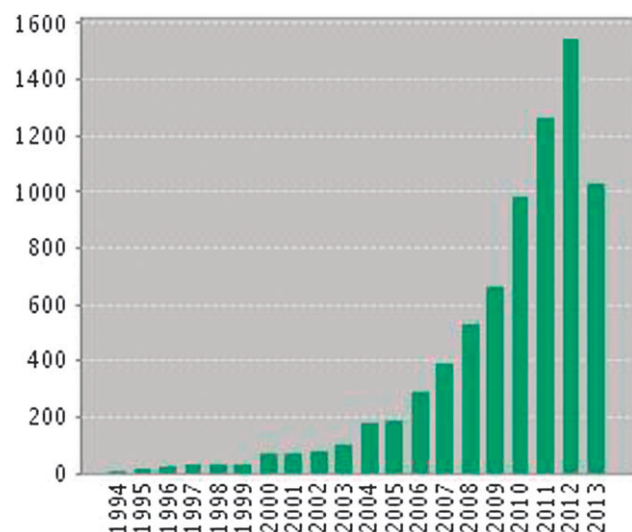


Fig. 8 OPV publications each year over the last 20 years.³⁵

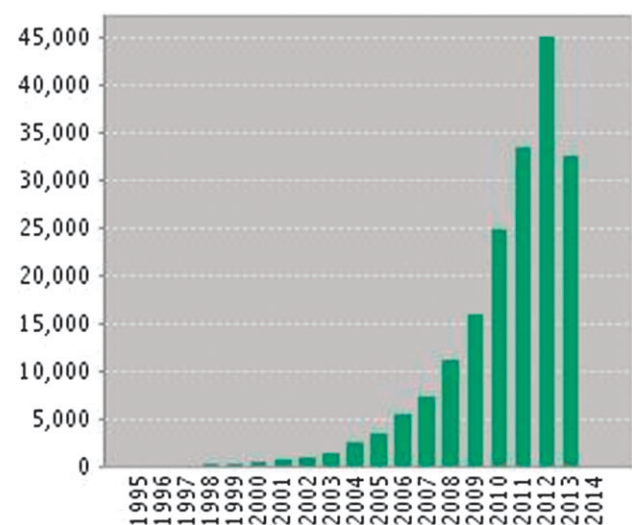
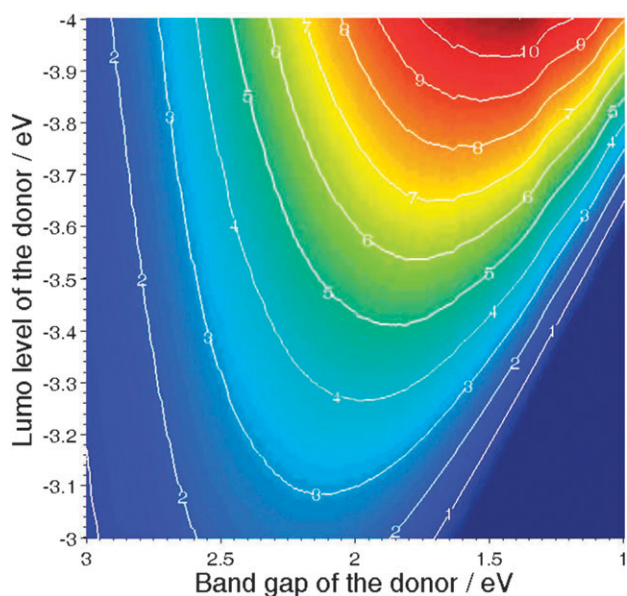


Fig. 9 OPV citations each year over the last 20 years.³⁶

1 researchers interested in the commercialization of cost-effective,
 low-weight and flexible technology for solar cells.³² While Brabec
 and coworkers pointed out in 2009 that OPV would compete with
 other energy sources at an efficiency of around 7% and a lifetime
 5 of the module of 7 years,⁷ Mishra and Bäuerle are now looking
 toward an efficiency of 10–15% for commercialization.²⁴ Other
 than PCE, another key aspect for commercialization of OPV is the
 stability of the solar cell over time. Krebs has reviewed the recent
 advances in that particular field and he is considering the idea of
 10 developing SC with a one-day energy payback for the factories of
 the future.^{33,34} All this is nowadays conceivable due to tremen-
 dous improvements made both by chemists on the composition/
 properties of the D–A layer and by physicists and engineers on the
 architecture of the solar cell.

15 Theoretically, researchers working on the photoactive layer
 in OPV are expecting to reach a maximum PCE of about 10% for
 a single donor material. This assumption is based on a model
 for BHJSC investigated by Scharber *et al.* and they put in
 relation LUMO's energetic level of the polymeric D with its
 20 band-gap in eV (Fig. 10).^{7,22} A recent review from Gendron and
 Leclerc presented four polymer classes with high potential for
 commercialization within a few years based on this concept.¹²
 For their part, both Lupton and the group of Scholes have
 investigated the importance of conjugation in polymeric materi-
 25 als for charge transport and electronic energy transfers.^{37,38}

On the other hand, several researchers are casting doubt on
 the use of fullerene-based derivatives as the “ideal” acceptor
 material. Therefore, they are exploring to replace them either by
 graphene or by other organic non-fullerene electron-
 30 conducting molecules.^{39,40} The use of dyes as the A is especially
 interesting in a context where it has the potential to remedy the



35 Fig. 10 Contour plot showing the calculated energy-conversion effi-
 ciency (contour lines and colors) versus the bandgap and the LUMO level
 of the donor polymer.⁷ (Reprinted with permission from *Adv. Mater.*, 2009,
 40 **21**, 1323–1338. Copyright © 2009 WILEY-VCH Verlag GmbH & Co. KGaA,
 Weinheim.)

poor light-absorption of the fullerene-based acceptors, which
 decreases the overall PCE.²⁶

In an attempt to refine the OPV model and help researchers
 design more suitable materials for BHJSCs, Marks and coworkers
 pointed out the differences this field expresses compared to tradi-
 5 tional inorganic solar cell models.⁴¹ Hence, they put in perspective
 three important points for OPV: (1) geminate pair and bimolecular
 recombination, (2) effects of interfacial layers inserted between the
 electrodes and the active layer, and (3) resistance effects.

In order to reach up to 15% of PCE within a few years, the
 10 design of new solar cell architectures seems imperative. Tandem
 solar cells, conceptually integrating many layers of complemen-
 tary light-absorbing D materials to expand the overall spectrum
 coverage, are an example under exhaustive investigation.^{41–43} In a
 similar fashion, the incorporation of photosensitizers proposes
 15 PCE efficiencies above the theoretical 10% for reasons described
 in Section 1.1 and Fig. 5. Another interesting approach consists of
 conjugated polymer–inorganic solar cells, but further improve-
 ments are still needed to pass from ~3% PCE to the ~10% of
 PHJSC and BHJSC.⁴⁴ Probably the most encouraging result in OPV
 20 architecture is the parallel-like bulk-heterojunction solar cell
 reported by You *et al.*⁴⁵ This conceptually new approach main-
 tains the simple device configuration and low-cost processing of
 single-junction BHJSCs while inheriting the major benefit of
 incorporating multiple polymers in tandem cells. In fact, J_{SC} of
 25 tandem cells is nearly identical to the sum of J_{SC} of the two
 corresponding individual polymeric cells, an increase of about
 40%, while the V_{OC} is in between their respective values. Overall,
 an improvement of 30% in PCE was achieved with preliminary
 optimization of this architecture.

A last noteworthy avenue of exploration in OPV is the utilization
 of organometallic polymers/metallo-polymers. In a review of 2009
 on challenges in organometallic chemistry, Wong argued for the
 increased possibility of fine-tuning the chemical and photophysical
 properties of optoelectronic materials containing metals, either
 35 complexes or polymers, in comparison with purely organic
 devices.⁴⁶ For example, transition metals allow MLCT transitions
 of relatively low-energy band-gap due to their d orbitals, an
 important aspect toward an increased absorption of NIR photons.
 This relatively underexploited avenue in OPV will be extensively
 40 considered throughout this review due to the inherent advantages
 of the incorporation of metals in the photoactive D materials.

Hopefully, this short overview will give a better taste to readers
 of the general concepts in OPV, numerous challenges and param-
 45 eters to control, commercial considerations and new avenues
 under investigation. From this point, focus will be devoted toward a
 critical analysis of how dipyrromethene and azadipyrromethene
 can be integrated into photoactive donor materials, either as small
 molecules or polymers, to achieve important gains of PCE.

Dipyrromethene derivatives

In the past decades, several synthetic methods have been
 developed and photophysical properties widely studied concern-
 55 ing the 4,4-difluoro-4-bora-3a,4a-diaza-s-indacene (BODIPY)

dye (Fig. 1) and its derivatives.^{47–49} These dyes are of particular interest owing to their strong absorption in the UV region and sharp fluorescence emissions generally beyond 600 nm occurring with high quantum yields. In addition to numerous synthetic advantages offered by this family of dyes, they are tolerant to a wide range of thermal, photochemical, pH and polarity conditions. Their stability in physiological environments also makes them of prime choice for imaging techniques and protein labeling. Their use in other advanced applications such as laser dyes, fluorescent indicators and as components of light-harvesting (LH) systems is noteworthy. The groups of Boens and Lin recently published reviews on fluorescent indicators based on BODIPY,^{50,51} You *et al.* on BODIPY-based photosensitizers for photodynamic therapy,⁵² Chujo *et al.* discussed their use as advanced luminescent materials,⁵³ Boyle *et al.* their use as light active material components,⁵⁴ while Ziessel and Harriman discussed as early as 2010 their function in artificial LH antennae.⁵⁵ This pool of applications originated from the intrinsic properties of this half-porphyrin and is now strongly compelling the development of new derivatives with fine-tuned properties. Therefore, we propose in this section an overview of how BODIPY can be optimized toward their incorporation into OPV materials.

2.1. Synthetic aspects and photophysical tuning of DPMs

2.1.1 The quest for NIR dyes.

As mentioned in Section 1.1, the OPV field is currently searching for NIR dyes with high extinction coefficient (ϵ) and good photostability. In such a context, many synthetic tools have been developed lately in order to further push the absorption and emission properties as far as possible in the NIR for BODIPYs. Four main strategies have been used to take the 470 nm absorption of the generic BODIPY core **1** (Fig. 11) up to almost a 1000 nm: (1) fusing rings on the pyrrole units to extend its π -conjugation; (2) fusing an aromatic unit on the zigzag edge of the core by an intramolecular oxidative cyclohydrogenation; (3) generating a push-pull motif by derivatization at the α -, β - and/or *meso*-positions; (4) replacing carbon 8 by a nitrogen, giving rise to the aza-BODIPY dye family (Fig. 1).⁵⁶

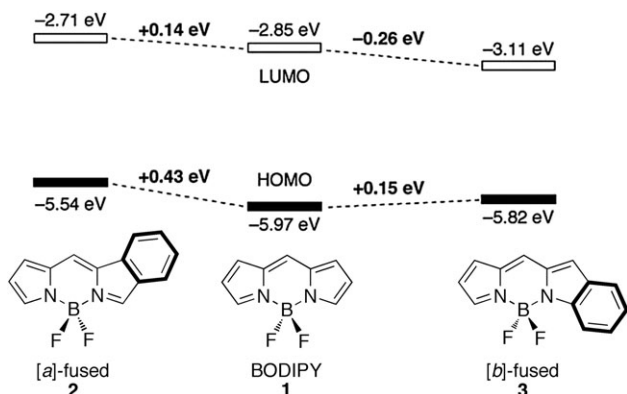


Fig. 11 Effect on the electronic structures of benzene-fusing at the *a* and *b* bond positions of a BODIPY as obtained by DFT calculations (B3LYP/6-31G(d)).⁵⁷ (Adapted from ref. 57 with permission from The Royal Society of Chemistry.)

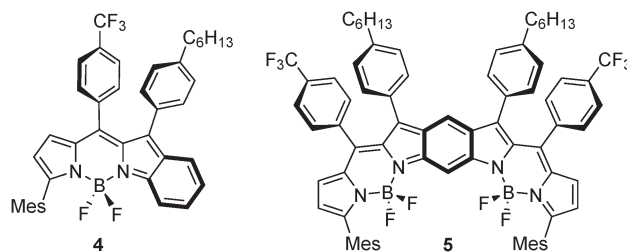


Fig. 12 Benzene-fused BODIPY and its corresponding dimer.⁵⁷

First, Wakamiya *et al.* looked at the impact of fusing rings on the pyrrole units.⁵⁷ Evaluation of the electronic impact of ring-fusing a benzene at the [*a*] bond (**2**) and the [*b*] bond (**3**) on the BODIPY skeleton **1** was achieved (Fig. 11). DFT calculations first showed that benzene fusing at the [*a*] bond led to an increase of the HOMO level while the fusing at the [*b*] bond mainly gave rise to LUMO stabilization. Based on these *in silico* results, synthesis of the benzo-[*b*]-fused BODIPY **4** and the fully fused BODIPY dimer **5** was achieved (Fig. 12). An X-ray crystal structure analysis of benzo-[*b*]-fused BODIPY revealed a significantly perturbed π -conjugation with system enhancement of its electron-accepting azafulvene character. Dimer **5** showed a large deviation of the central benzene from the aromatic benzene geometry, a situation leading to a significantly low-lying LUMO delocalized along the periphery. This was further supported by electrochemical characterization. In addition, the benzene-fused BODIPYs **4** and **5** showed broad and intense absorption bands in the visible/NIR region (reaching up to 900 nm for the latter) along with weak fluorescence in the deep red ($\lambda_{em} = 690$ nm, $\Phi_F = <0.01$) and NIR region ($\lambda_{em} = 940$ nm, $\Phi_F = <0.01$), respectively.

Another nice example of extending the π -conjugation system by fusing a benzene ring on the pyrrole unit was presented in 2010 by Jiao *et al.*⁵⁸ They reported the asymmetrical synthesis of benzo-fused BODIPYs showing a red-shifted absorption and bearing an additional point of functionalization based on chloro- or bromo-substituents in the 3-position (Fig. 13). With this structural platform, Sonogashira-coupling was made possible to further expand the π -conjugation with various aryl and thiophene groups. Nucleophilic substitution reactions were also possible on the same position, allowing notably for the construction of push-pull derivatives. Vicente and coworkers also reported the synthesis of a series of symmetric benzo-appended BODIPYs by two different routes, along with their computational modeling for a better rationalization of the observed properties.⁵⁹

An additional way to extend the π -conjugation system is to fuse two or more BODIPY units together. Shinokubo *et al.*

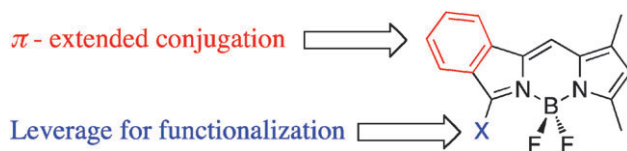


Fig. 13 Asymmetrical benzo-fused BODIPY platform.⁵⁸

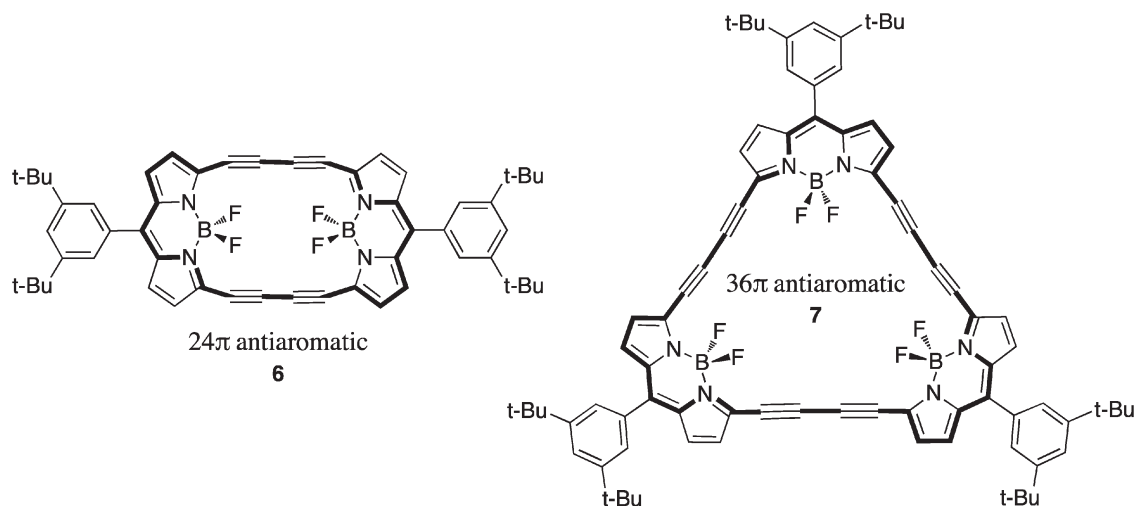


Fig. 14 BODIPY-based antiaromatic porphyrinoid structures of 24 and 36 π electrons.⁶¹

reported a facile synthesis of biphenyl-fused BODIPY obtained by oxidative cyclization of peripheral aryl-substituents at the β -position of the BODIPY.⁶⁰ NIR properties and strong π - π interactions in the solid state are associated with this extension of the π -system. The same group also used BODIPY precursors to generate antiaromatic porphyrinoid structures **6** and **7** (24 and 36 π electrons, respectively) by metal-mediated synthesis (Fig. 14).⁶¹ The photophysical properties of the extended conjugation system revealed absorption in the NIR past 950 nm, albeit quite weakly. Pursuing their research toward the smallest antiaromatic porphyrinoid structure possible, they also reported a nickel-mediated reductive homocoupling of a homoleptic dipyrin complex for the formation of a Ni(II) norcorrole (16 π electrons).⁶² In contrast, Bröring *et al.* recently reported the preparation of aromatic 10-heterocorroles (18 π electrons) integrating a Group 16 element (O, S, Se) in the backbone through a

two-step macrocyclization approach from 3,5-dibrominated dipyrin precursors.⁶³ They first used these precursors in order to obtain bromine-terminated linear tetrapyrrole Cu(II) chelates by using a *n*-BuLi/Cu(II) protocol. In a second step, cyclization to the desired Cu(II) 10-heterocorrole complexes was achieved by using different nucleophilic O, S, or Se transfer reagents. After reductive demetalation with SnCl₂·2H₂O-HCl in a mixture of acetonitrile and dichloromethane, the desired 10-heterocorroles were isolable as pure free-base compounds.

The group of Wu investigated fusion of aromatic rings on the zigzag edge of BODIPY by an FeCl₃-mediated intramolecular oxidative cyclohydrogenation reaction. They reported in 2011 three examples of π -extended systems based on porphyrin (**8**), anthracene (**9**) and perylene (**10**) (Fig. 15).^{56,64,65} Absorption in the NIR up to almost 1000 nm was observed, in addition to good solubility and high photostability. These observations are

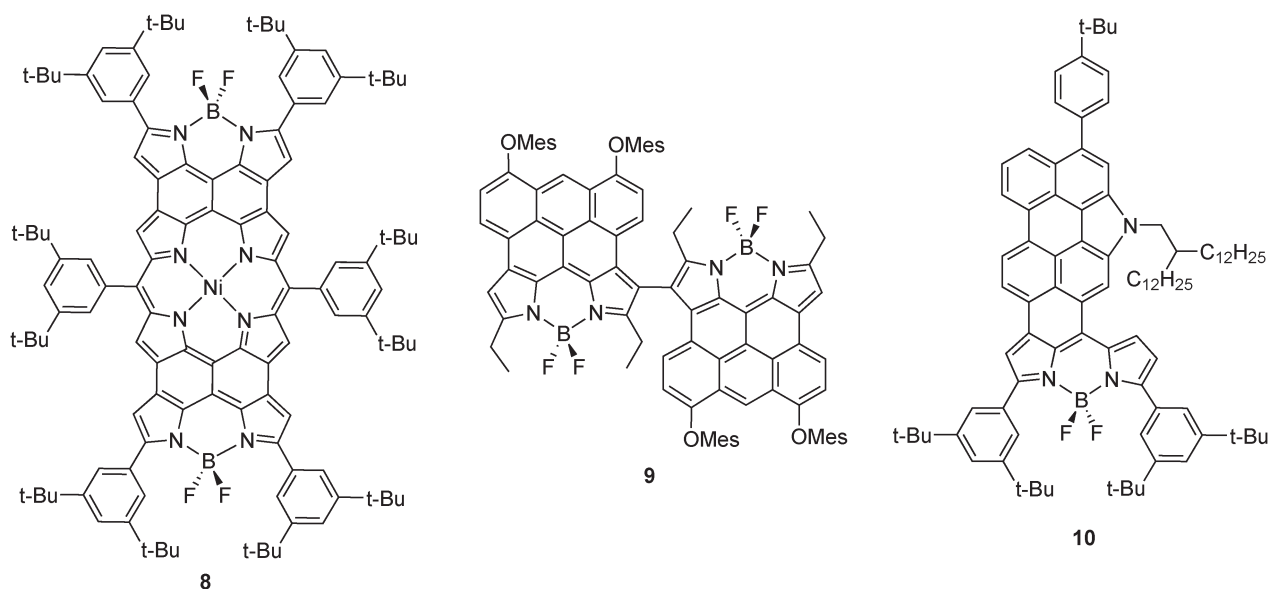


Fig. 15 Porphyrin-, anthracene- and perylene-based BODIPY NIR dyes.^{56,64,65}

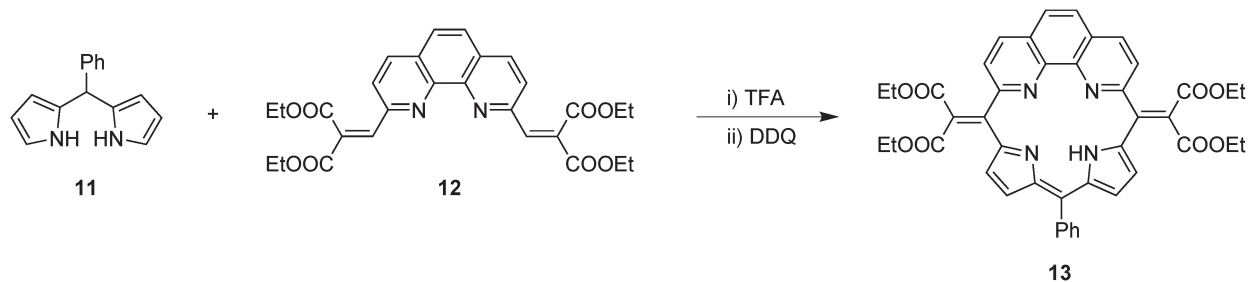


Fig. 16 Synthesis of a porphyrin-related macrocycle with embedded DPM and 1,10-phenanthroline subunits.⁶⁶

undeniably of great interest for OPV. Remarkably, the use of organometallic chemistry with the Ni^{II} based porphyrin core offers supplementary leverage for fine-tuning of the energy levels in addition to axial coordination of an acceptor such as PCBM derivatives.

Ishida *et al.* reported another example of the formation of porphyrin related macrocycles starting from a DPM building block.⁶⁶ Their synthetic approach for **13** was based on a one-pot [2+2] acid condensation of the *meso*-phenyldipyrromethene **11** with the corresponding 1,10-phenanthroline vinyl derivative **12**, advantageously avoiding formation of a complex mixture of compounds (Fig. 16). Photophysical and X-ray characterization were reported, along with DFT calculations. Interestingly, modelization showed that both the HOMO and LUMO are mainly centered on the DPM part of the porphyrin-related macrocycle, with almost no contribution at all from the phenanthroline moiety. The MgCl-coordinated derivative was also obtained and compared to the metal-free macrocycle.

Boens *et al.* performed a comprehensive study concerning the effect on photophysical properties of conformationally constrained BODIPY dyes by means of annulation.⁶⁷ To do so, they prepared six different related dyes (**14–19**, Fig. 17) to compare how pending phenyl groups in the α -position affect the rigidity. Dyes were compared in solvents of variable polarity and showed that the small solvent-dependent shifts observed were primarily determined by solvent polarizability. The authors also witnessed that symmetrically disubstituted compounds **15** and **19** have bathochromically shifted absorption and fluorescent spectral maxima compared to dyes **14** and **18** bearing asymmetrically monosubstituted DPM cores. Experimental results were backed up by quantum mechanical calculations of the lowest electronic excitation and by comparison with corresponding dyes of related chemical structure but without conformational restriction. They concluded that the fusion of conjugation extending rings to the 2,3- and 5,6-positions of BODIPY is an especially efficient method for the construction of dyes absorbing and emitting at longer wavelengths.

Back in 2010, the group of Ohe prepared structurally rigid BODIPY dyes having spirofluorene moieties as a means to force the conformation (**20–24**, Fig. 17).⁶⁸ These dyes exhibited intense bathochromic shift in the absorption and fluorescence maxima, along with a significant increase in fluorescence quantum yield due to high rigidity and good planarity induced

by spirofluorene moieties. DFT calculations also proved the implication of spirofluorene units in the π -system of the BODIPY derivatives. Furthermore, the fluorescent ON/OFF phenomenon observed upon changing solvent for compound **9** was due to photo-induced electron transfer from an *N,N*-dimethyl-aminophenyl unit to the BODIPY core.

The group of You reported the synthesis of NIR BODIPY dyes with thiophene or furan fused on the *b* bonds of the pyrrole (**25–30**, Fig. 17).⁶⁹ They also took advantage of the heavy atom effect brought about by bromine substituents to efficiently apply their NIR dyes to singlet oxygen generation. The theoretical, optical and singlet oxygen generation characteristics of these NIR dyes were assessed and proved the potential for their use in imaging and photodynamic therapy. More recently, they also published a study on the use of thieno-pyrrole-fused BODIPY intermediate as a platform to multifunctional NIR agents.⁷¹ On their side, Chujo recently studied thiophene-fused BODIPY dyes (**31–34**, Fig. 17).⁷⁰ They took two distinct substitution strategies to modulate the optical properties of the new dyes. First, introduction of iodine groups (**32** and **33**) allowed them to observe bathochromic shifts (15 nm for **32** and 30 nm for **33**) and the enhancement of molar extinction coefficients compared to the reference compound **31** (from 127 000 up to 184 000 M⁻¹ cm⁻¹ for **33**) due to the heavy atom effect. Second, the insertion of a -CF₃ group at the *meso*-position in compound **34** led to a bigger bathochromic shift (60 nm) arising from the lowering of the LUMO energy level, as observed by calculations. Overall, this thiophene-fused BODIPY family showed large molar extinction coefficients with sharp absorption bands down to 623 nm in the case of **34** and low emissions. We believe that such strong absorbers in the NIR would make interesting candidates as additives in OPV applications.

Finally, Krumova and Cosa reported in 2010 the preparation of 16 new BODIPY dyes with tunable redox potentials and functional groups for further tethering (**35–50**; Fig. 18).⁷² Insertion of electron-withdrawing and -donating groups in 2,6-positions gave rise to redox potentials tunable by ~0.7 eV without significantly affecting the band-gap or absorption/emission properties. The integration of hydroxymethyl or formyl groups at the *meso*-position allowing for covalent tethering on receptors and labeling of biomolecules was noteworthy. The absence of emission in the *meso*-formyl derivatives also allows for their application as exceptional fluorogenic probes for studying the mechanisms of nucleophilic attack.

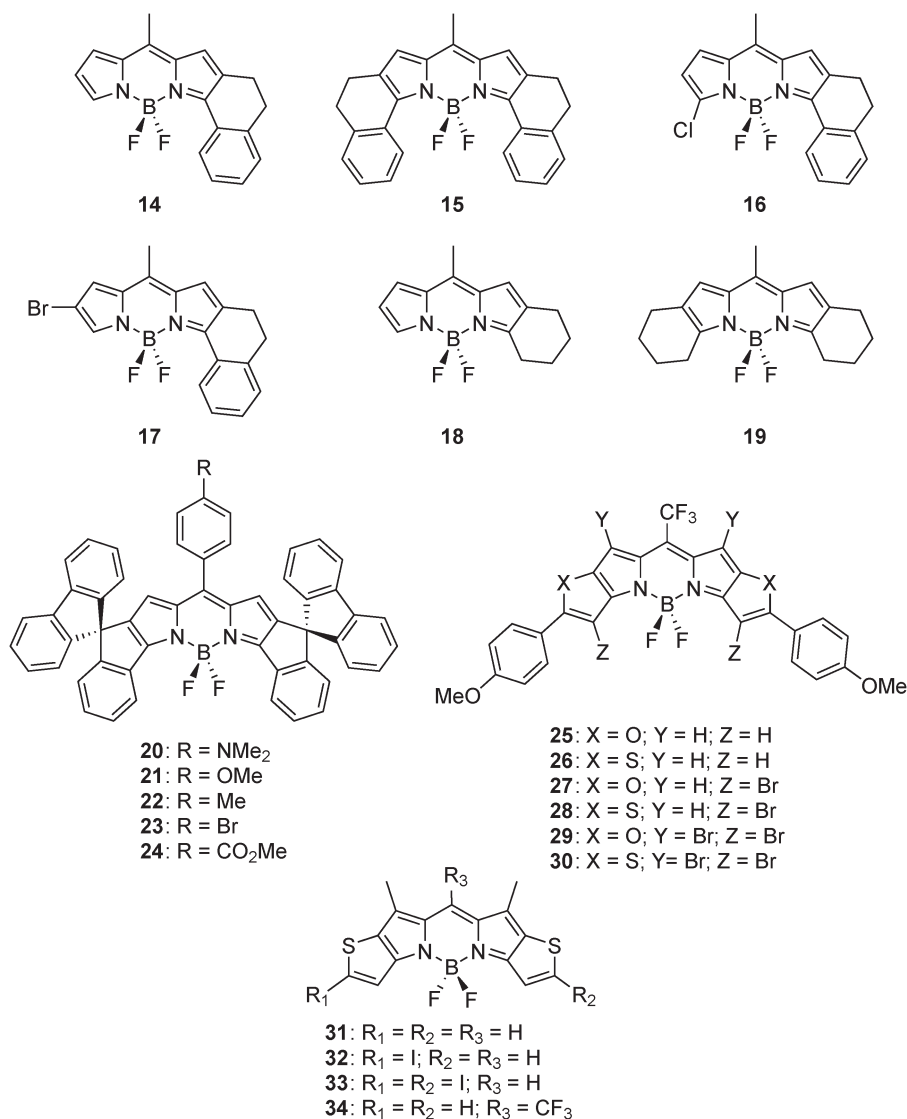


Fig. 17 Conformationally constrained BODIPY dyes by means of annulation and their analogues.^{67–70}

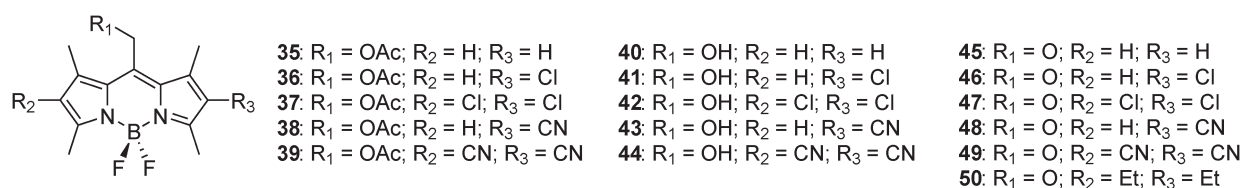


Fig. 18 BODIPY dyes with tunable redox potentials.⁷²

2.1.2 Tuning of emission. Looking more specifically at the tuning of emission properties, another example of quenching by structural derivatization was described by Ravikanth *et al.*⁷³ Synthesis of sterically crowded polyarylated BODIPYs 51–55 from brominated precursor 51 revealed that while the propeller-like conformation derivatives obtained were highly fluorescent, the unsubstituted precursors were almost not at all (Fig. 19). Electrochemical studies also indicated a reversible oxidation for polyarylated derivatives that was absent for

unsubstituted ones. In a continuation of this paper, the same group published the photophysical and electrochemical properties of new sterically crowded polyarylated BODIPY derivatives.⁷⁴ Using another synthetic procedure based on the reaction of tetraarylcyclopentadienones with ammonium acetate in a one-pot cascade process, the groups of Lu and Wang collaborated together to study a large variety of heptaaryl-DPM and their corresponding BODIPYs (Fig. 20).⁷⁵ Along with their exhaustive photophysical characterization of the derivatives

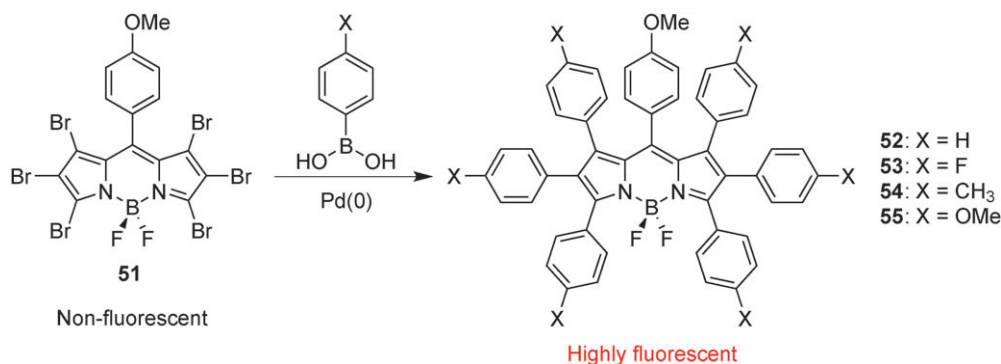


Fig. 19 Polyarylated BODIPY derivatives exhibiting high fluorescence compared to unsubstituted ones.⁷³

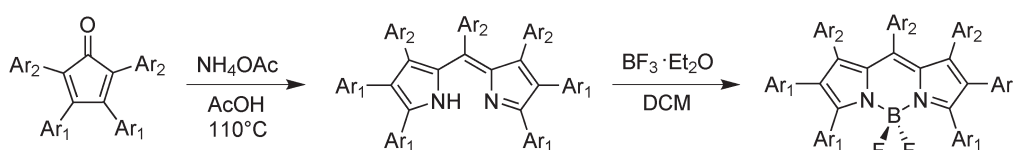


Fig. 20 Heptaaryl-DPM derivatives obtained from the one-pot cascade process and their corresponding BODIPYs.⁷⁵

obtained, they were able to show a fluorescent response to environmental acidity.

Zhao and collaborators looked at the concept of geometry relaxation-induced Stokes shift in red-emitting BODIPY.⁷⁶ They prepared 2-thienyl and 2,6-bisthieryl BODIPY derivatives (56 and 57, respectively; Fig. 21) that showed intense absorption and a large Stokes shift (96 nm) vs. the small Stokes shift of typical BODIPY (<15 nm). DFT calculations proposed that the large Stokes shifts are due to the remarkable geometry relaxation upon photoexcitation and its substantial effect on the energy levels of molecular orbitals. Interestingly, fluorophores were used for fluorescent thiol probes, with 2,4-dinitrobenzenesulfonyl (DNBS) as the fluorescence switch.

Interestingly, Cole reused compound 57 in a recent theoretical work comparing four organic fluorophore families (coumarin, cyanine, stilbene and BODIPY) to establish rules for molecular design of UV-vis absorption and emission properties.⁷⁷

Solvent is another environmental parameter that can strongly affect the spectral properties when observing a chromophore. In this sense, the relationship between the spectral properties of alkylated BODIPYs in solution and the physico-chemical parameters of various solvents is of interest.⁷⁸ Marfin *et al.* established that the negative solvatochromic effect is intrinsic for BODIPY. They also concluded that specific interactions contribute substantially to the properties of the chromophore, which are determined by the electron donor properties of the solvent.

The tuning of emission properties can also be achieved by addition of Cu^{II} and Hg^{II} cations. Kobayashi *et al.* prepared BODIPY derivative 58 with an -NH₂ and -OH substituted *meso*-phenyl ring (Fig. 22), which undergoes a specific fluorescence enhancement under biological conditions in the presence of Hg^{II} cations. In addition, the presence of Cu^{II} cations leads to the J-aggregation of the dye. This behavior is of particular interest for OPV, since J-aggregation gives rise to a red-shifted absorption spectrum due to the parallel alignment of transition dipoles.⁷⁹ This type of aggregation appears to be a potentially strong tool for the control of morphology of the photoactive layer in the solid state. Interestingly, special behavior arising from aggregation was also observed from tetraphenylethene-containing BODIPY derivatives 59–61 (Fig. 22), which exhibited aggregation-induced emission (AIE) tunable from the visible to the NIR.⁸⁰ In fact, the study of Tang and coworkers revealed how subtle structural changes can modulate the emission color, solvatochromism and AIE features of these BODIPYs. In the same vein, Vu *et al.* looked at the spectroscopic properties and the aggregation process of the new sterically hindered

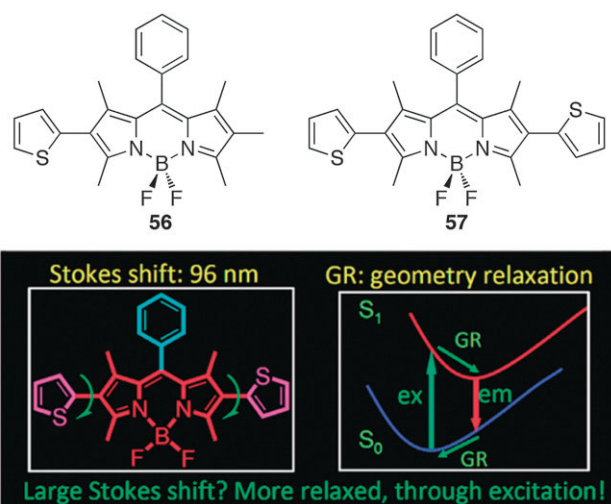


Fig. 21 2-Thienyl and 2,6-bisthieryl BODIPY derivatives showing geometry relaxation-induced large Stokes shifts.⁷⁶ (Adapted with permission from *J. Org. Chem.*, 2012, **77**(5), 2192–2206. Copyright© 2012 American Chemical Society.)

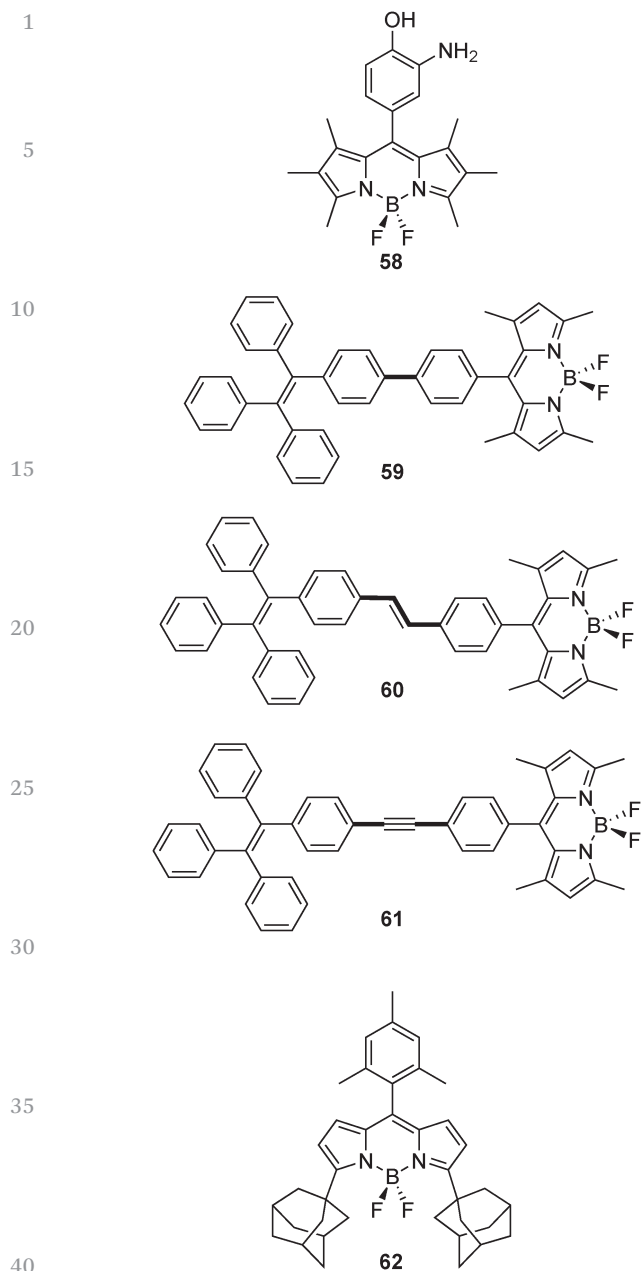


Fig. 22 BODIPY derivatives exhibiting aggregation behavior.^{79–81}

BODIPY **62** bearing adamantyl moieties in the 3,5-positions (Fig. 22).⁸¹ They observed that the aggregation process could be described by three components, namely the monomer species along with J and H aggregates. Analysis of fluorescence and anisotropy decays also showed that excitation energy was transferred from the monomer to the J dimers, while it might most probably be trapped by H aggregates.

The group of Li reported the possibility of inducing green color emission from a BODIPY dye *via* energy transfer from the polysilane S_1 state to the S_2 state of the BODIPY in the solid state.⁸² This was achieved by irradiation of a film made of a poly(methylphenyl)silane containing less than 3 mol% of BODIPY dye. Interest in this type of BODIPY-doped polysilane

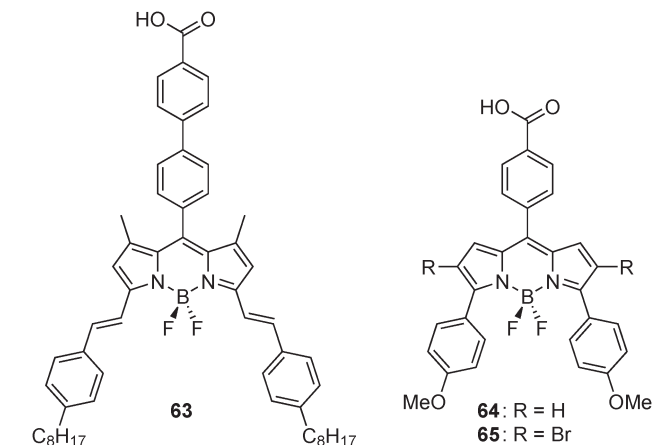


Fig. 23 Dual-emissive BODIPY derivatives.^{83,84}

systems resides in the usually nonfluorescent behavior of BODIPY dyes in the solid state due to aggregation and self-quenching. According to the authors, new optoelectronic devices for electroluminescence can be envisioned based on their results.

With the idea of preparing new photoactive materials for solar cells, Wang *et al.* reported BODIPY derivative **63** and its use in functionalizing highly monodispersed PbS nanoparticles (Fig. 23).⁸³ Their system (**63**-PbS nanoparticles) reaches absorption and emission in the NIR region past 1100 nm, mainly due to the intrinsic photophysical properties of PbS nanoparticles. However, electronic communication between the BODIPY ligand and the nanoparticle was established. Interestingly, the BODIPY derivative used presented dual-emission behavior at $\lambda_{\text{max}} = 585$ and 655 nm in toluene that was further studied as it was observed for the first time in this family of dyes. They assigned it to an intramolecular electronic transition for the higher energy emission and aggregation plus intermolecular interactions for the lower energy emission as the explanation for such a dual emissive behavior. A simple solar cell was constructed based on **63**-PbS nanoparticles as the photoactive layer and this actually presented a photocurrent. This represents a true improvement compared to their control, oleic acid capped PbS nanoparticles that did not display any PV properties.

On their side, Cho and coworkers also observed S_2 emission from chemically modified BODIPYs.⁸⁴ Those new BODIPYs **64** and **65** (Fig. 23) showed atypical emission from the second excited state at shorter wavelength (~ 440 nm) in addition to the one in the red region (631 and 636 nm, respectively). This dual-emission behavior was investigated by fluorescence up-conversion and transient absorption to reveal a dependence of the emission decay time on the internal conversion and the intersystem crossing process. TD-DFT calculations were also performed for the assignment of electronic transitions implied.

The group of Banfi and coworkers reported the synthesis of eight new variously substituted BODIPY dyes (**66**–**73**; Fig. 24) and their photodynamic activity.⁸⁵ Photophysical data were presented along with the ability for singlet-oxygen generation.

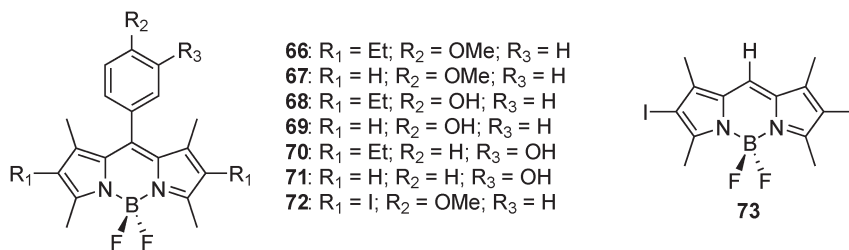


Fig. 24 BODIPY derivatives showing singlet-oxygen generation properties.⁸⁵

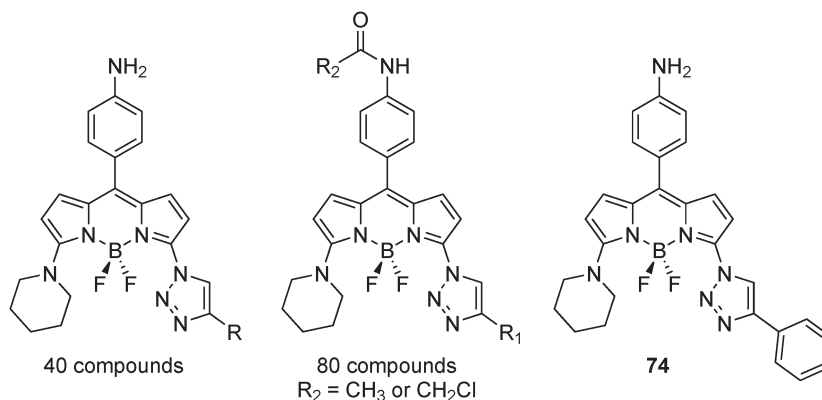


Fig. 25 BODIPY-triazole derivatives exhibiting large Stokes shifts.⁸⁶

This last parameter is of interest for OPV because it represents a form of susceptibility toward energy transfer of the dyes. From the observations made, halogenated compounds **72** and **73** quickly generated singlet-oxygen, although they presented the lowest quantum efficiency of fluorescence.

Finally, the group of Chang prepared a library of 120 BODIPY-triazole derivatives on solid-phase using a click-chemistry protocol (Fig. 25).⁸⁶ The compounds prepared exhibited large Stokes shifts (up to 160 nm) and remarkable environmentally sensitive quantum yield increments that asserted their potential as turn-on fluorescent chemosensors. Out of their library, they identified **74** (Fig. 25) as the best fluorescent chemosensor, which displayed high sensitivity and species-selectivity towards human serum albumin. In addition to the interesting photophysical behavior observed by the authors, we strongly believe in the potential of click-chemistry as a powerful synthetic tool for integration of BODIPYs in new OPV materials, either in complex small molecules of D-A type or in various polymeric architectures.

2.1.3 Regioselective functionalization. As described in Sections 2.1.1 and 2.1.2, substitutions on the DPM/BODIPY core can greatly affect its absorption and emission properties. This section therefore aims at discussing the various routes of derivatization of the DPM/BODIPY core. Modifications at the 3,5-, 2,6- and 8-positions are well documented. It is possible to operate electrophilic aromatic substitution (S_EAr), direct hydrogen substitutions and Pd-catalyzed cross-coupling in the 2,6-positions. The 3- and 3,5-positions can undergo S_NAr (including thiol-halogen nucleophilic substitution), electrophilic substitution with NBS on methyl groups, direct hydrogen substitutions,

direct styrylation, and Pd-catalyzed cross-coupling.^{87–91} S_NAr and Liebeskind cross-coupling at the 8-position are possible, similar to the installation of a *meso*-CF₃ group during the formation of symmetric or asymmetric 3(5)-aryl(hetaryl)- and 3,5-diaryl(dihetaryl)-BODIPY dyes.^{92–95} Finally, nucleophilic substitutions (S_N) with oxygen or carbon nucleophiles on the boron center in the 4-position are also possible.^{96–98} Fig. 26 gives a schematic overview of the different synthetic routes for the derivatization of the BODIPY core.

In an unprecedented synthetic effort to open a wider access to the chemistry on 1,7-positions, the group of Dehaen focused on the synthesis of 1,7-dihalogenated BODIPY dyes and further substituted them by either nucleophilic aromatic substitution (S_NAr) or Pd-catalyzed cross-coupling reactions (refer to Fig. 26).⁹⁹ By doing so, they gave the last synthetic tools chemist

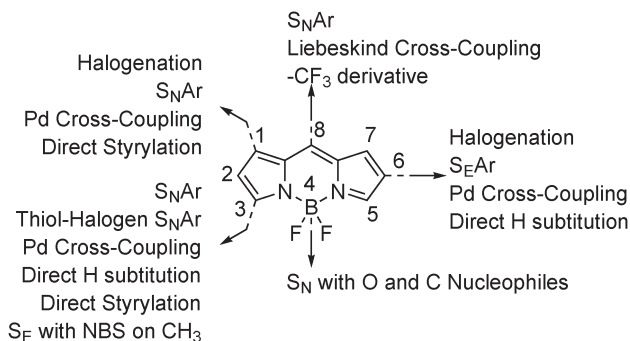


Fig. 26 Overview of the synthetic routes for derivatization of the BODIPY core.

needed to fully decide on regioselectivity in their design of BODIPY derivatives. Shortly after, Ziessel *et al.* also reported derivatization at 1,7-positions based on direct styrylation of methyl groups leading to highly substituted BODIPYs of the type AB, A₂B₂ or ABCD.¹⁰⁰ In addition to derivatization at the newly accessible 1,7-positions, Ziessel also reported the possibility of preparing carbonyl derivatives of BODIPYs *via* catalytic CO insertion.¹⁰¹ In fact, their methodological study dealt with carbopalladation reactions on BODIPY dyes bearing aryl-halogen functions. The functional groups could be positioned directly on the BODIPY core, *i.e.* at the *meso*- or β -positions, or in the periphery of the boron-substituted and on styryl-BODIPY derivatives (75–86; Fig. 27). Using this versatile technique, several ester and amide groups were efficiently introduced on the dyes. The authors reported that these changes do not significantly affect the optical properties and thus allow the construction of new BODIPY-based functional dyes with carboxylic anchoring groups or peptide linkages.

The groups of Hao and Jiao reported a straightforward acid-catalyzed synthetic procedure for the preparation of

pyrrolyl-dipyromethene (Fig. 28).^{102,103} Numerous derivatives having different functional groups were efficiently synthesized from POCl₃-promoted condensations between 5-chloro-2-formylpyrrole or isoindole derivatives and suitable pyrrole or indole fragments through a nucleophilic aromatic substitution of the initially formed protonated azafulvene rings. In addition, these groups further reported the preparation of 3-pyrrolylBODIPYs by an alternate synthetic procedure using pyrrole and acyl chlorides in the presence of oxygen (Fig. 29).¹⁰⁴ On his side, Ravikanth reported the synthesis of *meso*-unsubstituted 3-pyrrolyl BODIPY in one pot by treating the *meso*-free DPM with pyrrole in chloroform followed by oxidation with DDQ, neutralization with triethylamine and complexation with BF₃·Et₂O.¹⁰⁵ These three metal-free one-pot protocols are of great interest to prepare new tridentate ligands with extended π -conjugation able to coordinate a variety of metallic cations, allowing further tuning of the photophysical properties.

Regioselective halogenation of the BODIPY core is still under study as it generates valuable synthetic precursors. Jiao

20

20

25

30

35

40

45

50

55

25

30

35

40

45

50

55

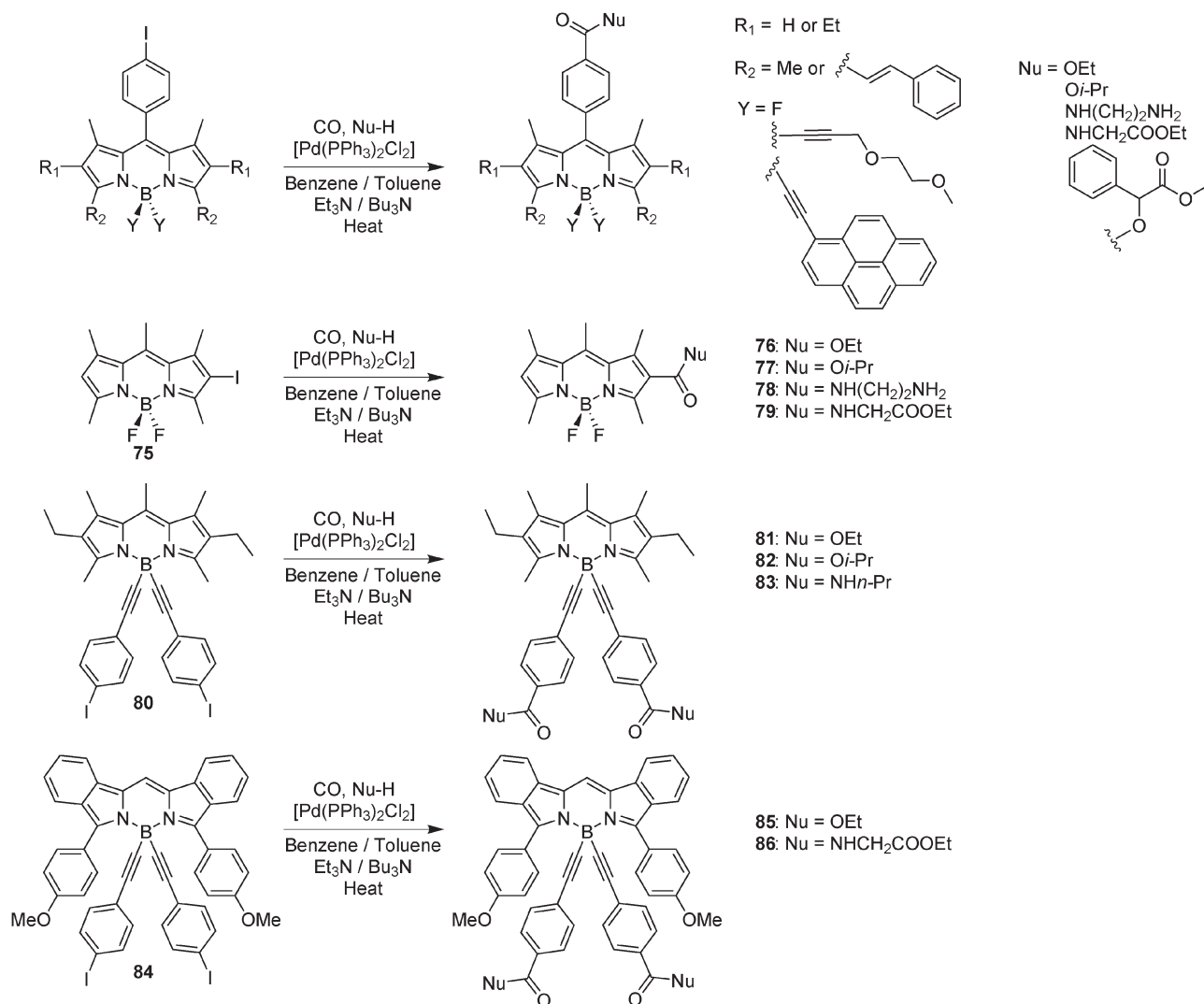


Fig. 27 Preparation of carbonyl derivatives of BODIPYs *via* catalytic insertion.¹⁰¹

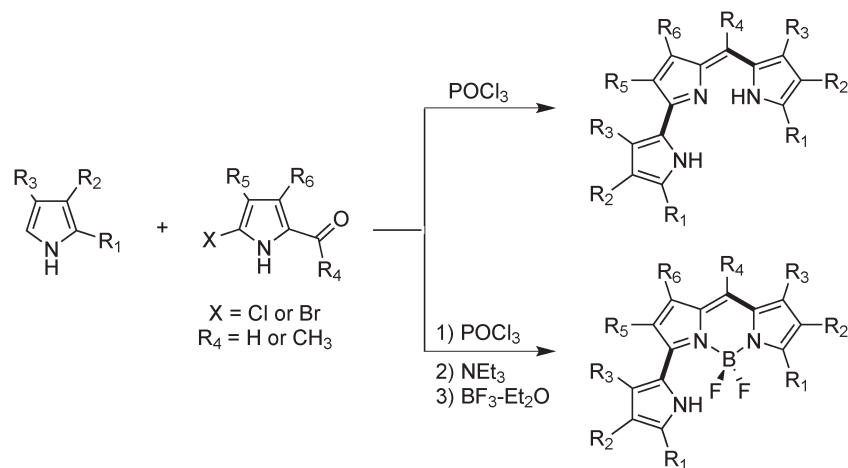


Fig. 28 Straightforward acid-catalyzed synthesis of pyrrolyl-dipyrromethenes and 3-pyrrolylBODIPYs.^{102,103}

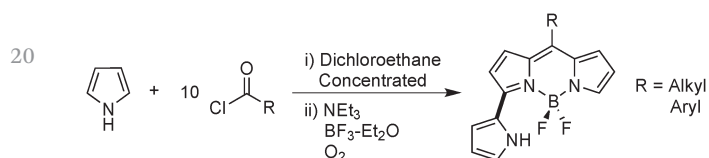


Fig. 29 One-pot synthesis of 3-pyrrolylBODIPYs from pyrrole and acyl chlorides.¹⁰⁴

et al. reported that electrophilic bromination of pyrrolic unsubstituted BODIPYs using bromine can regioselectively generate mono- to hepta-bromo substitution in a stepwise fashion.¹⁰⁶ According to their results, the bromination of **87** occurs first at 2,6- (**88** and **89**), then at 3,5- (**90**) and eventually at 1,7-positions (**91**) when a large excess of bromine is used (Fig. 30). Bromination of the *meso*-phenyl at the *meta*-position can even occur when using up to 400 equivalents of bromine with a methoxy-group present in the *para*-position. Regioselective substitution and Suzuki coupling reactions were attempted on the brominated BODIPYs, giving good to excellent yields. Results also showed that regioselective substitution occurred first at

the 3,5- and then at the 1,7-positions of the chromophore. The spectroscopy of the compounds was included. Interestingly, Zhang and Yang conducted a further study on these brominated BODIPYs to determine their potential for singlet oxygen generation and triplet excited-state spectra.¹⁰⁷ In the same period, they also looked at a covalent BODIPY dimer linked at the 2-position for the exact same application selectively in nonpolar environments.¹⁰⁸

Likewise, Ortiz *et al.* reported a theoretical and experimental study on the iodination of BODIPY dyes with different degrees of substitution for the preparation of various derivatives bearing asymmetrical DPM cores.¹⁰⁹ Their study was the first to present polyhalogenated BODIPYs with different halogen atoms (*e.g.* **92–94**; Fig. 31), allowing for selective functionalization. Photophysical properties and singlet oxygen generation were also presented. The group of Zhang recently reported the preparation of various iodo-BODIPYs that were further used as visible light-driven metal-free organic photocatalysts.¹¹⁰ Another recent study from Dehaen *et al.* proved the possibility of preparing *meso*-halogenated BODIPYs and accessing useful *meso*-substituted analogues either by S_NAr or by Pd-catalyzed cross-couplings.¹¹¹

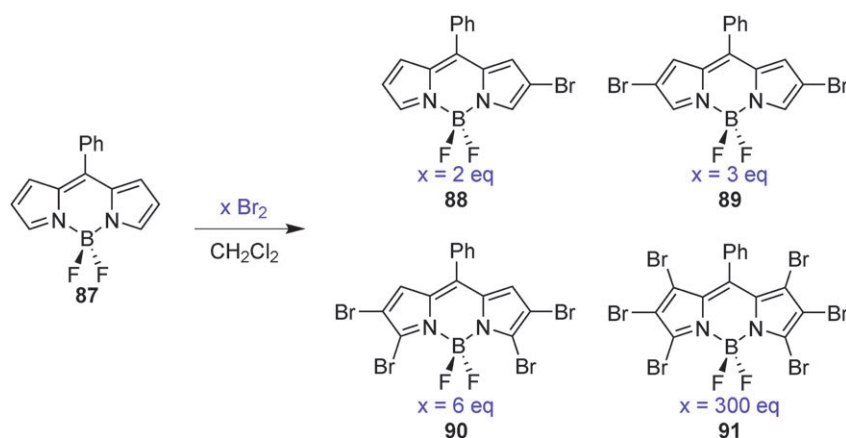


Fig. 30 Regioselective stepwise bromination of the BODIPY core.¹⁰⁶

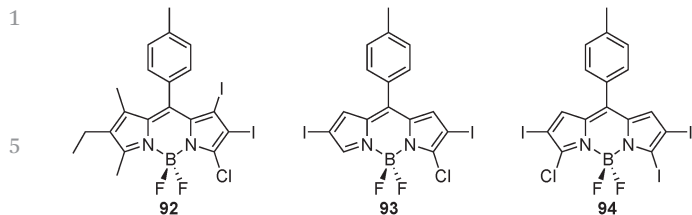


Fig. 31 Selection of hetero polyhalogenated BODIPYs.¹⁰⁹

Yang *et al.* reported an example of BODIPY-based fluorescent sensors taking advantage of regioselectivity.⁸⁸ Highly selective detection of glutathione (GSH) over cysteine (Cys) and homocysteine (Hcy) was obtained based on the rapid replacement of mono-chlorinated BODIPYs **95** to **100** by biothiols through thiol-halogen nucleophilic substitution and the significantly different photophysical properties of sulfur-compared to amino-substituted BODIPYs (Fig. 32). The sensor **95** was further successfully applied to the detection of GSH in living cells. More recently, Ravikanth and coworkers also used 3,5-bis(acrylaldehyde) BODIPYs for the detection of Cys and Hcy in living cells.¹¹²

On their side, the group of Chattopadhyay took advantage of the steric strain in *meso*-methyl BODIPYs **101** and **102** to functionalize that position regioselectively by a Knoevenagel-type condensation of various aromatic aldehydes (**103–108**; Fig. 33).¹¹³ Driven by alleviation of the structural strain of alkylated BODIPYs, the difference of acidity of the methylic protons at the pyrrole rings was overruled. Aware of the attractiveness of resultant *meso*-styryl BODIPYs for optoelectronic applications, the authors mentioned that they intend to study DSSC applications. This synthetic strategy is also valuable for the rational design of small-molecule planar-heterojunction solar cells.

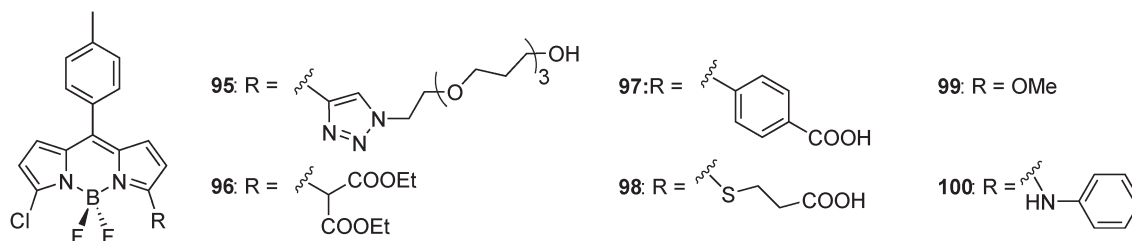


Fig. 32 Mono-chlorinated BODIPYs used for biodetection of glutathione by thiol-halogen nucleophilic substitution.⁸⁸

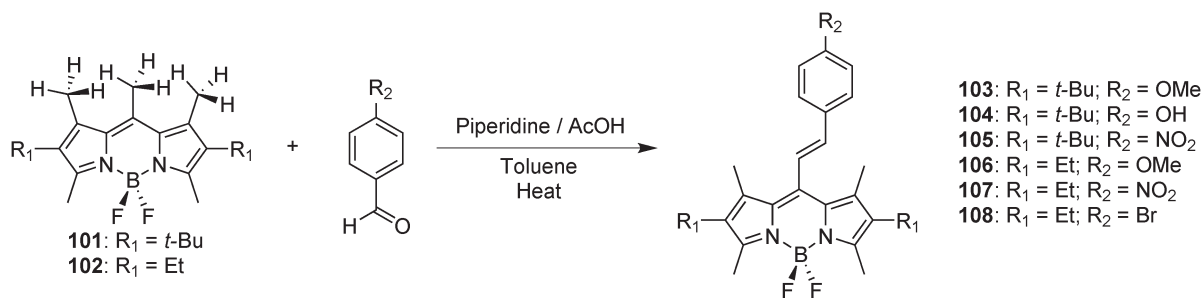
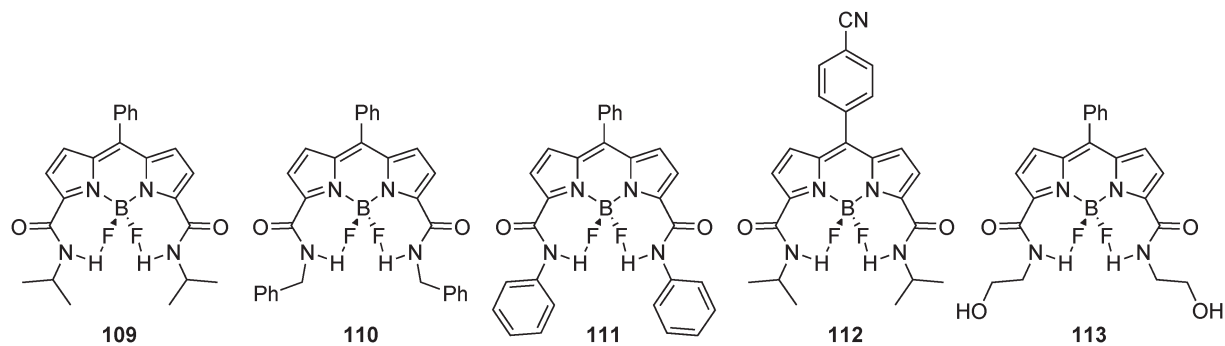
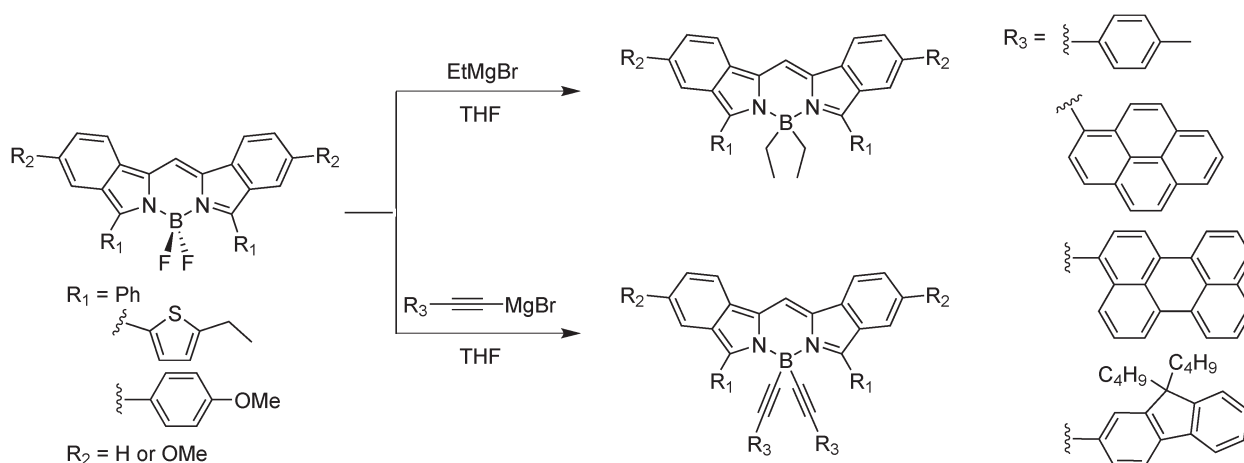
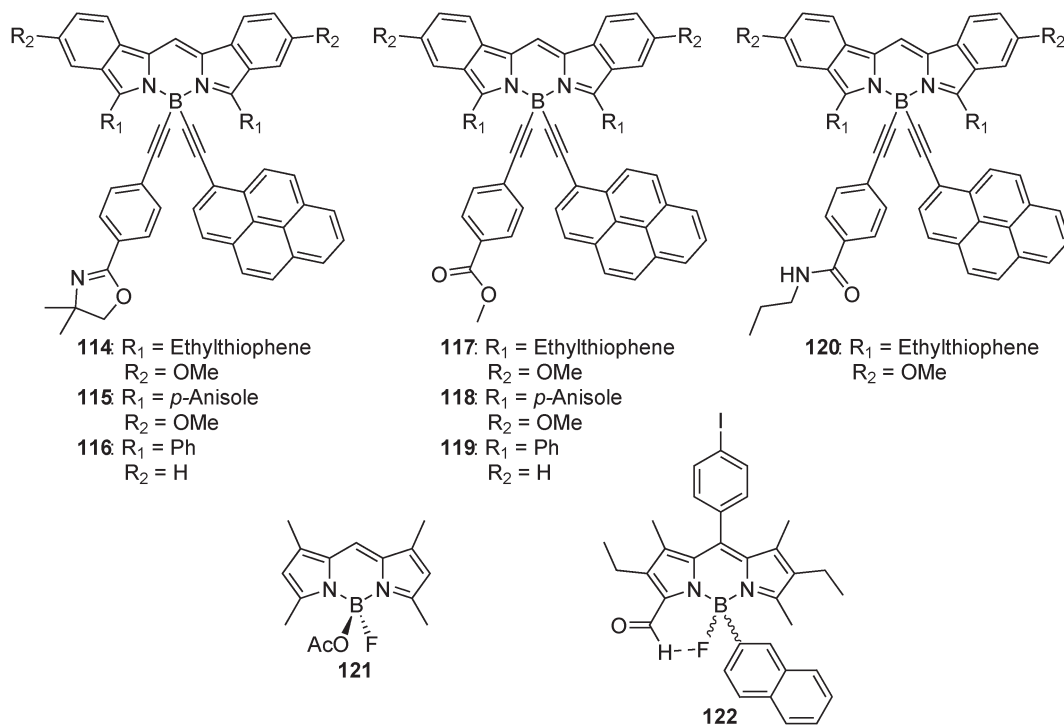


Fig. 33 Steric strain release-directed regioselective functionalization of the *meso*-position.¹¹³

In a recent paper, the group of Ortiz refined the regioselective functionalization at the *meso*-position by Knoevenagel condensation on alkyl-substituted-3,8-dimethyl BODIPYs.¹¹⁴ They noted that the change in hybridization of the carbon at the 8-position (from sp³ to sp²) determines the fluorescence emission, while the presence of EDG or EWG groups leads to ICT processes.

Other interesting results concerning the tuning of BODIPY properties were reported in 2010 by the group of Cohen.¹¹⁵ Persistent intramolecular hydrogen bonds between the –NH and F– groups were used to rigidify BODIPY dyes (**109–113**; Fig. 34). This behavior was supported by X-ray crystallography and solution ¹⁹F NMR experiments. The modular synthesis and robust photophysical properties led the authors to suggest their potential as materials for photochemical applications.

Derivatization at the boron center is also an interesting way to modify the photophysical properties of the BODIPY family. The most common ways for the substitution of fluorides are with oxygen- or carbon-based groups. It allows for either rigidification of the skeleton, addition of complementary chromophores and/or tuning of the electronic levels through reduction of the electron-withdrawing effect brought about by fluorides. This approach has gained a lot of attention in the last few years and might also be extended to the ADPM family. Ziessel presented an excellent article in which they reported an extensive study of boron chemistry on a diisoindolomethene framework.¹¹⁶ A general synthetic approach was developed to obtain the various difluorobora-diisoindolomethene dyes substituted with phenyl, *p*-anisole or ethyl-thiophene. A Grignard-based strategy was further used to introduce ethynyl-aryl or ethyl ligands on the boron center in replacement of the fluorides, either in a homo- (Fig. 35) or a hetero- (**114–120**; Fig. 36) manner. The numerous X-ray crystal structures

Fig. 34 Hydrogen-bond rigidified BODIPY dyes.¹¹⁵Fig. 35 Red to NIR fluorescent dyes based on boron-substituted diindolomethene frameworks.¹¹⁶Fig. 36 Heterodisubstitution at the boron in BODIPY derivatives.^{116,118,119}

1 obtained allowed the authors to determine a structure–fluorescence relationship to explain the modulation of emissions from
 2 650 to 780 nm. They observed that when the steric crowding around the boron center is severe, the aromatic substituents α to
 3 the diisindolomethene nitrogens are twisted out of coplanarity, and hypsochromic shifts up to 91 nm with ethynyl substituents
 4 are observed in the absorption and emission spectra. Electrochemical studies also revealed the redox active behavior of the dyes.
 5 The boron substitution strategy explored in detail was already used by the group of Ziessel back in 2010 when they reported
 6 BODIPY dyes with pentane-2,4-dione anchors designed for incorporation in electrochemical solar cells (123–129; Fig. 37).¹¹⁷ Facile
 7 anchoring on TiO₂ powder was achieved and studied by FT-IR spectroscopy to evaluate the potential for integration in this type
 8 of solar cells. The authors reported that the quench of fluorescence of TiO₂-linked dyes was indicative of a good electron
 9 injection in the conduction band of the semiconductor.

10 Ziessel's group also reported the resolution of a racemic mixture of a BODIPY derivative with an asymmetric boron
 11 center (122, Fig. 36).¹¹⁸ The dissymmetrization of the BODIPY core was achieved by oxidation of the 3-methyl group to the
 12 corresponding carboxaldehyde. In addition, ¹H NMR and X-ray structures both provided proof of H-bonding between the
 13 carboxaldehyde proton and the remaining fluoride ligand. Preparative chiral HPLC allowed resolution of the racemic
 14 mixture and circular dichroism showed persistence of enantiomers over time at room temperature.

15 Jiang *et al.* successfully prepared the mono-acetate (127, Fig. 37) and di-acetate substituted BODIPYs on the boron
 16 center from TM-BDP by *in situ* generation of the TMSOAc reagent.¹¹⁹ X-Ray structures were obtained and photophysical
 17 studies proved that derivatives retained the principal properties of the parent TM-BDP. In addition, their results showed an
 18 increased solubility in water for the acetate-modified BODIPYs,

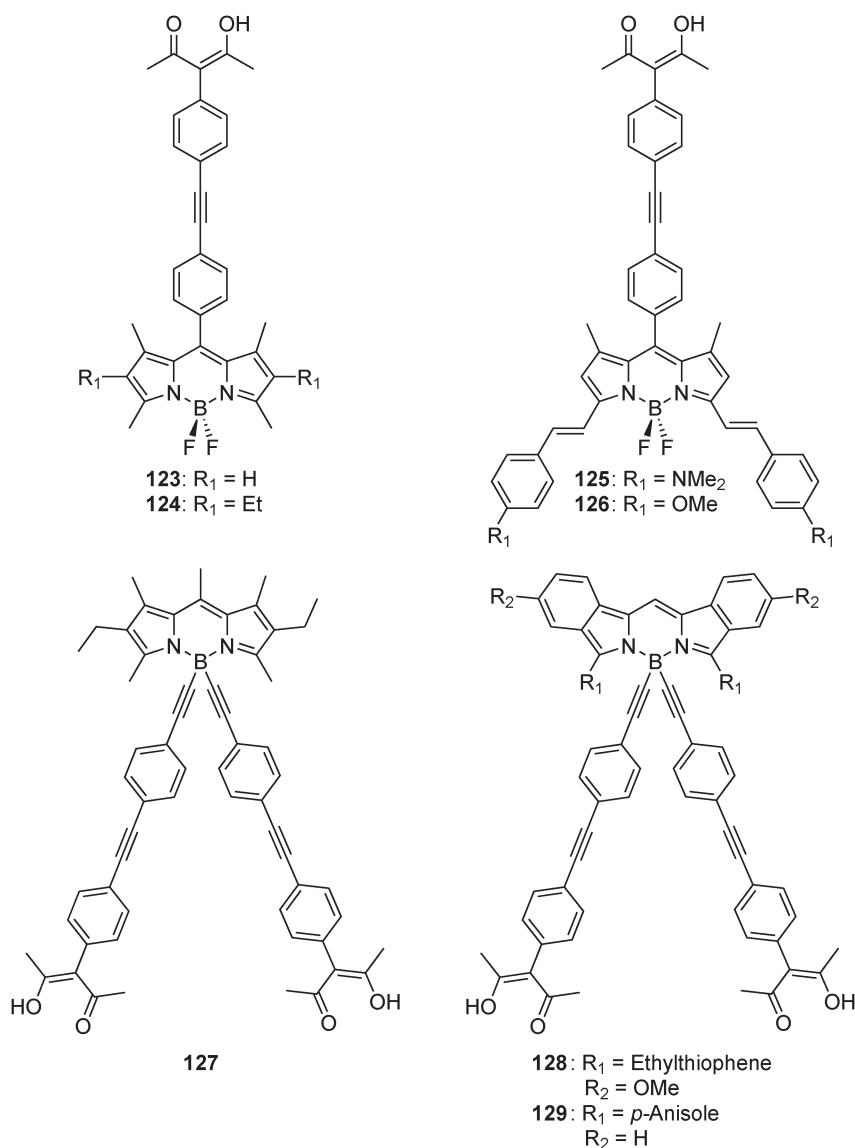


Fig. 37 BODIPY dyes with pentane-2,4-dione anchors.¹¹⁷

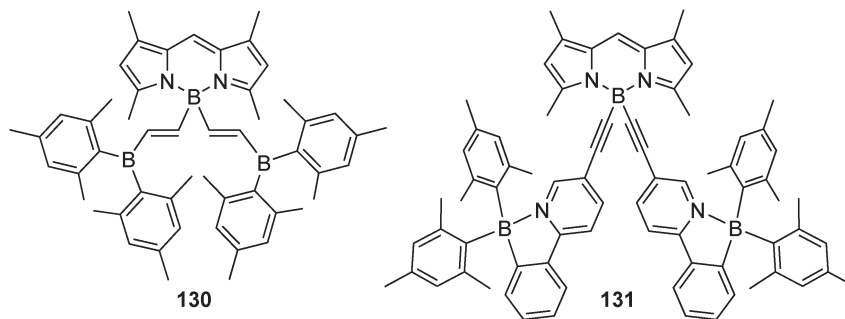


Fig. 38 BODIPY derivatives bearing three- and four-coordinated boron groups.¹²¹

which is highly suitable for incorporation in biological applications. Other examples of water-soluble BODIPY derivatives were also reported by Romieu in 2009 based on either boron chemistry or integration of sulfonated peptide chains that were subsequently quaternized by reaction with propanesultone.¹²⁰

The group of Wang prepared two new BODIPY derivatives decorated with three- and four-coordinated boron groups. In the first case, a Lewis acidic $\text{BMe}_2(\text{vinyl})$ group was used to prepare **130** and in the latter case it was a photochromic four-coordinated boron chromophore that gave **131** (Fig. 38).¹²¹ X-Ray structural analysis along with absorption and emission properties in solution and solid phases either as neat or doped PMMA films were studied. Significant mutual influence on photophysical and photochemical properties by the different boron-containing units was observed. For instance, the $\text{BMe}_2(\text{vinyl})$ unit in **130** greatly enhanced the BODIPY fluorescence efficiency in a PMMA matrix while the photoreactivity of the N,C -chelate boron unit in **131** was completely switched off by BODIPY *via* intramolecular energy transfer.

Finally, noteworthy publications on chemistry at the boron center have appeared lately from the group of Thompson. They reported a new class of BODIPYs, namely Cl-BODIPYs, bearing chloride instead of fluoride atoms on the boron center that allows for extremely easy substitution at the center.¹²² This work followed another paper published in 2009 where they prepared perfluoroaryl-substituted boron dipyrinato complexes, also including spiro BODIPY derivatives (**132–136**; Fig. 39).¹²³ In another recent article, they optimized the BF_2 removal from BODIPYs that they previously proposed in 2010 (Fig. 40).^{124,125} This breakthrough based on a standard lab microwave synthetic methodology using potassium hydroxide as the base is opening up the way for an efficient use of F-BODIPYs as a protective strategy of DPM. The authors

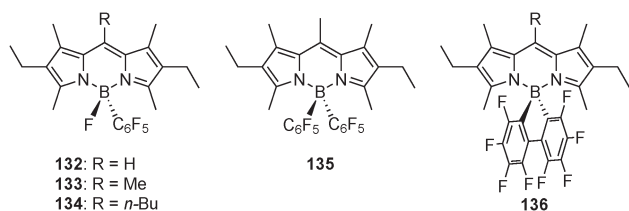


Fig. 39 Perfluoroaryl substituted BODIPYs.¹²³

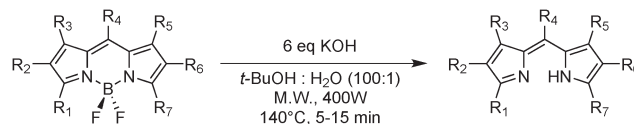


Fig. 40 Deprotection conditions for F-BODIPYs.¹²⁴

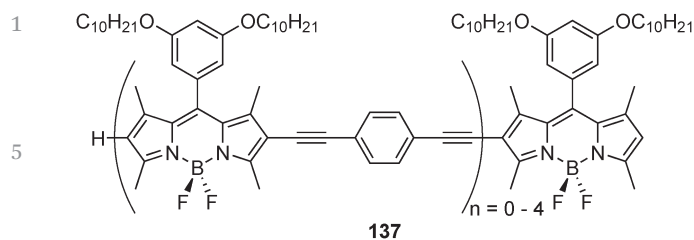
proposed a mechanism for the deprotection implying *tert*-butoxide as the active reagent due to the observation of a $t\text{-BuO-BODIPY}$ intermediate in the course of their study. The application of their protection–deprotection strategy to the synthesis of known and new pyrrolyldipyrromethenes is providing a good argument for the use of BF_2 protection in achieving challenging target compounds. Such a general procedure appears interesting in the perspective of expanding it to aza-BODIPYs as well.

2.2. Oligomers and polyads incorporating DPM

The integration of oligomers and polyads as photoactive donor materials in OPV is usually made possible through planar heterojunction solar cells. This is mainly due to their relatively low molecular weight allowing for vacuum deposition or solution processing on the ITO substrate. However, a few examples have been recently reported in which they have been used as sensitizers to expand the panchromaticity of solar cells, as mentioned in Section 1.1. Owing to the multiple ways to integrate them in OPV, this section will be dedicated to the review of energy transfer (ET) studies made on BODIPY oligomers and tetrads, including porphyrinoids, and their integration in heterojunction solar cells either as donor materials or additives.

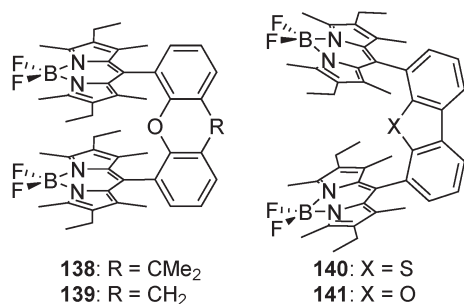
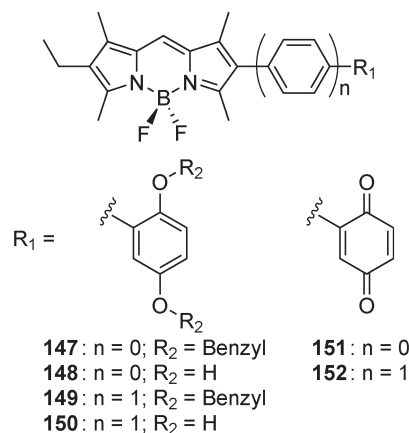
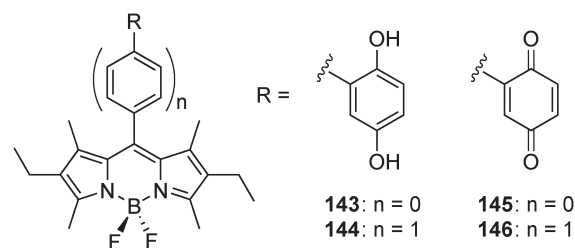
2.2.1 DPM-based oligomers and polyads in energy transfer studies.

Energy transfer in molecular polyads necessitates particular attention in order to fully understand the potential of molecules to harvest the energy from light and make it flow in a specific direction in complex systems. The assessment and control of the exact mechanism of energy transfer upon photoexcitation are therefore of great value for rational design. Possible mechanisms can either be through a poorly efficient radiative process or one of the two types of radiationless processes (through-space (Förster type) or through-bond (Dexter type)). The last few years have seen the development of many systems incorporating BODIPY derivatives able to

Fig. 41 Phenylethynyl-BODIPY oligomers.¹²⁶

transfer their absorbed energy to molecular partners or emit energy received from tetrad partner units. Akkaya and Cakmak have reported the preparation of various phenylethynyl-BODIPY oligomers (**137**; Fig. 41), notably *via* a Sonagashira coupling approach.¹²⁶ This study has revealed that such highly soluble, bright dyes should also be considered as fluorescent building blocks to create macromolecular assemblies.

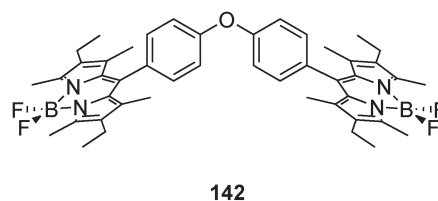
Another exciting study has been reported concerning BODIPY dimers by Benniston and co-workers in which they looked at charge delocalization and exciton coupling of their newly synthesized compounds (**138–142**; Fig. 42).¹²⁷ **138** to **141** are shown to adopt a cofacial conformation allowing for systematic variations of both the mutual orientation and mean separation of both BODIPY residues. X-Ray data support this assumption for complexes **138** and **139**. This cofacial conformation allows charge delocalization and exciton coupling which are revealed by electrochemical and spectroelectrochemical investigations. The group further studied the photophysical properties of those dimers under the condition of variation of temperature and pressure in a recent paper.¹²⁸ Recently, in 2010, Benniston *et al.* also studied the effect of substitution with covalently linked redox active hydroquinone/quinone groups at the *meso* vs. the 2-position in donor-acceptor BODIPY dyads (**143–152**; Fig. 43).¹²⁹ A complete investigation of the photophysical and electrochemical properties was reported along with special attention devoted to the electron transfer from the hydroquinone toward the BODIPY unit. Lately, another study was undertaken in collaboration with the groups of Lemmetyinen and Clegg to assess the effect of charge transfer and charge recombination by insertion of a naphthalene-based bridge in molecular dyads.¹³⁰ In order to do so, photophysical and electrochemical properties of two related dyads based on a *N,N*-dimethylaniline donor coupled to a fully alkylated BODIPY acceptor were described (**153** and **154**; Fig. 44) and they concluded that

Fig. 42 Cofacial BODIPY dimers.¹²⁷Fig. 43 BODIPY-based molecular dyad incorporating hydroquinone/quinone redox active groups.¹²⁹

the naphthalene spacer group is extremely efficient at promoting back electron transfer. Benniston and coworkers also studied Förster energy transfer over 20 angstroms from a pyrene-based donor to a BODIPY acceptor in compound **156** and in comparison with its phenyl derivative **155** (Fig. 44).¹³¹

In a similar fashion, a reversible fluorescence probe based on the Se-BODIPY D–A system for the redox cycle between HClO oxidative stress and H₂S repair in living cells was reported lately by the group of Han.¹³² Interestingly, the electron transfer process is quenched upon oxidation to the selenoxide derivative **158** under HClO conditions and is restored by H₂S reducing conditions, giving back the selenide derivative **157** (Fig. 44). Liu and Wu removed the methoxy group and the group of Li used a *meso*-hydroxymethyl BODIPY derivative by publishing similar concepts a few weeks later.^{133,134}

Audebert and collaborators also reported BODIPY–tetrazine multichromophoric derivatives where the BODIPY units were



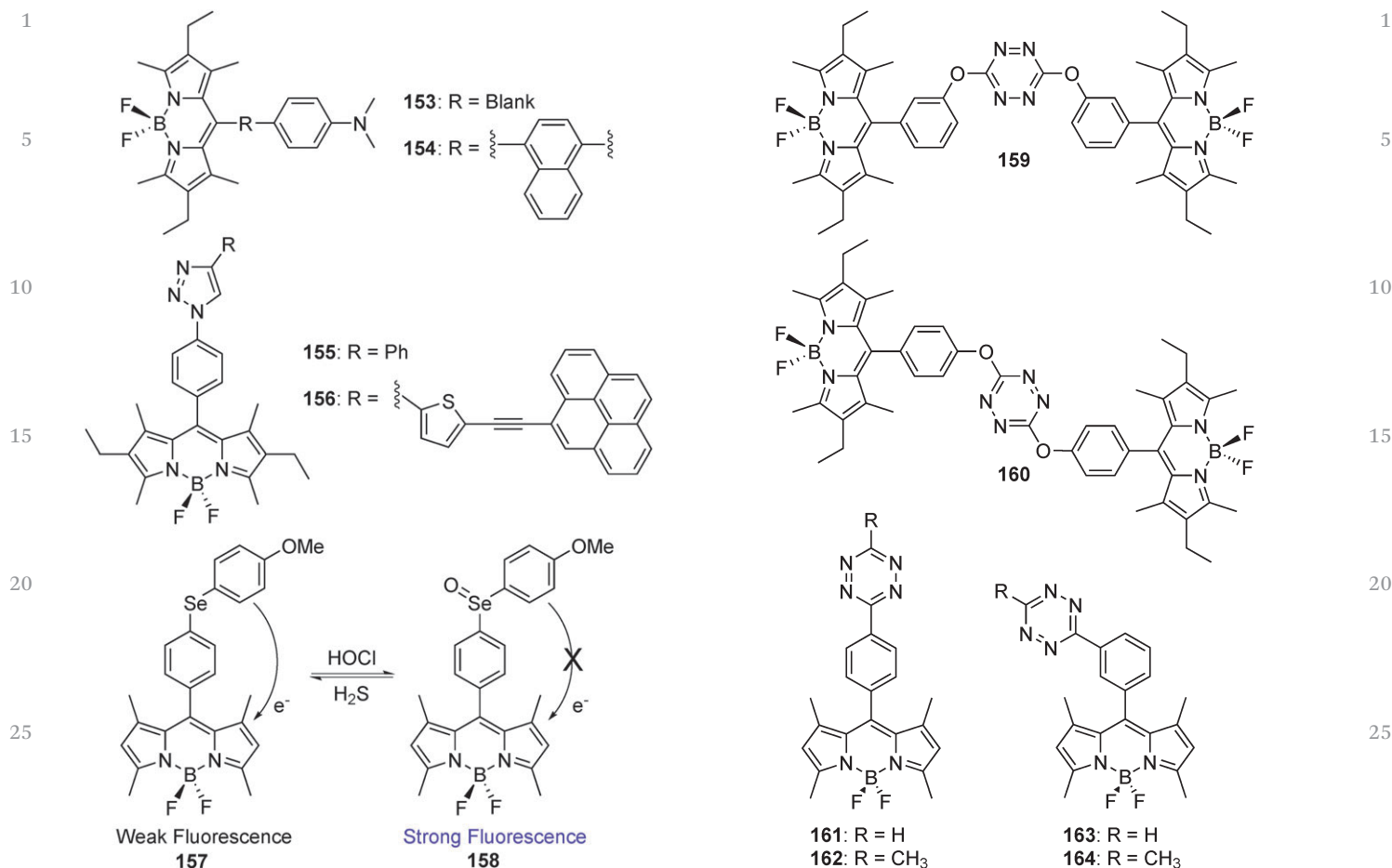


Fig. 44 BODIPY-based molecular dyads bearing a naphthalene, triazole or selenium bridge.^{130–132}

closely held together (159 and 160; Fig. 45).¹³⁵ BODIPY and tetrazine fluorophores were connected through a phenyl spacer and the resulting derivatives were characterized by photophysical and electrochemical means. Furthermore, DFT calculations and spectroelectrochemistry experiments demonstrated that photoinduced electron transfer and ET remain possible when the tetrazine moiety is reduced electrochemically, which shuts OFF the BODIPY unit's fluorescence. Interestingly, the group of Weissleder recently took advantage of the tetrazine moiety as an acceptor group that can quench the emission of the BODIPY in the differently positioned dyads 161–166 (Fig. 45).¹³⁶ Upon reaction with a double bond, the conjugation of the tetrazine moiety is broken and BODIPY's emission is turned back on with an enhancement of up to 1600-fold (164), making such derivatives very interesting for superbright bioorthogonal turn-on probes.

Thilagar looked at the dual-emission properties of borane-BODIPY dyads 167 and 168, which differ mainly by their molecular conformations (Fig. 46).¹³⁷ In addition to the dual emissive behavior, they observed intramolecular charge transfer between boryl and BODIPY chromophores along with a difference in emission enhancement and quenching upon fluoride binding. This discrepancy was further investigated by

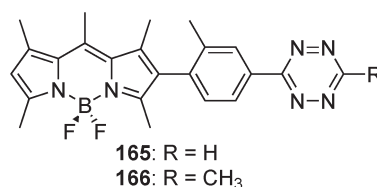


Fig. 45 BODIPY-tetrazine multichromophoric derivatives.^{135,136}

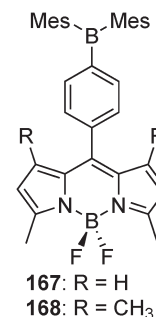


Fig. 46 Borane-BODIPY dyads.¹³⁷

structural and computational methods in order to better understand the effect of molecular conformations accessible.

Bard and collaborators recently studied BODIPYs in the context of electrogenerated chemiluminescence (ECL) in a

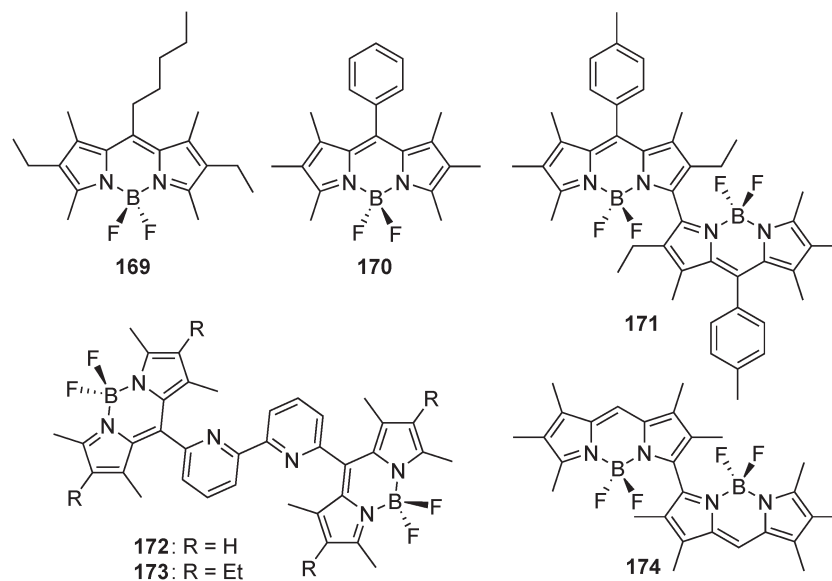


Fig. 47 BODIPYs for ECL.^{138,139,141}

series of papers. In the first one, *n*-pentyl-, phenyl- and a dyad of BODIPY derivatives were synthesized and their electro- and photochemical properties were studied (169–171; Fig. 47).¹³⁸

The second one appended BODIPY units by a 2,2'-bipyridine linker (172 and 173, Fig. 47).¹³⁹ These 2,2'-derivatives may be used as building blocks for further incorporation in LH or photocatalysis systems. Molecular electronics is also reported as a potential application for such dyads. In fact, Nepomnyashchii *et al.* recently prepared devices with interdigitated array electrodes to produce ECL with a BODIPY derivative.¹⁴⁰ A third paper from Bard *et al.* focused on the preparation of BODIPY dimers (*e.g.* 174; Fig. 47) by chemical or electrochemical oxidation and their monitoring by the ECL technique.¹⁴¹ Hong also reported an interesting example of selective anion sensing of pyrophosphate by means of ECL using a BODIPY-based derivative.¹⁴² Finally, a review on this specific ECL subject was published lately by Bard.¹⁴³

In the context of creating molecular polyads with donor-acceptor functionalities for directed ET, the group of Haley reported a systematic study of six structural isomers incorporating dibutylamine as donor moieties and BODIPY acceptors on a tetrakis(arylethynyl)benzene (TAEB) core (175–180; Fig. 48).¹⁴⁴ To evaluate the effectiveness of the donor group, all-acceptor derivatives based on either the TAEB core (181), the tetrakis(arylethynyl)-1,4-pyrazine (TAEP) core (182) or bis(arylethynyl)benzene (BAEB) core (183 and 184) were also synthesized using the same cross-coupling strategy (Fig. 49). Photophysical studies were made and corroborated with computational methods. The study revealed an assortment of intriguing optical properties that can be fine-tuned through small isomeric and structural variations. Comparison of D-A compounds with the all-acceptor related 181 to 184 proved the importance of strong donor moieties in molecular systems for efficient charge transfer pathways. BODIPY acceptors were also found to have a remarkable impact on the overall phenylacetylene scaffold, quenching any form of solvatochromism that is most

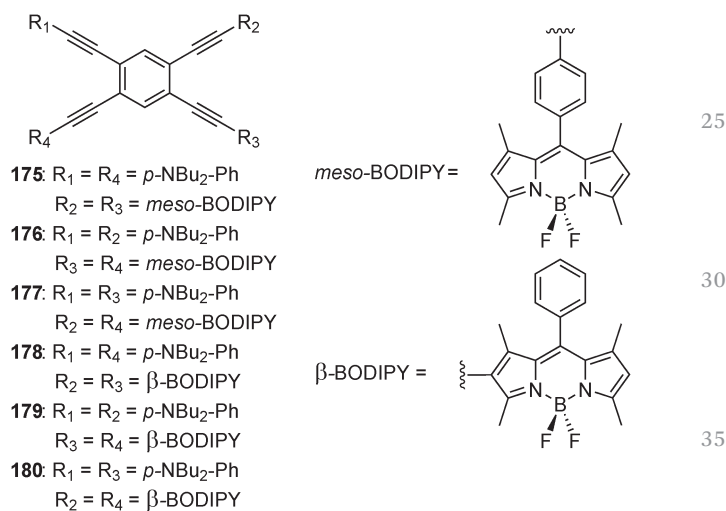


Fig. 48 Incorporation of BODIPY fluorophores on tetrakis(arylethynyl)-benzenes.¹⁴⁴

often found in these systems. Finally, despite the tendency to quench in polar solvents, the BODIPY unit was able in some instances to enhance the quantum yields to levels not yet seen with previously known TAEB molecules.

Donor-acceptor molecular dyads based on BODIPY modified 9-cycloheptatrienylidene fluorene derivatives were used by Wang and collaborators for detecting Cu^{II} cations.¹⁴⁵ Two fluorescent chemosensors 185 and 186 were designed taking advantage of the 9-cycloheptatrienylidene as the Cu^{II} receptor and BODIPY based fluorophores (Fig. 50). Both of them present high selectivity toward this specific cation and high selectivity with acidity independence. In addition, the authors report a turn-on fluorescent behavior, which should be more practical in the design of fluorescent chemosensors for detection of Cu^{II} anions.

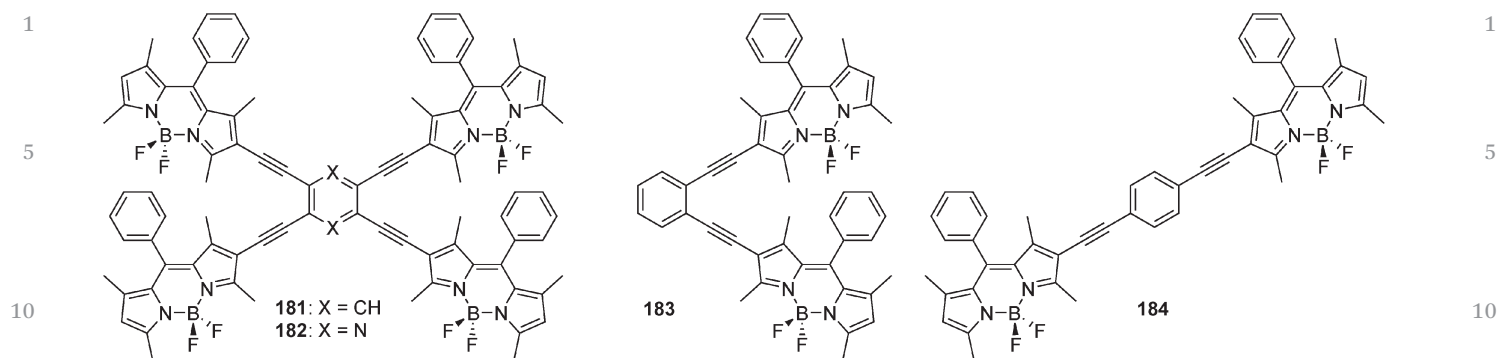


Fig. 49 All-acceptor TAEB, TAEP and BAEB derivatives incorporating BODIPYs.¹⁴⁴

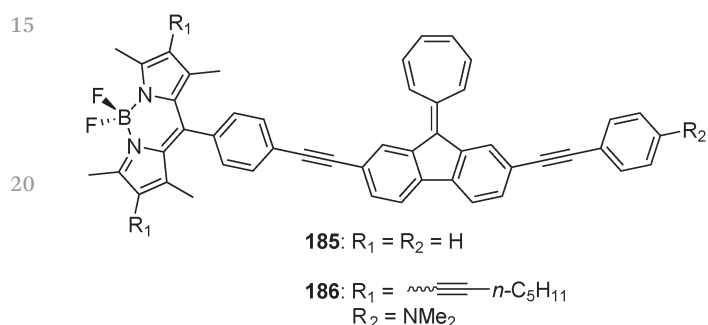


Fig. 50 Donor-acceptor molecular dyads based on BODIPY modified 9-cycloheptatrienyliene fluorene derivatives.¹⁴⁵

Bichromophoric energy-transfer cassettes based on a BODIPY donor linked *via* Sonogashira cross-coupling to cyanine acceptors were reported by Burgess (**187–173**; Fig. 51).¹⁴⁶ Upon excitation of the BODIPY moiety at 488 nm, the excitation energy was transferred through an acetylene bridge to various cyanines with emission tunable from about 600 up to 800 nm as the length of the oligomeric polyene increased. A through-bond ET was proved to occur in **187** and **188** cassettes due to measured rates 2 orders of magnitude faster than that reported for the classical through-space Förster type ET. However, assessment of a specific ET mechanism for **189** was not possible from rate measurements. The water solubility of the lipophilic fluorescent-imaging probes was further enhanced by encapsulation in calcium phosphate/silicate nanoparticles (*ca.* 22 nm). Only minor changes in the photophysical properties of encapsulated cassettes were noted and labeling of organelles with a model nanosystem containing **187** was accomplished by permeation in clone 9 rat liver cells.

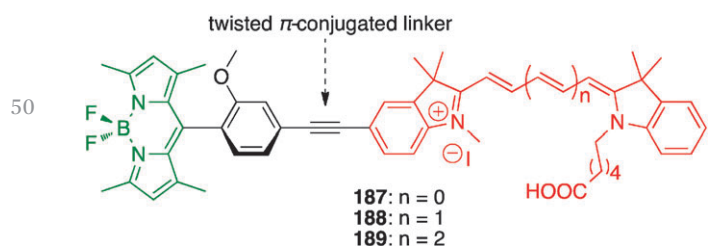


Fig. 51 Bichromophoric cassettes bearing a BODIPY donor with various cyanine acceptors.¹⁴⁶

Also using a cross-coupling strategy, Zissel *et al.* reported the synthesis and length dependence for intramolecular energy transfer in three- and four-color D-spacer-A arrays.¹⁴⁷ Interestingly, the molecular triads used the boron center of one π -extended BODIPY, acting as the A, to connect two conventional BODIPY donor moieties through their *meso*-position (**190–193**; Fig. 52). The spacer (S) units were based on oligomers of 1,4-phenylene-diethynylene repeating units, allowing for variation of the distance between D and A units from 18 to 38 Å. The same strategy was further used to incorporate pyrenes on the terminal BODIPYs (**194**; Fig. 52). The photophysical

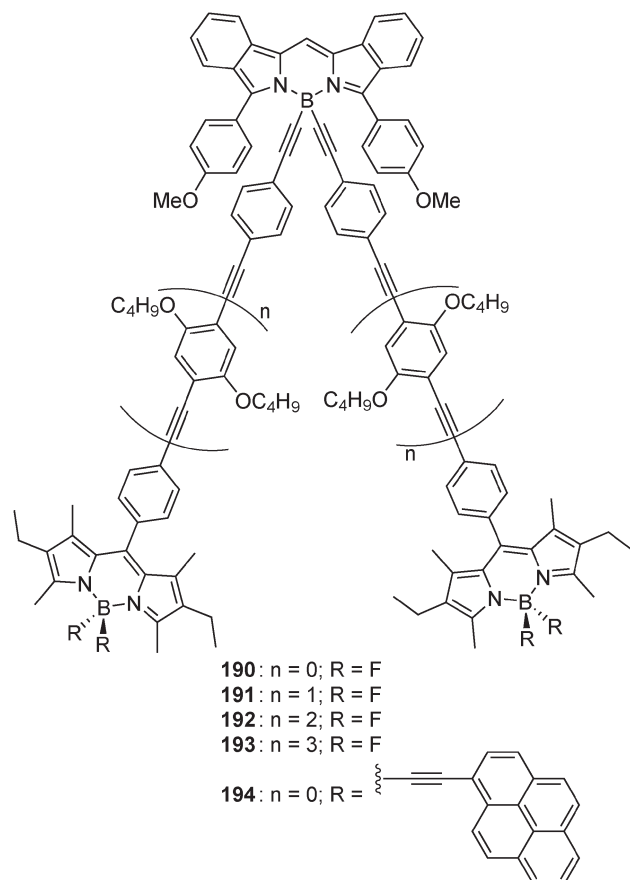


Fig. 52 BODIPY molecular triads based on D-spacer-A architecture.¹⁴⁷

1 studies of the series revealed a highly efficient electronic energy
 2 transfer (EET) through conjugated bonds occurring from the
 3 first-excited singlet state of the conventional BODIPYs toward
 4 the extended-one with a nonlinear evolution of the rate constant
 5 upon variation of separation distance. With only a 4-fold
 6 decrease in the rate constant, the length dependence appeared
 7 to be a consequence of the energy gap between D and S units
 8 becoming smaller as the molecular length increased. Remarkably,
 9 a simple relationship based on the effective conjugation
 10 length exists between the measured electronic resistance of the
 11 spacer unit and the Huang-Rhys factor determined by emission
 12 spectroscopy. Also, excitation of the spacer alone led to a fast
 13 EET to both D and A units followed by a slow second EET from
 14 the D to the A. When pyrenes are involved in the system, fast
 15 EET occurs toward the conventional BODIPYs from the pyrenes
 16 followed by a slow long-range EET to the opposite terminal. The
 17 authors suggested that they are highly attractive materials for
 18 solar concentrators when incorporated in transparent plastic
 19 media used under conditions where both inter- and intra-
 20 molecular EETs occur.

21 In collaboration with Ziessel's group, Harriman and cow-
 22 orkers further studied systems incorporating pyrene- and
 23 perylene-substituted BODIPYs (**195** and **196**; Fig. 53) to resolve
 24 the contribution of intramolecular EET in closely coupled
 25 molecular dyads.¹⁴⁸ The study was achieved in pressurized
 26 methyltetrahydrofuran solution and showed that illumination
 27 into the aryl polycycles leads to rapid intramolecular EET to
 28 BODIPY but also that fluorescence from these units is partially
 29 restored under high pressure. The argument made was that the
 30 applied pressure restricts torsional motions around the link-
 31 ages and imposes a near orthogonal geometry for transition

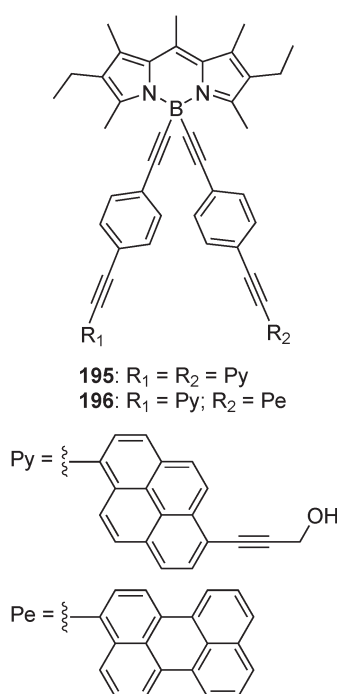


Fig. 53 Pyrene- and perylene-substituted molecular cassettes.^{147,148}

dipole moment vectors on the reactants. In turn, this pressure-
 induced conformational restriction switches off Förster-type
 EET within the system (contributions of *ca.* 5% for pyrene
 and *ca.* 25% for perylene), leaving the main contribution to
 the Dexter through-bond electron-exchange EET. Anthracene-
 BODIPY dyads fused by conjugated phenylacetylenyl bridges at
 the *meso* position were also reported by Nierth *et al.* in 2010.¹⁴⁹
 Finally, Ziessel and Harriman recently published the prepara-
 tion of an artificial LH array comprising 21 discrete chromo-
 phores strongly inspired by a combination of the various
 BODIPY and pyrene dyes previously discussed (*i.e.* **190** and
194).¹⁵⁰ The convergent synthetic approach led to a molecular-
 scale funnel having an effective chromophore concentration of
 0.6 M condensed into *ca.* 55 nm³ that can direct the excitation
 energy to a focal point. Interestingly, the energy obtained from
 photoexcitation can also travel in the opposite direction, there-
 fore becoming spread around the array before being trapped by
 the acceptor. The authors undertook preliminary tests for the
 incorporation of their new LH cassette as a sensitizer for
 amorphous silicon solar cells and promising results were
 obtained.

21 The collaboration of Ziessel and Harriman groups presented
 22 an interesting study on spirofluorene-bridged BODIPY dyads
 23 (**197–201**; Fig. 54).¹⁵¹ They used various combinations of the D
 24 and A BODIPYs attached to the spirofluorene spacer to explore
 25 the limits of Förster theory at a separation of 20 Å. This was
 26 achieved by comparing the agreement between computed and
 27 measured coulombic matrix elements and the net result was

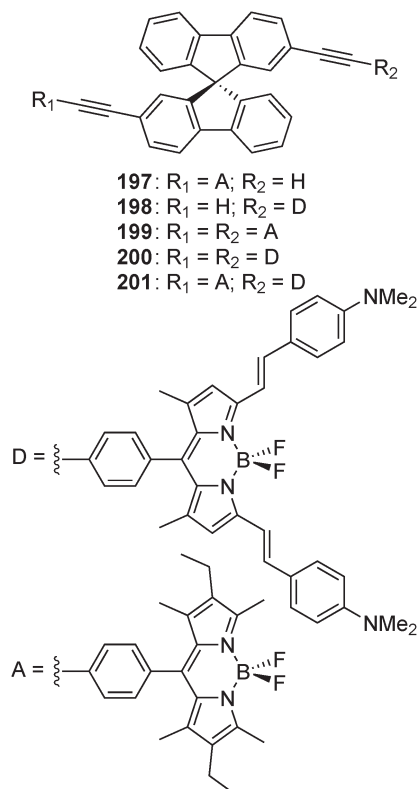


Fig. 54 Spirofluorene-bridged BODIPY dyads.^{151,152}

1 that Förster theory remains applicable to these closely spaced,
 intramolecular systems. The solvent polarity effects on the rate
 of Förster-type energy transfer were studied in a subsequent
 paper published one year later using the **199**, **200** and **201**
 5 adducts previously reported.¹⁵² The group of Caprasecca *et al.*
 further studied by quantum mechanics the solvent-dependence
 of EET rates observed for dyad **201**.¹⁵³

More recently, Ziessel and Harriman groups studied the
 nanomechanical properties of molecular-scale bridges as visual-
 10 ized by intramolecular EET.¹⁵⁴ In that paper, a series of linear
 molecular dyads of the type D–S–A (**202–206**; Fig. 55) were
 prepared where the donor is a BODIPY, the spacer is built by
 accretion of ethynylene–carborane units and the acceptor is
 based on a dipyrrolopyrrole (DPP). The authors found out that
 15 the probability of one-way EET between terminals depends on
 the length of the spacer and also on temperature and applied
 pressure. Based on their results for the given system, the
 dynamics of EET can be used to estimate the strain energy
 associated with molecular contraction, the amount of work
 20 done in effecting the structural change and the Young's mod-
 ulus for the bridge. In a subsequent paper, the authors further
 investigated the effect of the spatial configuration (linear *vs.*
bent) between a similar BODIPY donor and a DPP acceptor on
 through-space EET (**207** and **208**, Fig. 55).¹⁵⁵ To mention, other
 25 examples of highly fluorescent BODIPY-based nanocars incor-
 porating carborane and adamantane groups as wheels were
 reported by the group of Tour.^{156,157}

The group of Ziessel also prepared four other families of
 small D–A dyads using a BODIPY moiety. A first paper

combined the 2-(2'-hydroxy phenyl)benzoxazole (HBO) frag-
 1 ment to the BODIPY through an amide linker (**209**,
 Fig. 56).¹⁵⁸ Photophysical studies were performed on this dyad
 and evidence of energy transfer from the HBO moiety toward
 the BODIPY was revealed. The authors also observed the
 5 absorption spectrum to be a linear combination of the two
 subunits, a situation favored by their orthogonal conformation.
 A second paper combined an electro-attractor BODIPY deriva-
 tive with either julolidine (**210**) or triazatruxene (**211**) donor
 moieties (Fig. 56).¹⁵⁹ In those push–pull derivatives, there is a
 10 low-energy charge-transfer state observable by both absorption
 and emission spectroscopy. Charge-recombination fluores-
 cence was found to be weak and decayed over a few picoseconds
 to the ground state. Electrochemistry and DFT calculations
 were also used to support photophysical studies. Finally, a
 15 third paper showed that photoinduced electron transfer is also
 possible from the BODIPY subunit toward a methyl-4,4'-
 bipyridinium (methylviologen) acceptor (**212** and **213**,
 Fig. 56).¹⁶⁰ This observation was supported by photophysical
 studies, including transient absorption technique, and electro-
 20 chemistry. However, the dyes were not able to generate any
 catalytic amounts of hydrogen under standard conditions, a
 behavior expected *a priori* due to the presence of
 methylviologen.

Ziessel's group joined forces with Harriman and Nierengar-
 25 ten to prepare and study a sophisticated artificial light-
 harvesting model built on hexa-adduct C₆₀ fullerenes decorated
 with two types of BODIPY derivatives, namely a yellow absorber
 (Y) and a blue absorber (B), introduced by a click-chemistry

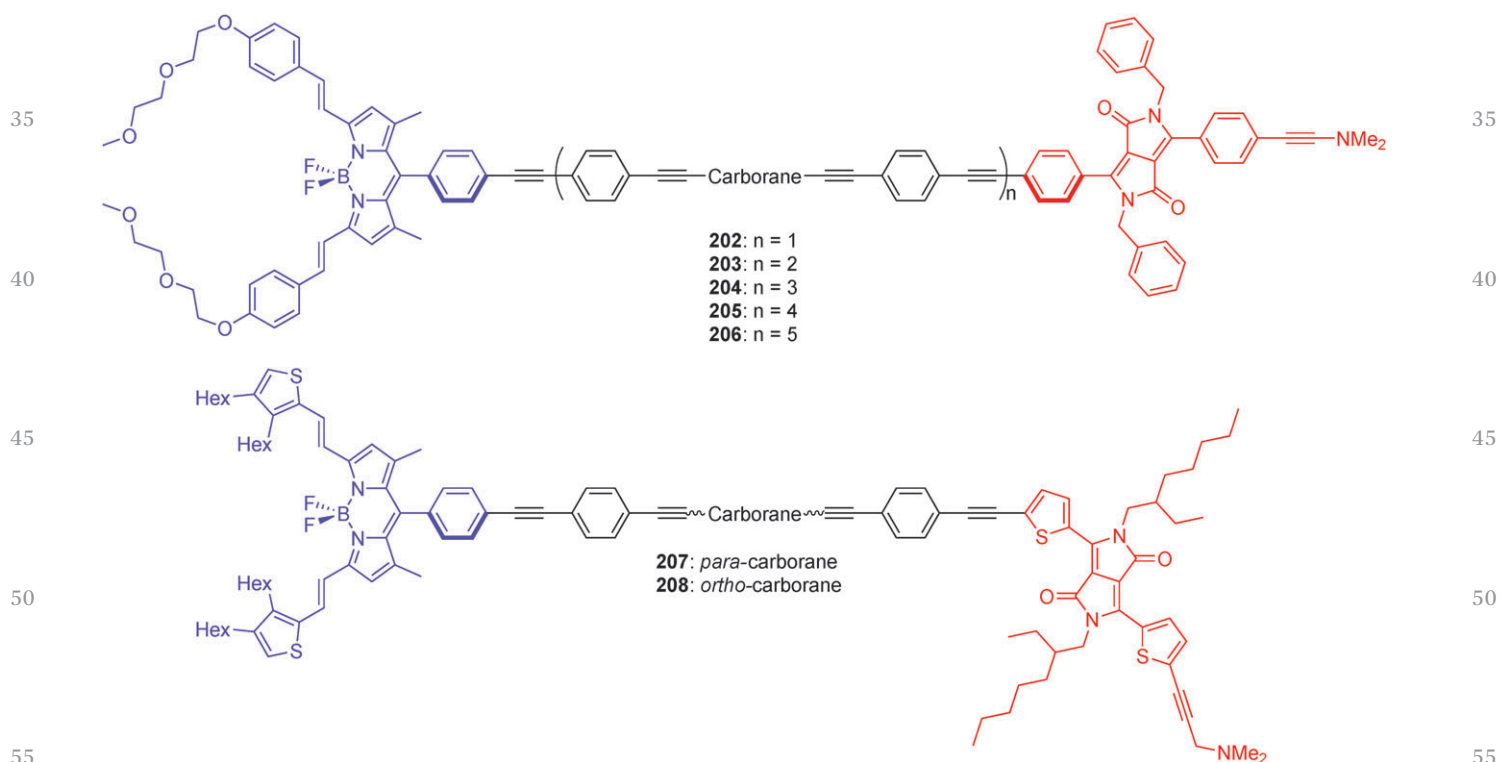


Fig. 55 Molecular dyads based on a BODIPY donor that uses ethynylene–carborane units to separate the DPP acceptor.^{154,155}

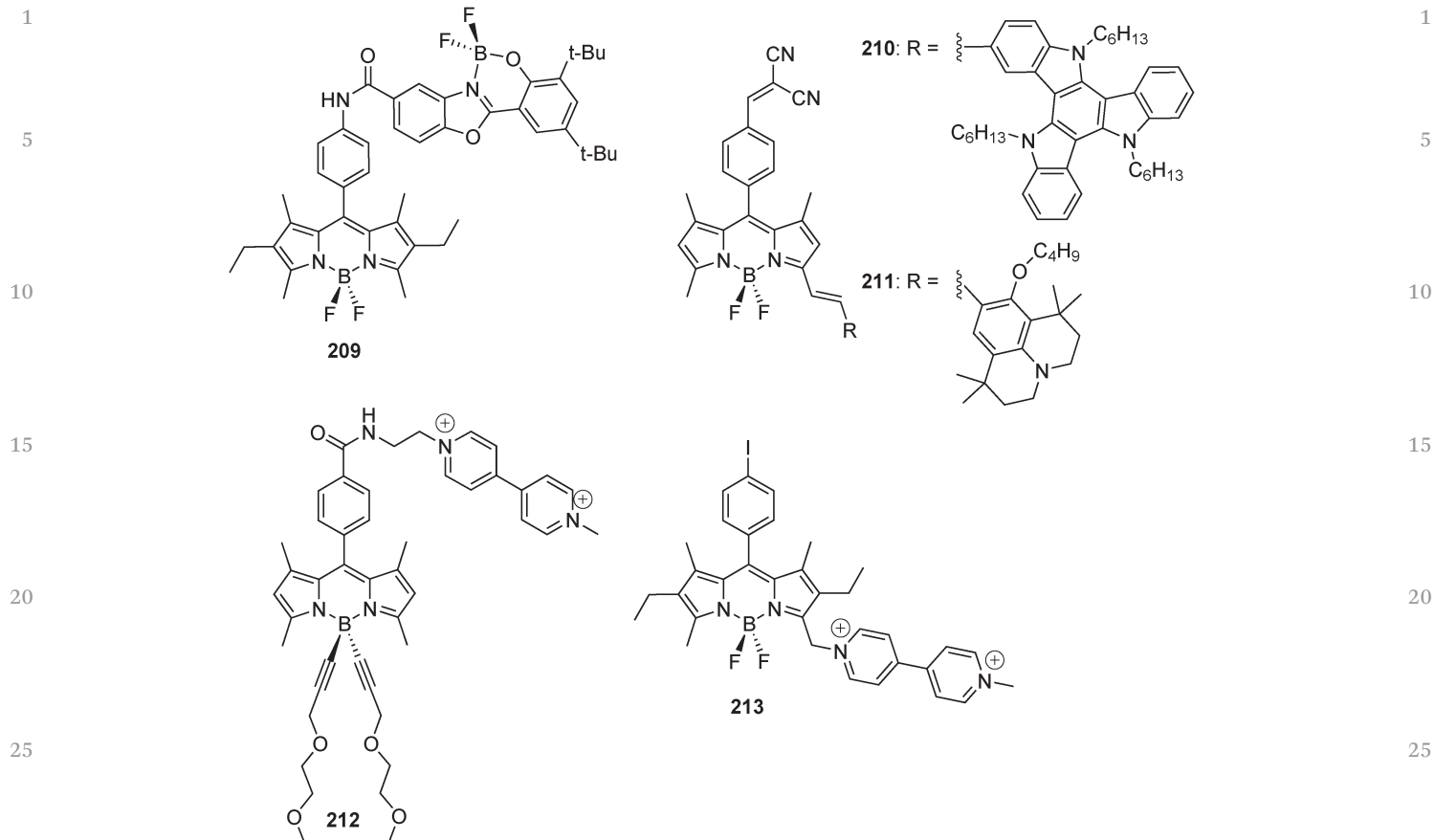


Fig. 56 BODIPY dyads incorporating HBO, julolidine, triazatruxene or methylviologen.^{158–160}

approach (**214** and **215**; Fig. 57).¹⁶¹ The BODIPY derivatives retained their individuality in the system and assisted the solubility of the fullerene. Fascinatingly, the fullerene spheres did not act as electron acceptors under photo-excitation. Instead, an electronic energetic migration pathway is favored in solution between appended yellow light-absorbing BODIPYS (Y) toward the energetically low-lying stilbene-derived BODIPYS (B), which can emit around 660 nm. When spheres **214** containing only yellow BODIPYS are mixed in high concentration with spheres **215** containing also trapping blue dyes to form a polymeric thin film by spin coating from solution, intersphere long-range energy transfer occurs between Y dyes until they are trapped by B dyes. Such a phenomenon is a bio-mimic of natural LH in photosynthesis, although a much lower efficiency is reported. The authors also reported the preparation of a luminescent solar concentrator based on **215** able to sensitize amorphous silicon photocells with a PCE of *ca.* 5%.

Another system incorporating C₆₀ as the electron acceptor in BODIPY-based dyads has been studied lately by Zhao and collaborators (**216–219**; Fig. 58).¹⁶² They prepared two different dyads incorporating a BODIPY chromophore attached by the π -core *via* an ethynyl linker to one (**217**) or two (**219**) carbazole subunits, one of which was bearing the C₆₀. For comparison purpose, related light-harvesting antennas **216** and **218** were also prepared. The new dyads reported show strong absorption

of visible light with long-lived excited states as organic triplet photosensitizers for triplet–triplet annihilation (TTA) upconversion (quantum yields up to 2.9%). In a very similar fashion, the group also reported visible light-harvesting triphenylamine ethynyl C₆₀–BODIPY dyads **221** and **223** (Fig. 58) for the same type of application along with their corresponding LH antennas **220** and **222**.¹⁶³ In fact, this group was the first to report in 2010 a library of organic triplet sensitizers based on a single BODIPY chromophore (**224–227**; Fig. 59) with long-lived triplet excited states for TTA upconversion.¹⁶⁴ This type of photosensitizers usually rely on phosphorescent transition metal complexes, showing poor tuning of UV/Vis absorption properties and T₁ excited state energy levels. Their intrinsic problems were overcome by the use of BODIPY dyes. More recently, they also prepared BODIPYS conjugated to 2-(2-hydroxyphenyl) benzothiazole/benzoxazoles (**228–231**; Fig. 59) and reported their application as organic triplet photosensitizers for photooxidation of 1,5-dihydroxynaphthalene.¹⁶⁵ Recently, the group prepared new triplet photosensitizers taking advantage of the resonance energy transfer to enhance their visible light absorption (**232–234**, Fig. 59).¹⁶⁶ Photophysical studies were used to prove that the intramolecular energy acceptor (iodo-BODIPY moiety) and the donor (BODIPY moiety) had different and complementary absorption bands in the visible that explained this overall enhanced behavior. Time-resolved transient

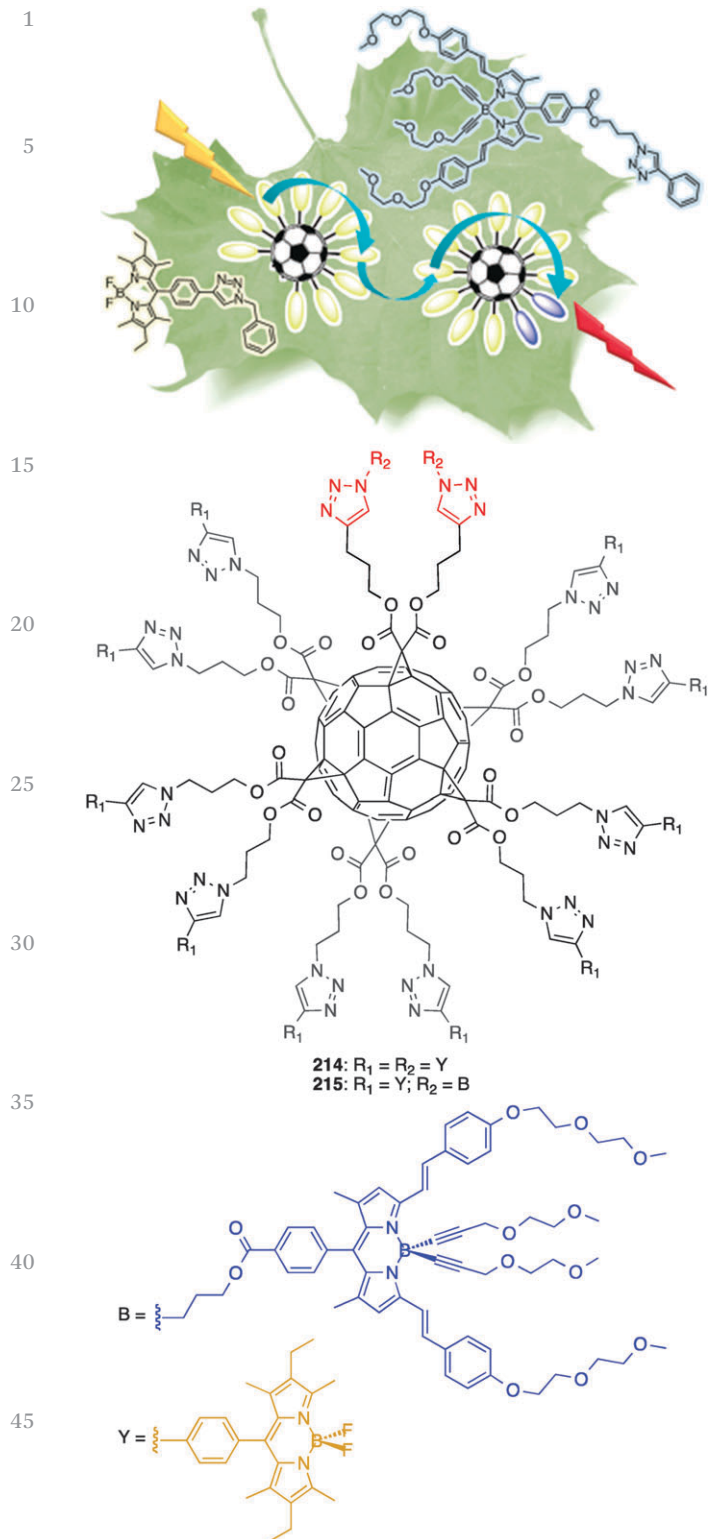


Fig. 57 Artificial light-harvesting arrays based on BODIPYs and fullerene derivatives.¹⁶¹ (Adapted with permission from *J. Am. Chem. Soc.*, 2012, **134**(2), 988–998. Copyright© 2011 American Chemical Society.)

absorption spectroscopy has also confirmed the triplet excited states to be distributed on both D and A moieties, which is the result of bidirectional energy transfer in the dyads and a rare

example for organic molecular arrays. Again, their application as organic triplet photosensitizers for photooxidation of 1,5-dihydroxynaphthalene and as triplet–triplet upconverters was studied. The authors also saw potential for the integration of their various types of organic triplet sensitizers in photovoltaic applications.

Zhao further used BODIPY for triplet-sensitizer applications by integrating the chromophore into a $N^{\wedge}C^{\wedge}N$ Pt^{II} -acetylide complex (235; Fig. 60).¹⁶⁷ The result was room temperature long-lived NIR phosphorescence from the BODIPY part, maximized by the heavy-atom effect of Pt^{II} cores connected to the chromophore by π -conjugation. A complex that displays such strong absorption of visible light and long-lived triplet intra-ligand state (3IL) is suitable for upconversion, photocatalysis and photovoltaic applications.

Other Pt^{II} complexes incorporating BODIPY chromophores were previously reported by Eisenberg and coworkers (236–239; Fig. 60).¹⁶⁸ The potential for light-harvesting of Pt^{II} (diimine)-(dithiolate) complexes, which are poorly absorbing in the visible but present long-lived charge-transfer excited states applicable in photocurrent generation or H_2 production, was greatly improved by the presence of the highly absorbing BODIPY core. Photo-physical, electrochemical and TD-DFT studies were presented in order to gauge the different energetic migration mechanisms within the dyads. More recently, Mirkin *et al.* prepared a new class of hemilabile ligands with BODIPYs that can signal changes in the coordination mode through changes in fluorescence when complexed to Pt^{II} (240–242, Fig. 60).¹⁶⁹

The idea of forcing DPM dyes to stand as close as possible to each other as discussed previously in this section was further advanced by Dolphin *et al.*, who prepared triple stranded organometallic complexes using bis(DPM) ligands.¹⁷⁰ Co^{III} , Ga^{III} and In^{III} cations were used to template those helicate and mesocate assemblies. X-Ray crystal structures of Co^{III} (243) and Ga^{III} derivatives were obtained and that of the former is presented in Fig. 61 (*meso*-phenyl and hydrogens were omitted for clarity). UV/Vis characterization showed extinction coefficient values reaching up to about $250\,000\ M^{-1}\ cm^{-1}$. With the many possibilities for fine-tuning the absorption of DPM derivatives, the authors pointed out the potential for the triple-stranded complexes to serve as self-assembled functional chromophores. Maeda *et al.* also prepared covalently strapped double helices of bis(DPM)– Zn^{II} complexes presenting two double helical modes (244–247; Fig. 61).¹⁷¹ This last behavior was assessed through UV/Vis, circular dichroism and 1H NMR spectra examinations and was further supported by modelization studies. The existence of the two modes of the double helix has been proven to be dependent on the dihedral angles between two of the dipyrromethene units at the pyrrole α – α bond. In fact, the changes of the modes were observed according to the temperature as well as the length of the straps. In a similar fashion, homoleptic complexes of Cu bearing various DPM ligands were prepared by both Servaty *et al.* (248 and 249; Fig. 62) and Qu *et al.* (250 and 251), in the latter case for application as fluorescent turn-on probes for H_2S detection in living cells.^{172,173}

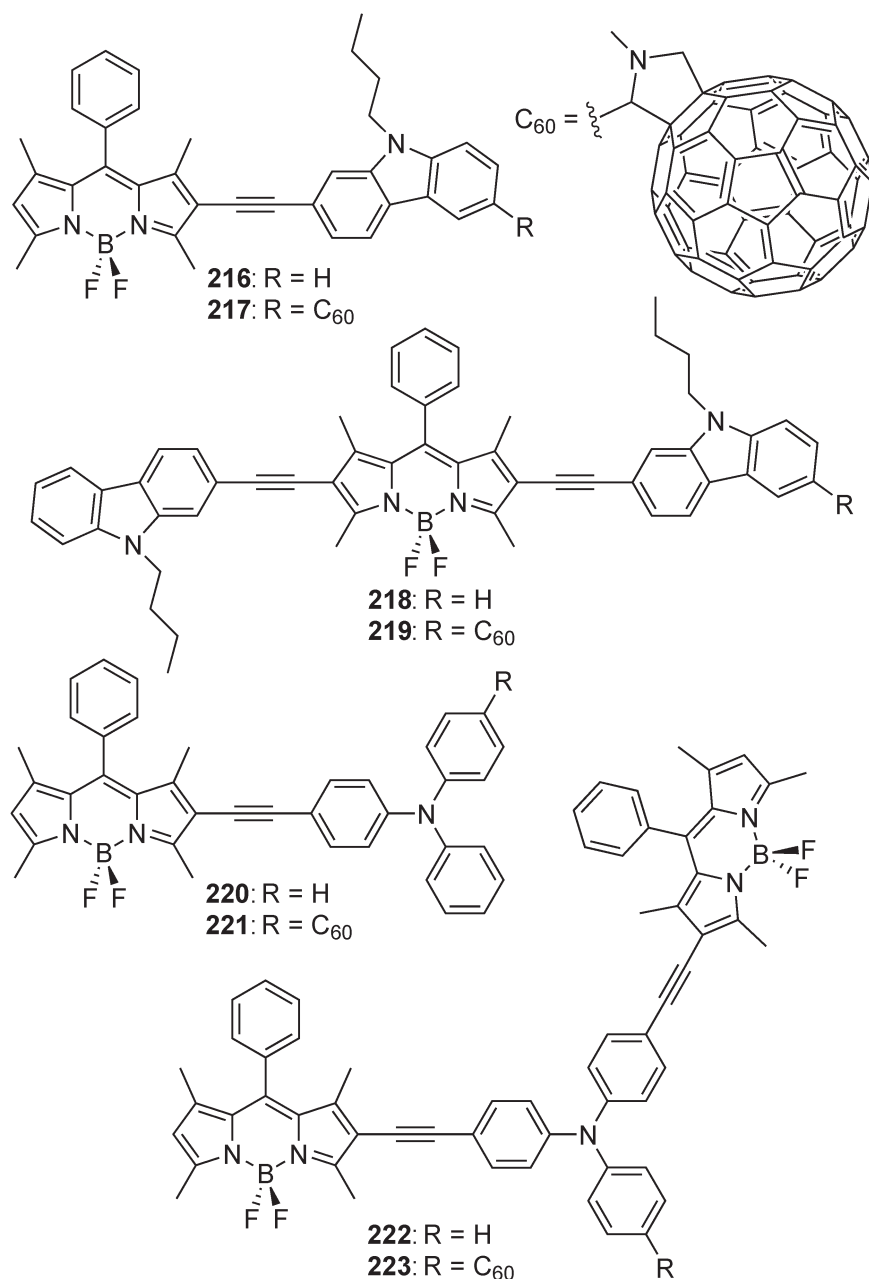


Fig. 58 C₆₀-BODIPY dyads for triplet-triplet annihilation upconversion and their related light-harvesting antennae.^{162,163}

The report in 2011 by Nozaki of new tetravalent metal complexes **256–259** based on DPM derivative **252** (Fig. 63) inspired the group of Thomas to prepare anionic Co^{II} and Ni^{II} analogues (**260⁻** and **261⁻**, respectively; Fig. 63).^{174,175} The former group prepared titanium, zirconium, germanium and tin complexes **256–259** for their use as a new class of catalysts in copolymerization of epoxides with carbon dioxide. The latter group looked at the ligand-centered redox behavior of **260⁻** and **261⁻** complexes. In fact, the one-electron (radical) and two-electron oxidized forms of these complexes were structurally characterized by X-ray diffraction and their electronic structure was confirmed by spectroscopy and DFT calculations. On their side, Neumann *et al.* reported use of trianionic DPM derivatives

253–255 for coordination with either a boron or a Mn^{III} chelate (**262–264** and **265–267**, respectively; Fig. 63).¹⁷⁶ They further proved the use of Mn^{III} complexes **265–267** as peroxytrite scavengers *via* a two-electron oxidation mechanism, thereby forming the corresponding Mn^V-O species. In addition, X-ray structures of **266** and its boron derivative **263** were obtained.

Another paper discussing the synthesis of DPM based organometallic complexes was reported by the group of Betley.¹⁷⁷ They prepared three-coordinate Co^{III} imido complexes **269–272** bearing a sterically crowded DPM ligand from the Co^I synthon **268** (Fig. 64). The Co^{III} complexes reported exhibit either spin crossover or C–H bond activation properties. In fact, Co-imido complex **269**, which is paramagnetic at room temperature,

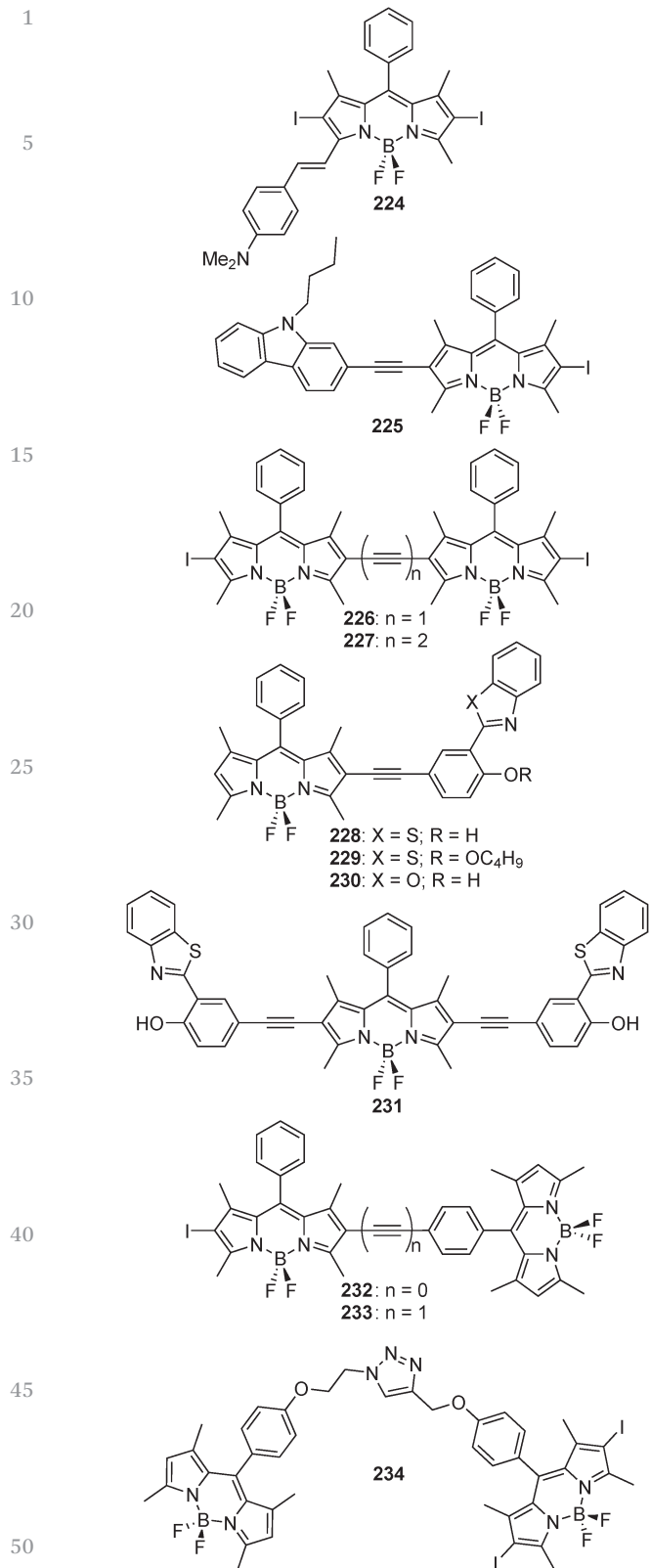


Fig. 59 A selection of organic triplet sensitizers based on BODIPY chromophores.^{164–166}

undergoes a thermally induced spin crossover from an $S = 0$ ground state to a quintet ($S = 2$) state as proved by variable

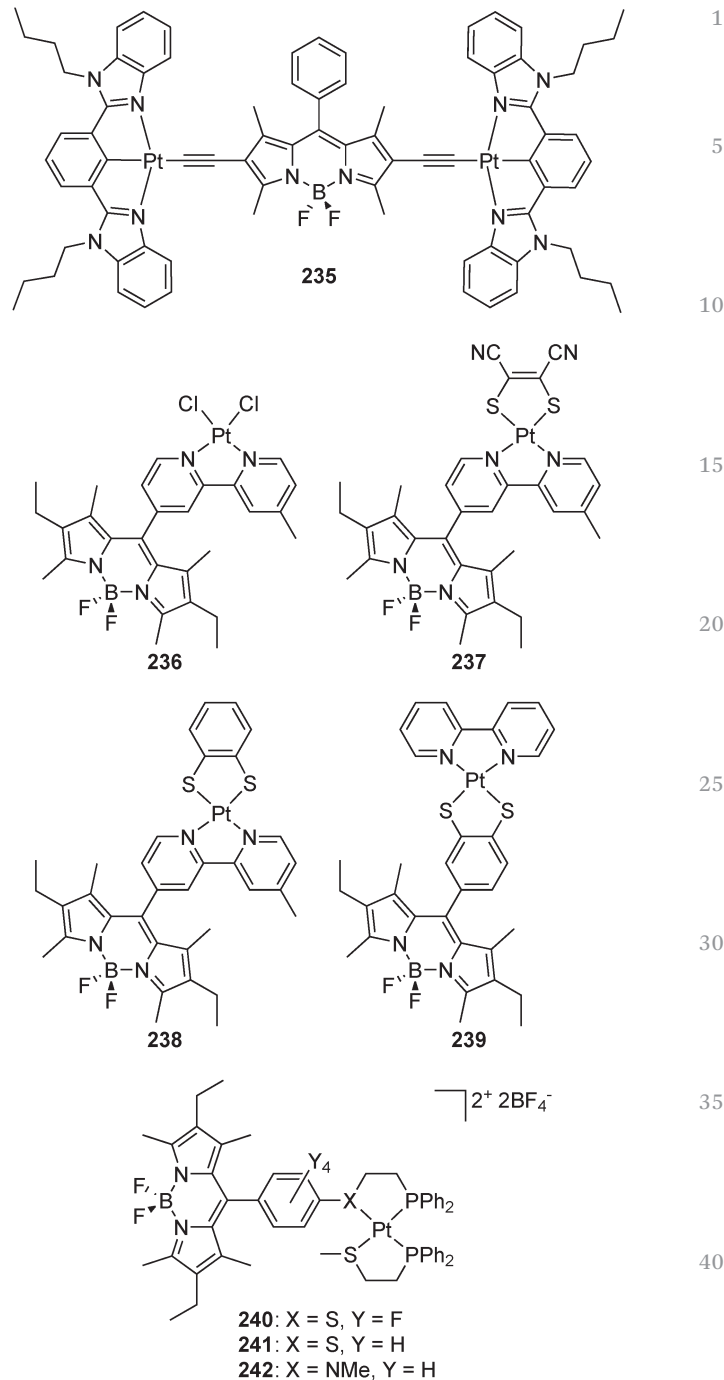


Fig. 60 Pt(II) complexes incorporating BODIPY chromophores.^{167–169}

temperature ^1H NMR spectroscopy, crystallography and magnetic susceptibility measurements. Complex **270** ($S = 1$) obtained from the reaction of **268** with mesityl azide can further be converted into the metallacycloindoline complexes **271** or **272** via benzylic C–H activation.

Examples of heteroleptic Rh^{III} and Ir^{III} complexes bearing DPM/ η^5 -pentamethylcyclopentadienyl (Cp*) with the general formula [(Cp*)MCl(DPM)] were prepared by the group of Pandey (273–277; Fig. 65).¹⁷⁸ Their reactivity with various species (e.g. NaN₃, NH₄SCN, PPh₃, bpy and dppe) was examined. The

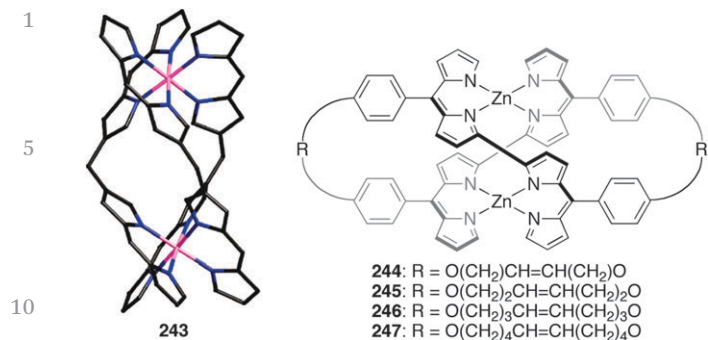


Fig. 61 DPM helical structures: X-ray structures of Co^{III} triple-stranded bis(DPM) complexes (*meso*-Ph and H omitted for clarity; left) (adapted with permission from *Inorg. Chem.*, 2010, **49**(24), 11550–11555. Copyright © 2010 American Chemical Society.); bis(DPM)–Zn^{II} complexes presenting two double helical modes (right).^{170,171}

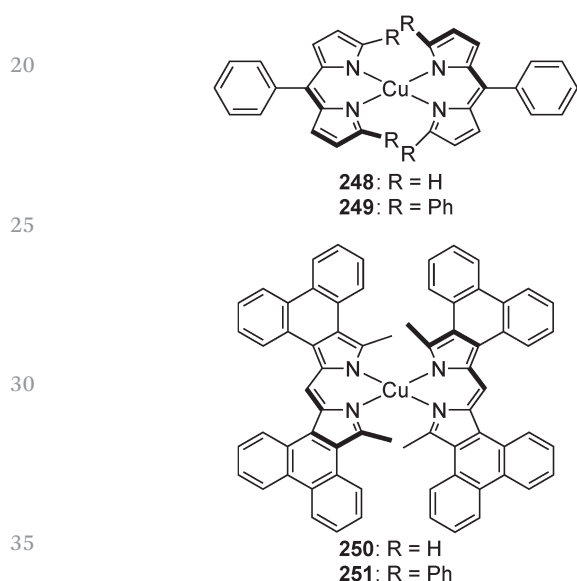


Fig. 62 Homoleptic Cu complexes with DPM derivatives.^{172,173}

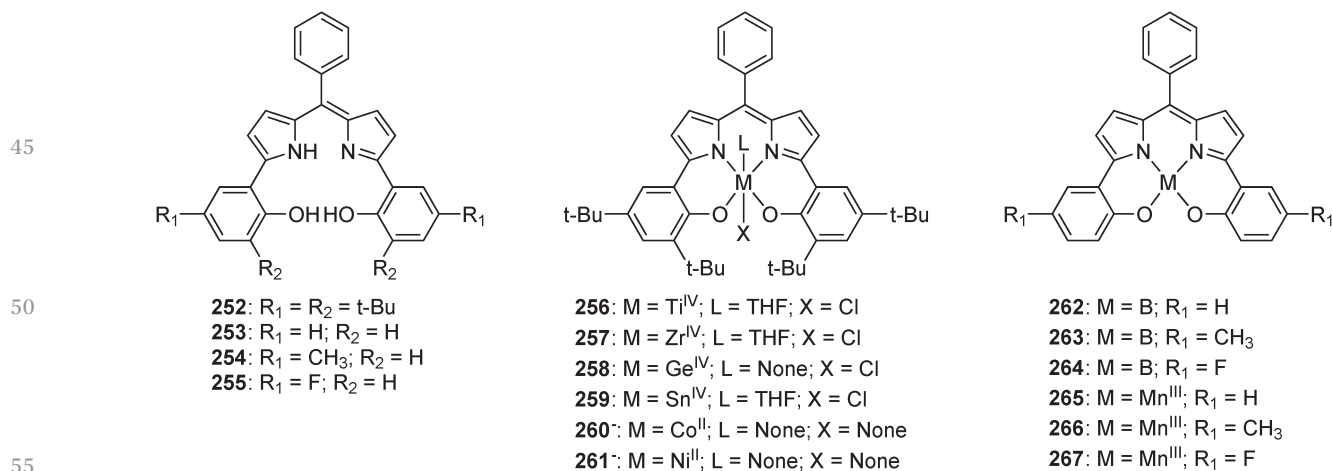


Fig. 63 Metal complexes based on trianionic DPM derivatives.^{174–176}

resulting complexes were characterized by elemental analyses, photophysics and electrochemistry. They further studied their catalytic activity for the reduction of terephthalaldehyde to 4-hydroxymethylbenzaldehyde in the presence of HCOOH/CH₃COONa in water under aerobic conditions. In a very similar fashion, they also prepared heteroleptic arene Ru^{II} complexes of general formula $[(\eta^6\text{-arene})\text{MCl}(\text{DPM})]$ based on *meso*-substituted DPM ligands (278–282; Fig. 65).¹⁷⁹

The group of Telfer reported the synthesis of a variety of luminescent Re^I–DPM complexes with the general formulas $\text{fac}[\text{Re}(\text{DPM})(\text{CO})_3\text{Cl}]^-$, $\text{fac}[\text{Re}(\text{DPM})(\text{CO})_3\text{PR}_3]$ and $\text{fac}[\text{Re}(\text{DPM})(\text{CO})_2\text{PR}_3\text{PR}'_3]$, where DPM is a *meso*-aryl dipyrromethene derivative (283–296; Fig. 65).¹⁸⁰ Structural characterization was achieved through X-ray crystallography in the solid phase and ¹H NMR in solution. Photophysical studies were also made, showing no emission for $\text{fac}[\text{Re}(\text{DPM})(\text{CO})_2\text{PR}_3\text{PR}'_3]$ derivatives and only weak emission for the $\text{fac}[\text{Re}(\text{DPM})(\text{CO})_3\text{Cl}]^-$ and $\text{fac}[\text{Re}(\text{DPM})(\text{CO})_3\text{PR}_3]$ ones. On the basis of the large Stokes shift, the authors ascribed the emission to phosphorescence from a triplet-excited state. They also reported in 2010 the synthesis, characterization and TiO₂ binding studies of a series of chromophoric complexes of 5-(4-carboxyphenyl)-4,6-DPM (297–303; Fig. 65).¹⁸¹ The synthesis of $[\text{Ru}(\text{bpy})(\text{DPM})_2]$, $[\text{Rh}(\text{DPM})_3]$ and $[\text{Pd}(\text{DPM})_2]$ was achieved by initial coordination of the methoxycarbonyl derivative of the DPM with the corresponding metallic center (299, 301 and 303, respectively) followed by hydrolysis of the ester group to give 298, 300 and 302, respectively. The authors reported interest for the use of such DPM complexes in DSSC, which suggests that they should be tested for OPV applications as well.

Wang and collaborators prepared the BODIPY-modified Ru^{II} arene complex 304 that can undergo ligand dissociation *via* a mechanism involving visible light (Fig. 66).¹⁸² Their design is based on a monodentate pyridine *meso*-substituted BODIPY ligand that effectively dissociates upon photoexcitation of the BODIPY chromophoric unit ($\lambda = >500$ nm; photoinduced ligand quantum yield of 4.1% at 480 nm). The authors showed that a

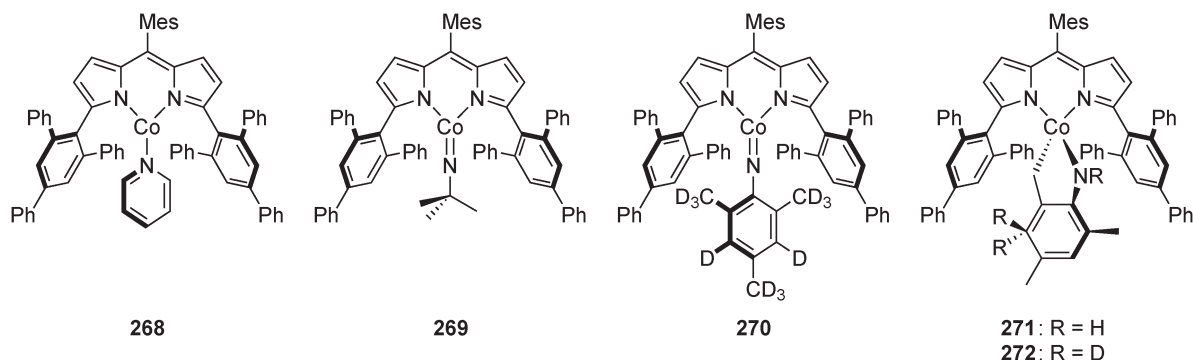


Fig. 64 Co^{III} imido complexes obtained from a Co^I synthon.¹⁷⁷

photoinduced electron transfer from this chromophoric unit toward the Ru^{II} arene moiety plays an important role. They further exploited this dissociation strategy to replace the pyridine-BODIPY ligand by the DNA base 9-ethylguanine (**305**; Fig. 66), a proof of concept for the photoactivated red-shift of anticancer metallodrugs' absorption within the phototherapeutic window.

The group of Zhao observed the room temperature phosphorescence of BODIPY in visible LH Ru^{II} polyimine complexes **306** and **307** (Fig. 67) and further tested them as triplet photosensitizers for triplet-triplet annihilation upconversion and photocatalytic oxidation.¹⁸³ Both compounds showed strong absorption in the visible region ($\epsilon = 65\,200\text{ M}^{-1}\text{ cm}^{-1}$ at 528 nm for **306** and $\epsilon = 76\,700\text{ M}^{-1}\text{ cm}^{-1}$ at 499 nm for **307**). Compound **306** exhibited phosphorescence of the BODIPY moiety, as well as the residual fluorescence of the BODIPY ligand. In comparison, **307** showed only the residual fluorescence of the BODIPY ligand. A long-lived BODIPY-localized triplet excited state was observed in both compounds upon photoexcitation in the visible region. Triplet-triplet annihilation studies revealed that the direct connection of the π -core of the BODIPY chromophore to the metal coordination center, as in **306**, is essential to enhance the effective visible LH of the ruthenium complexes.

The group of Ziesel also explored the idea of incorporating metals in their molecular dyads. In 2010, they published in collaboration with the group of Castellano the synthesis, structural characterization, electrochemistry and molecular photophysics of an Ir^{III}-based complex, [Ir(ppy)₂(bpy-ethynyl-BODIPY)](PF₆) (**308**; Fig. 68).¹⁸⁴ Compound **308** revealed a BODIPY-based phosphorescence that was assessed by comparison with appropriate model chromophores and proved to be due to the large spin-orbit coupling afforded by the Ir^{III} center. Preparation of hybrid organic-inorganic multichromophoric arrays arranged on a truxene-based platform was also reported by the group.¹⁸⁵ The synthesis, photophysical characterization and ET features of a series of hybrid truxene derivatives peripherally decorated with inorganic osmium-containing polypyridine and organic BODIPY dyes were reported (**309–311**; Fig. 68). The design allowed the photoactive terminal units to be coupled to the central truxene scaffold *via* rigid ethynyl linkers in a star-shaped arrangement. The results showed that the absorption range widely covers the UV/Vis spectrum and

that Os³MLCT and BODIPY triplet act as the final collectors of the absorbed energy. The authors noted the potential for the construction of arrays where the population of either organic or inorganic triplet levels can be indirectly and properly controlled by simple substitution at the BODIPY units.

Pistolis and coworkers reported an organic-inorganic hybrid system inspired from the LH photosystem II.¹⁸⁶ They used an efficient supramolecular synthesis driven by coordination self-assembly to prepare a robust multichromophoric D-A hexagonal wheel consisting of six BODIPY dyes in the corners arranged perpendicular to the circular plane made of Pt^{II} complexes with 4,4'-bpy spacers (see Fig. 69 for schematic 3D representation [BODIPY in green; Pt in pink]). Interestingly, photophysical studies revealed that such an assembly is completely fluorescent. Their one-step assembly of a solar-energy concentrator at $\sim 520\text{ nm}$ appears promising and closely resembles the natural supramolecular strategy. The authors therefore believed that such materials could open new horizons in the construction of sunlight concentrators that will boost solar energy research and emerging photonics.

2.2.2 DPM-ADPM and DPM-porphyrinoid polyads. As mentioned previously, DPM and ADPM are related to porphyrinoids, therefore making their combination very interesting in the context of light-harvesting systems to reach suitable and complementary photophysical properties. Many exciting polyads have been recently reported following this idea and demonstrate the powerful nature of such a combination for vectorial energy- and electron-transfer.

First looking at DPM-ADPM polyads, we note that the group of Nishihara and coworkers, inspired by their synthesis of the first Zn^{II} heteroleptic DPM-based complexes **312** and **313**, prepared the fluorescent heteroleptic ADPM-DPM hybrid Zn^{II} complex **314** (Fig. 70).^{187,188} This compound was obtained by means of a stepwise coordination method and led to a fluorescence maximum at 672 nm in toluene with a shoulder near 750 nm. The authors used DFT calculations from the X-ray crystal structure to prove that fluorescence exclusively originated from the ADPM ligand by thermal equilibrium among the two non-emissive charge-separated (CS) states and the favored ¹ π - π^* emissive excited state. They concluded that such fluorescence behavior opens the door for photochemical applications of ADPM metal complexes.

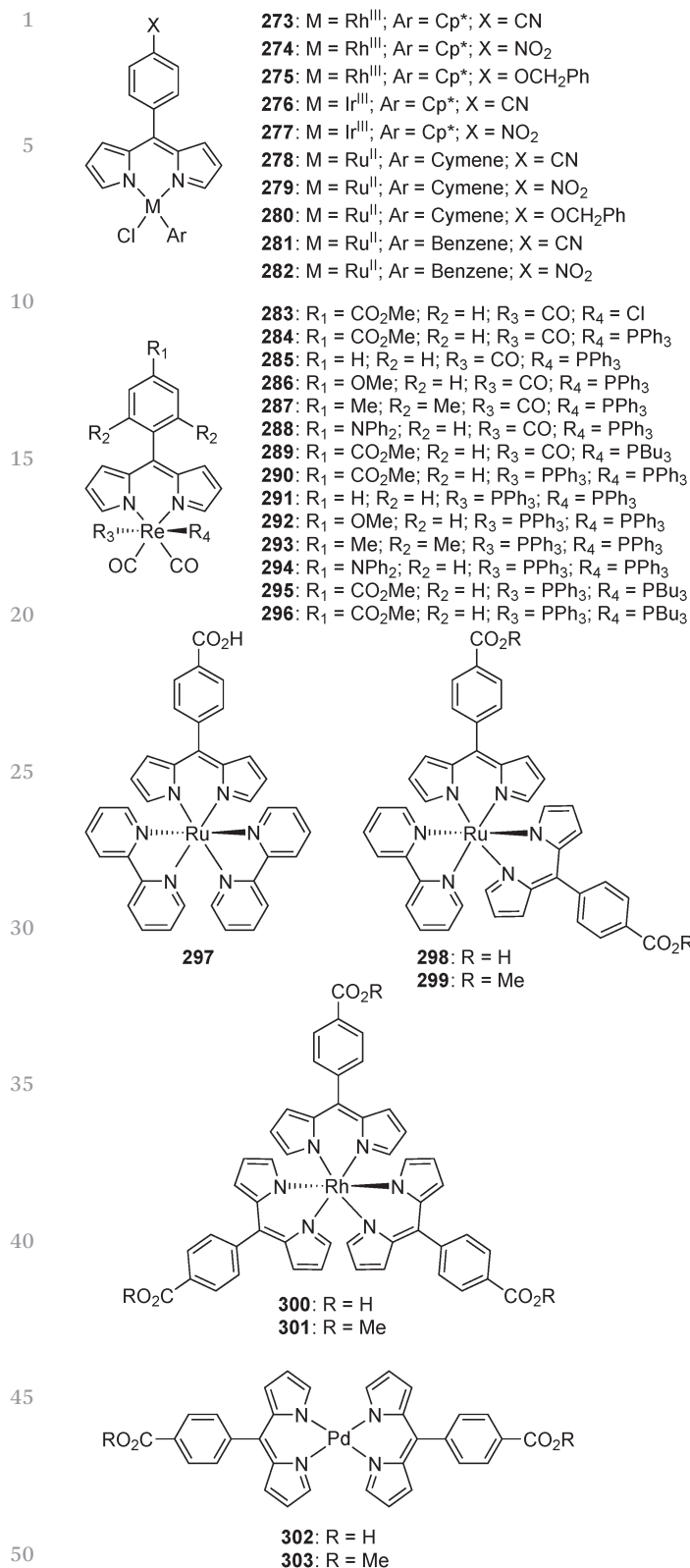


Fig. 65 Complexes coordinating *meso*-substituted DPM derivatives.^{178–181}

The group of D'Souza also reported in 2012 other examples of molecular dyads and triads implying both BODIPY and aza-BODIPY covalently connected together (315 and 316,

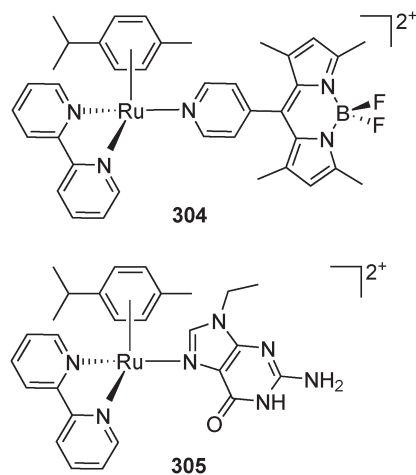


Fig. 66 Photo-dissociative BODIPY-modified Ru^{II} arene complex and its corresponding product of replacement by the DNA base 9-ethylguanine.¹⁸²

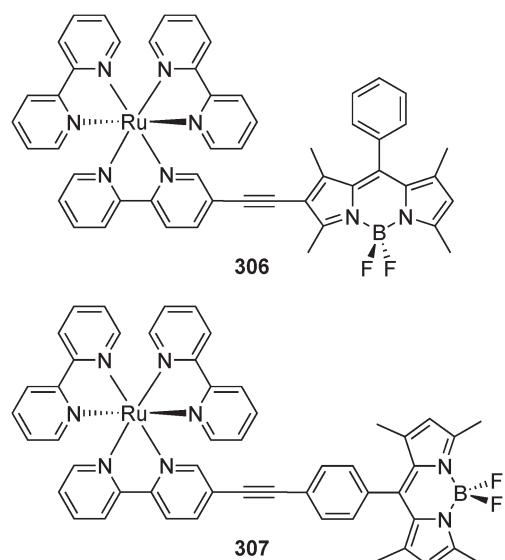


Fig. 67 BODIPY–Ru^{II} polyimine complexes for triplet–triplet annihilation upconversion and photocatalytic oxidation.¹⁸³

respectively; Fig. 71).¹⁸⁹ In these two systems, the aza-BODIPY acted as the acceptor, which was proved using computational, spectroscopic, photodynamic and electrochemical measurements. Actually, the kinetics of electron transfer *via* ¹aza-BODIPY*, as measured by monitoring the decay of the singlet aza-BODIPY at 820 nm, revealed a relatively fast charge-separation process from the BODIPY to ¹aza-BODIPY*. Lately, they further integrated a Zn porphyrin (ZnP) in their system, leading to an aza-BODIPY–BODIPY–ZnP triad 317 (Fig. 71).¹⁹⁰ Their photophysical studies revealed that the aza-BODIPY still acts as the acceptor for the whole system. In fact, both the BODIPY and the ZnP moieties transfer energy toward the aza-BODIPY, while the ZnP is also capable of electron transfer. Altogether, the new supramolecular triad combines the absorption and emission of the three subunits, making it a suitable

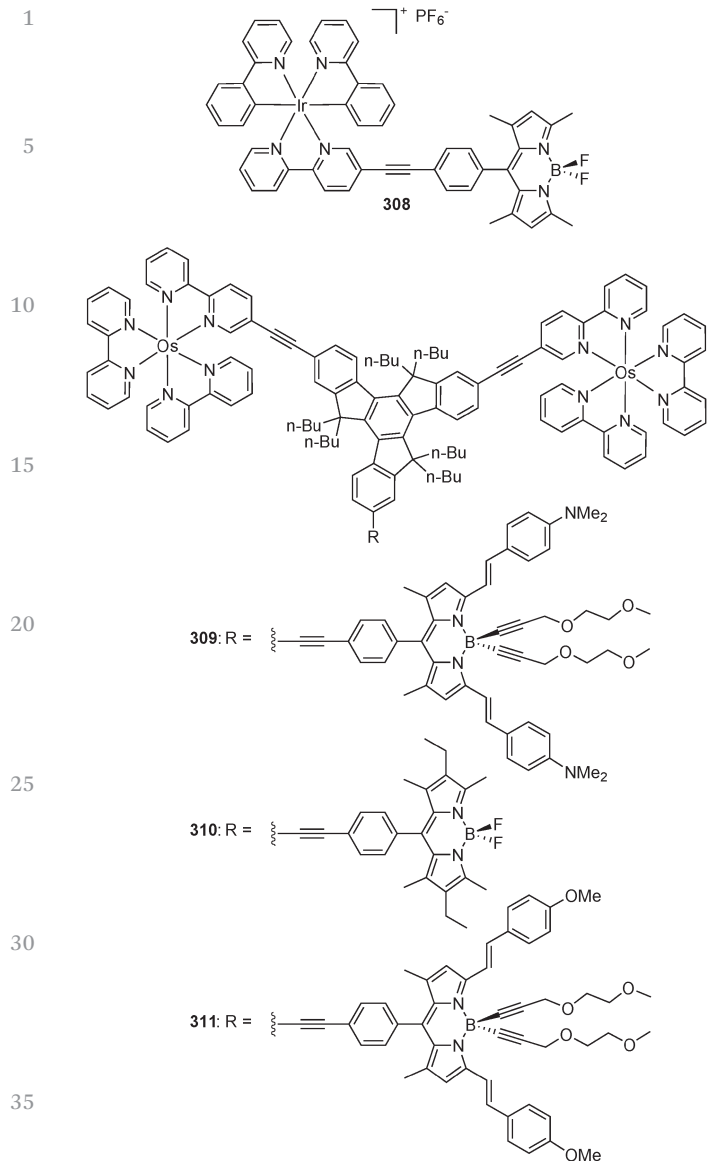


Fig. 68 Hybrid organic–inorganic multichromophoric arrays incorporating BODIPY and iridium or osmium complexes connected by ethynyl linkages.^{184,185}

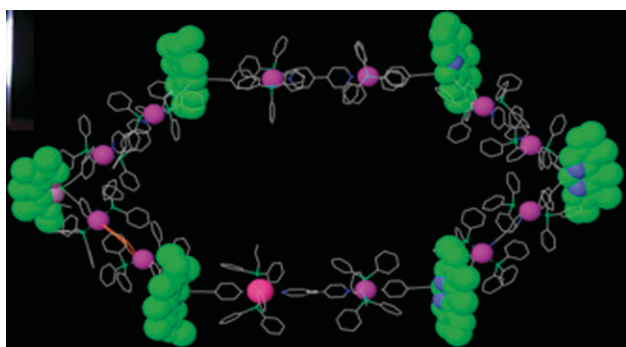


Fig. 69 Schematic 3D representation of a circular light-harvesting BODIPY-dye based array obtained through supramolecular assembly.¹⁸⁶ (Reproduced from ref. 186 with permission from The Royal Society of Chemistry.)

candidate for solar energy harvesting and developing optoelectronic devices.

On their side, the group of Ng prepared a photosynthetic antenna-reaction center mimic with a covalently linked monostyryl BODIPY–aza-BODIPY–C₆₀ triad **318** (Fig. 71).¹⁹¹ The aza-BODIPY was connected to the monostyryl BODIPY through a click reaction and to the fullerene C₆₀ using the Prato reaction. Intramolecular photoinduced energy- and electron-transfer processes were studied by steady-state and time-resolved absorption and fluorescence spectroscopy, in comparison to the corresponding BODIPY–aza-BODIPY and aza-BODIPY–C₆₀ dyads. Fast energy transfer from the BODIPY toward the aza-BODIPY (at a rate of $\sim 10^{11}$ s⁻¹), with subsequent electron transfer to the fullerene acceptor, was observed. They further looked at the electrochemistry of the triad to assess the origin of the electron transfer. The results indicated that a transfer from the singlet excited ¹aza-BODIPY* to the C₆₀, yielding the aza-BODIPY^{•+}–C₆₀^{•+} species, is energetically favorable. Upon photoexcitation, the lifetime of the resulting BODIPY–aza-BODIPY^{•+}–C₆₀^{•+} species was established at 1.47 ns. Finally, nanosecond transient absorption measurements revealed that the charge-separated state slowly decays to populate the triplet state of aza-BODIPY before returning to the ground state.

Now looking strictly at BODIPY–porphyrinoid polyads, a nice example of a multichromophoric array was reported by Thompson *et al.* based on four BODIPYs bound to a platinum^{II} benzoporphyrin (**319**; Fig. 72).¹⁹² This polyad exhibits intense panchromatic absorption due to the complementarity of BODIPY and porphyrin units. Fast bidirectional singlet and triplet ET processes are described, along with a resulting long-lived NIR-phosphorescence behavior. Overall, the paper reports a core–shell antenna system that efficiently captures a broad solar spectrum and shows quantitative ET from the antennae to the core but at the same time spreads the excited state energy over both the core and shell chromophores. This is of strong interest for OPV applications due to the inherent strict limitation of film thickness allowed for efficient exciton diffusion and carrier conduction.

Khan and Ravikanth recently reported a series of studies in which they linked BODIPY units to porphyrinoids by various methods to produce multichromophoric systems. They first developed a synthetic methodology based on the 3-bromo BODIPY key precursor **320** to yield covalently linked chromophore conjugates by cross-couplings (**321–327**; Fig. 73).¹⁹³ In addition to the porphyrinoid-based derivatives, it is noteworthy that a terpyridine compound has been prepared. Further coordination on a metallic center such as ruthenium is therefore conceivable.^{20,194,195} An anthracene-based dyad is also to be mentioned. Electrochemical characterization is reported, along with spectral studies showing a stronger interaction in ethynyl-bridged BODIPY–chromophore compared to ethynylphenyl-bridged one.

In the second paper of the series, Ravikanth *et al.* prepared covalently linked trichromophoric systems based on BODIPY–porphyrinoid conjugates with three different chromophores (**328–331**; Fig. 74).¹⁹⁶ The brominated α -positions of the

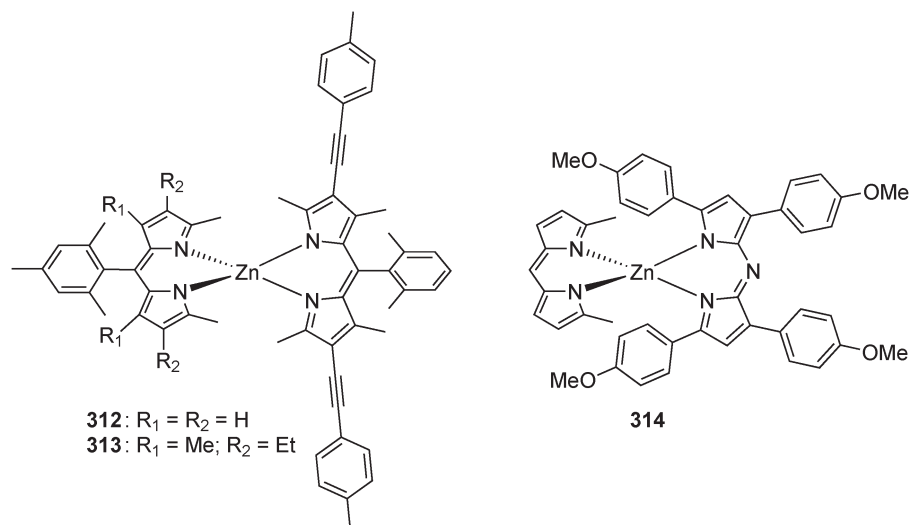


Fig. 70 Heteroleptic DPM and ADPM–DPM hybrid Zn^{II} complexes.^{187,188}

BODIPY were again exploited for convenient connection by a nucleophilic aromatic substitution strategy with porphyrinoids bearing an alcohol group. Good solubility in common organic solvents was reported, which is an interesting point for porphyrinoid derivatives. Absorption and electrochemical studies supported weak ground-state interactions between the three chromophoric units, while fluorescence studies indicated significant quenching of the BODIPY emission due to the transfer of energy to one or both macrocyclic units attached to it.

The third and final paper from Khan and Ravikanth relies on non-covalent coordination of BODIPYs to Zn^{II} and Ru^{II} metalloporphyrins for self-assembly of various dyads and triads (332–335 and 336–339, respectively; Fig. 75).¹⁹⁷ The coordination is ensured by oxypyridine-substituted BODIPYs in the α -positions, again arising from a nucleophilic aromatic substitution strategy. An X-ray structure obtained for BODIPY– Zn^{II} porphyrin dyad 333 revealed an oblique coordination with an angle between the porphyrin and the pyridyl ring of 70° . The absorption studies of the stable Ru^{II} –porphyrin conjugates exhibited overlapping absorption features of both chromophoric components, while fluorescence studies again presented a quenching behavior of the BODIPY emission on coordination with the $Ru(TPP)CO$ unit. Electrochemistry revealed the characteristics of both BODIPY and metalloporphyrin units in dyads and triads.

The group of Ng recently prepared a BODIPY–phthalocyanine pentad also using a non-covalent coordination strategy (340, Fig. 75).¹⁹⁸ The Si^{IV} phthalocyanine with two axial *p*-phenylene-linked BODIPY and monostyryl BODIPY (MSBDP) moieties absorbs strongly in the most part of the UV-vis region (up to 700 nm) and acts as an interesting artificial photosynthetic antenna-reaction centre model. The authors observed from the photophysical studies an energy transfer upon photoexcitation from the BODIPY to the MSBDP, followed by an electron transfer toward the phthalocyanine core. This work

was a follow-up of their photophysical study of the BODIPY–MSBDP dyad alone.¹⁹⁹

Harvey *et al.* recently prepared another system where the BODIPY chromophore was used to bridge two porphyrins.²⁰⁰ In that case, a strategy of derivatization at the boron center was used to prepare metal-free and Zn^{II} metalated *B,B*-diporphyrinbenzyloxy-BODIPY derivatives (341 and 342, respectively; Fig. 76). Singlet ET from BODIPY to the porphyrin units was analyzed and revealed an antenna effect due to the good spectral overlap between D fluorescence and A absorption that led to a notable quenching of the BODIPY fluorescence. However, the authors noted that further improvement in the system could be made by a gain in the appropriate relative orientation of the transition moments between the donor and the acceptor.

A panchromatic trichromophoric system using antenna effect was also reported by Odobel for incorporation as a sensitizer in DSSC (343; Fig. 77).²⁰¹ Such a trichromophoric system was used for the first time for DSSC application and the overall conversion efficiency was enhanced by 25%. Covalently linked BODIPY, Zn^{II} porphyrin and squaraine units have been synthesized by Heck alkylation and present an efficient intramolecular ET between all the chromophoric units. The antenna effect was assessed by the photoaction spectrum, which features all of a chromophore's absorption bands.

Coutsoulelos and colleagues recently presented a straightforward synthesis of BODIPY–porphyrin dyads connected *via* a cyanuric chloride bridge.²⁰² Their photophysical and electrochemical investigations led to a promisingly fast ET system (344; Fig. 78). In fact, the comparison of absorption spectra and cyclic voltammograms of metal-free and Zn^{II} dyads with those of their model compounds primarily showed retention of the individual properties of the chromophoric subunits. This indicated the negligible interaction between them in the ground state. In addition, the luminescence and transient absorption experiments revealed that excitation of the BODIPY unit into its first singlet excited state resulted in rapid ET from BODIPY to

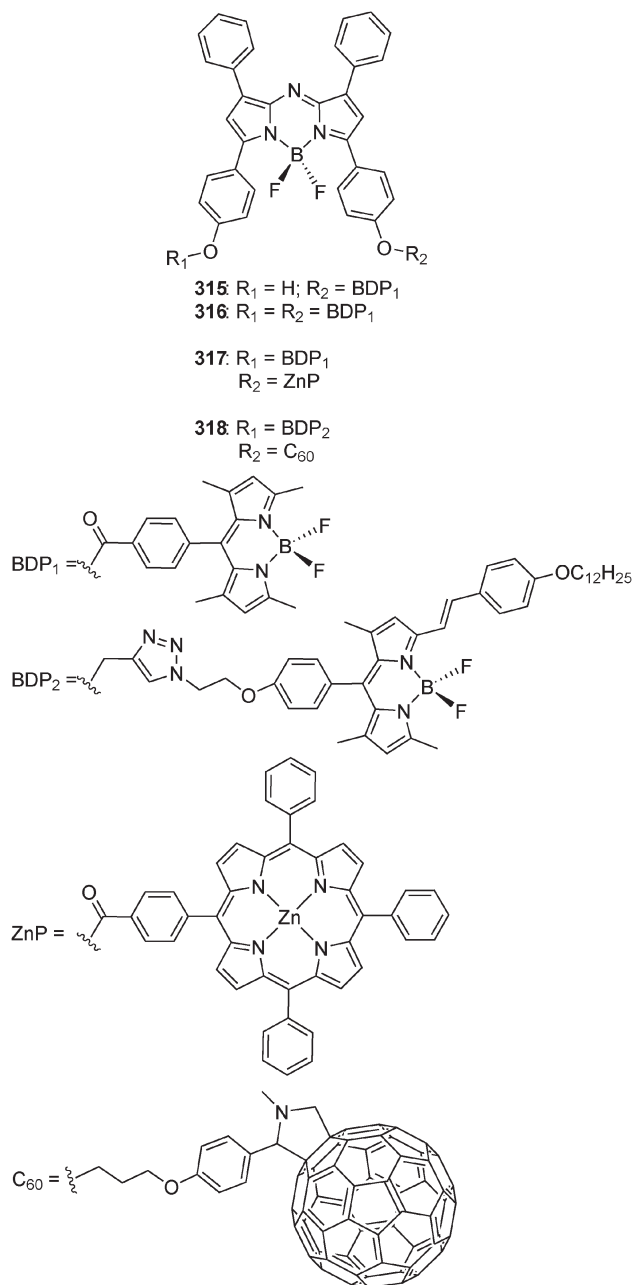
1
5
10
15
20
25
30
35
40

Fig. 71 BODIPY-aza-BODIPY D-A molecular dyads and triads.^{189–191}

porphyrin generating the first porphyrin-based singlet excited state. This last singlet state can give rise to fluorescence or undergo intersystem crossing to the corresponding triplet excited states. With the remaining chloride on the cyanuric acid moiety, a further substitution appears possible for incorporation in more complex light-harvesting systems. The same group also reported the preparation and photophysical characterization of BODIPY-porphyrin dyads connected both axially to a Sn^{IV} porphyrin *via* phenolate/benzolate bridges (**345** and **346**, respectively; Fig. 79) and peripherally to a *meso*-substituted Zn^{II} porphyrin *via* Pd-catalyzed amination (**347**; Fig. 79).^{203,204}

In a very similar fashion, the group of Dinolfo reported the preparation by Cu^I -catalyzed azide-alkyne cycloaddition

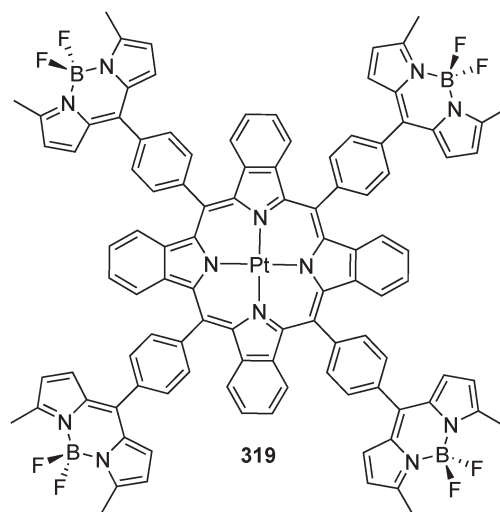


Fig. 72 Multichromophoric BODIPY-benzoporphyrin Pt^{II} complex for singlet and triplet generation.¹⁹²

(CuAAC) of a dyad, tetrad and pentad based on BODIPY donors connected to a Zn^{II} -tetraphenylporphyrin (ZnTPP) acceptor *via* 1,2,3-triazole linkages (**348–350**; Fig. 80).²⁰⁵ They further studied those arrays by UV/visible absorption and emission spectroscopy, fluorescence lifetime and DFT electronic structure modeling. Modelization provided insights that no excited state mixing of the D and A orbitals occurs in such systems. The results also showed that singlet excited state emission of the BODIPY is significantly quenched in all three arrays, which is consistent with ET to the porphyrin core. Furthermore, the fluorescence excitation spectra of the three arrays matched the through-space fluorescence resonance energy transfer (FRET) mechanism, with ET values >95%. The authors claimed the CuCAAC reaction to be a useful strategy for the creation of molecular systems for solar energy conversion and artificial photosynthesis.

The group of Wong reported the synthesis and photophysical properties of a series of D-A conjugates based on variously substituted Yb^{III} -porphyrinate (YbPor) electron-donor moieties bridged through an ethynyl linker to BODIPY electron acceptor units (**351–356**; Fig. 81).²⁰⁶ Photoluminescence studies demonstrated efficient ET from the BODIPY unit toward the YbPor counterpart. Once conjugated with the YbPor moiety, BODIPY serves as an antenna to harvest the lower-energy visible light and subsequently transfers it toward the former. Consequently, the sensitization of the Yb^{III} emission in the NIR region is achieved, with a quantum efficiency of up to 0.73% and a lifetime of around 40 μs . Moreover, these conjugates exhibited large two-photon-absorption cross-sections that ranged from 1048 to 2226 GM and strong two-photon-induced NIR emission.

Rational design and synthesis of a versatile FRET ratiometric sensor for Hg^{II} and Fe^{II} cations was achieved by Jiang *et al.*²⁰⁷ This fluorescent chemosensor is based on a flexible 8-hydroxyquinoline benzoate linked BODIPY-porphyrin dyad (**314**; Fig. 82) where the BODIPY acts as D and the porphyrin as A. Interestingly, the binding of this dyad with Hg^{2+}/Fe^{2+} induced

1
5
10
15
20
25
30
35
40
45
50
55

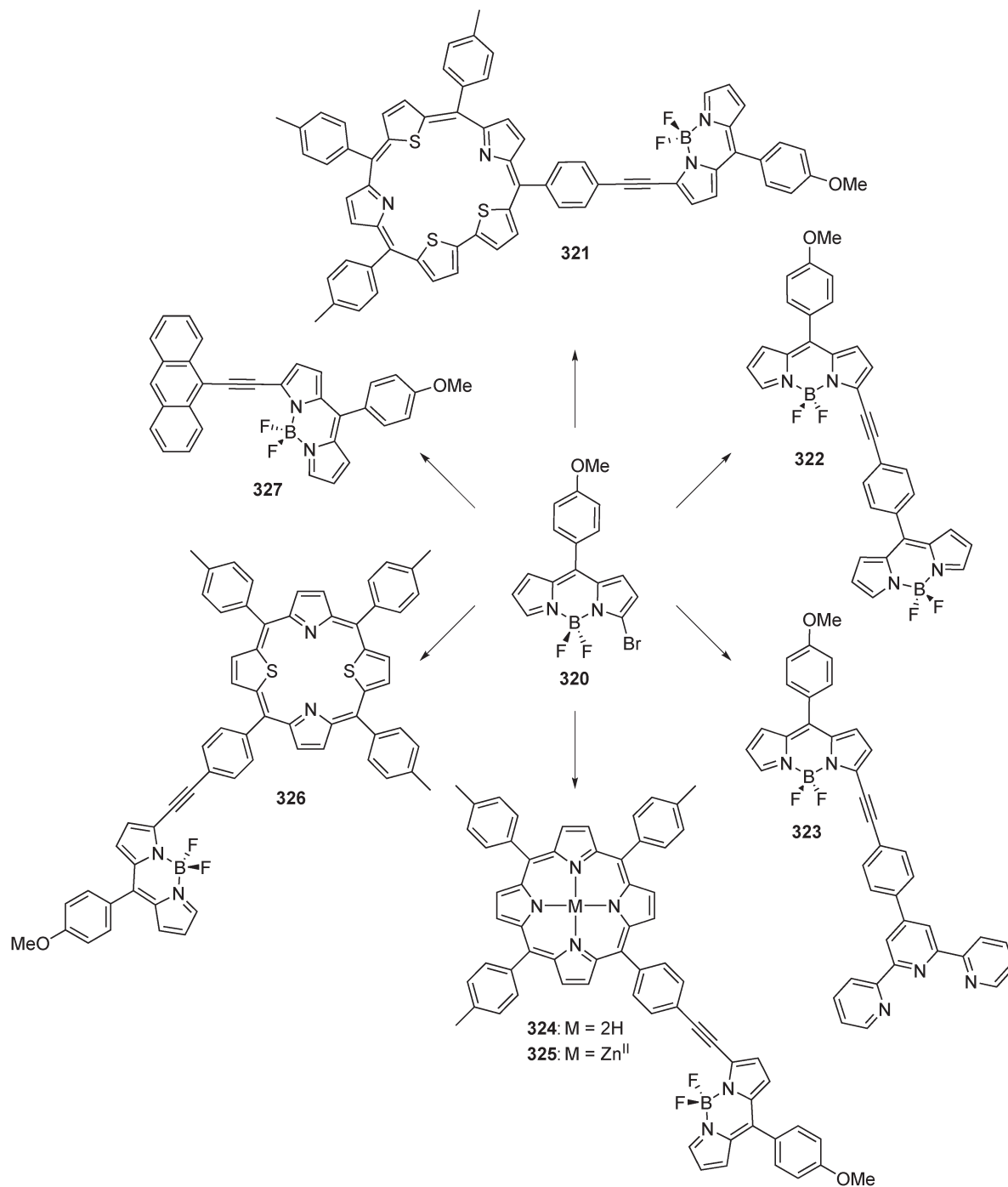


Fig. 73 Covalently linked BODIPY chromophore conjugates using a 3-bromo BODIPY as the key precursor.¹⁹³

just the opposite (promoting/restraining) influence on ET, resulting in a remarkably different ratio change of two signal emissions.

It is also of interest that the communication by Dolphin *et al.* presented a synthetic way to obtain a variety of BODIPY–hexaphyrin hybrids (358–360; Fig. 83).²⁰⁸ The authors intend to examine the detailed time-resolved photophysical properties and advanced multi-hexaphyrin–BODIPY arrays for incorporation in multichromophoric LH systems.

Another class of BODIPY–porphyrinoids based on subporphyrins was developed by Osuka and coworkers.²⁰⁹ BODIPY–subporphyrin hybrids bridged by a 1,4-biphenylene or 1,4-diphenylethyne spacer (361–362 and 363–364, respectively; Fig. 84) were obtained *via* either the palladium-catalyzed Suzuki–Miyaura cross-coupling or Sonogashira cross-coupling. The effects of the spacer and the BODIPY structures on structural and optical properties were put in relationship. The conclusion was that intramolecular excitation ET from the

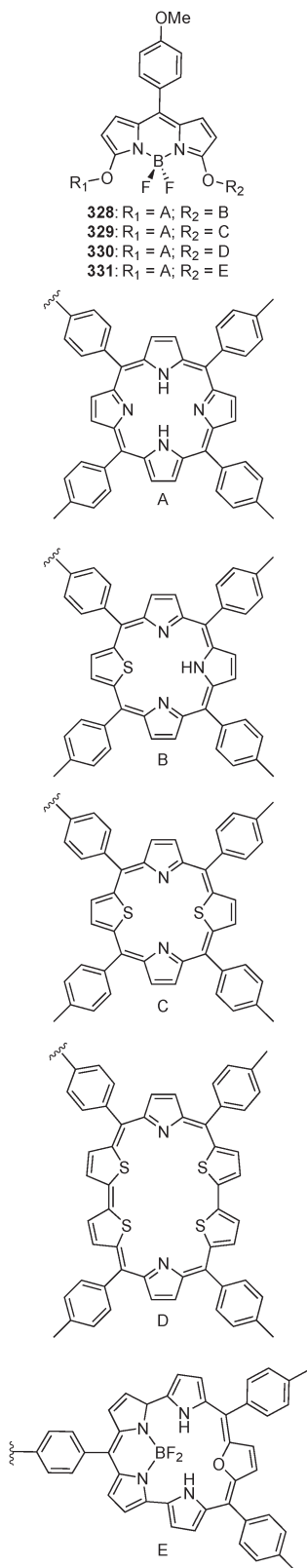


Fig. 74 Covalently linked trichromophoric systems based on BODIPY-porphyrinoid conjugates.¹⁹⁶

increased or decreased depending on the presence or absence of β -methyl groups adjacent to the *meso*-position of the BODIPY subunit. Finally, it was observed that electronic interaction between the subporphyrin core and the *meso*-(1,4-phenylene) substituents caused spectral changes for the subporphyrin part, a phenomenon not observed for their porphyrin counterparts.

An interesting BODIPY-porphyrinoid hybrid has been reported by Torres and coworkers.²¹⁰ This article presents a panchromatic supramolecular fullerene-based D-A assembly from a peripherally substituted BODIPY-zinc phthalocyanine dyad (**365**; Fig. 85). Photophysical characterization revealed that the BODIPY-zinc phthalocyanine (ZnPc) conjugated part of the assembly absorbs in two disparate but complementary sections of the solar spectrum (BODIPY = 525 nm; ZnPc = 680 nm). Its electrochemical characterization revealed that the photoactive ZnPc part has strong electronic interactions with the redox-active BODIPY part in the ground state. Under photoexcitation at 480 nm, the BODIPY-ZnPc complex reveals the photosensitization of the ZnPc moiety by means of BODIPY photon absorption. When self-assembled with the fullerene part, the entity forms a BODIPY-ZnPc^{•+}-C₆₀^{•-} radical-ion-pair state with an overall conversion efficiency of 25% and a lifetime 39.9 ns in toluene. This last value is quite high in comparison with the poor 5 ns of the simpler ensemble formed by ZnPc and pyridine-functionalized C₆₀. This complex also leads one to think that OPV thin films could be derived from it and it should give interesting photovoltaic results since there is a direct connection between the fullerene acceptor and the BODIPY-zinc phthalocyanine donor.

Following the same trend, the groups of Tkachenko and D'Souza jointly reported a few months later the preparation and electronic energy harvesting properties of multi BODIPY-zinc porphyrin dyads accommodating fullerene **369** as the photosynthetic composite of the antenna-reaction center.²¹¹ For the dyads bearing one, two and four BODIPY entities (**366-368**, respectively; Fig. 86), both steady-state and time-resolved emission and transient absorption studies revealed an efficient singlet-singlet ET from BODIPY units to Zn porphyrin in a timescale ranging from 28 to 48 ps. A decrease in the time constant of ET observed upon increasing the number of BODIPY units indicated a better antenna effect for dyads bearing a higher number of those chromophoric entities. Furthermore, supramolecular triads that mimic the antenna-reaction center in a naturally occurring photosynthetic process were constructed by coordination of **369**, a fullerene-pyrrolidine appended with an imidazole ligand, to the zinc porphyrin. The structural integrity of the supramolecular triads was measured by optical, computational and electrochemical studies. Energy calculations revealed the possibility of photoinduced electron transfer from ¹ZnP* to fullerene in the supramolecular triads and preliminary transient absorption studies involving pump-probe techniques further supported that hypothesis. Again, this type of system is suitable for incorporation in OPV thin films and should provide interesting photocurrent conversion.

subporphyrin core to the peripheral BODIPYs occurred in all cases and with great efficiency. Also, fluorescence was either

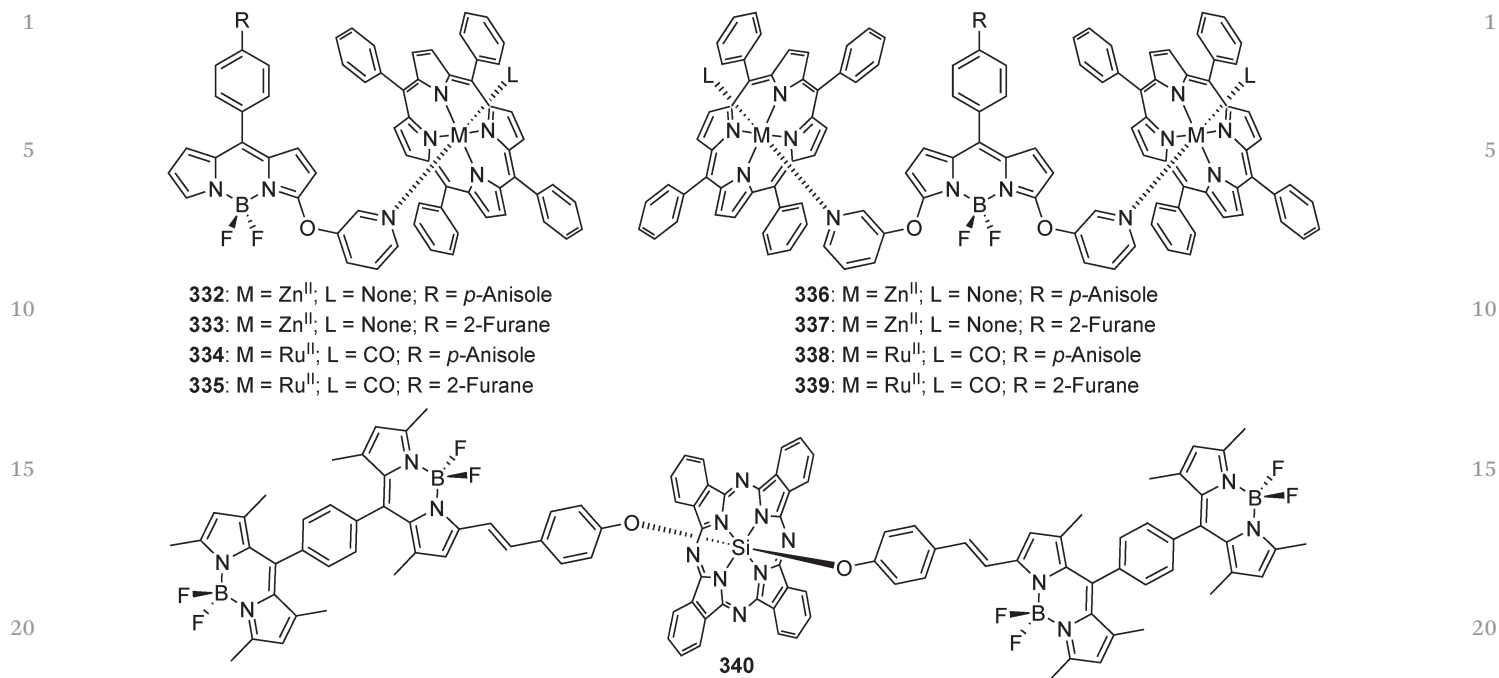


Fig. 75 Non-covalent BODIPY-metalloporphyrin dyads and triads.^{197,198}



Fig. 76 *B,B'*-Diporphyrinbenzyloxy-BODIPY derivatives showing antenna effect.²⁰⁰

2.2.3 DPM or ADPM polyads in OPV materials. With the numerous articles on DPM-based oligomer and polyad studies reported, their integration in real OPV devices has recently started to emerge in the literature. Many examples of their use as photosensitizer additives and as donor materials, along with their use as potential materials, according to their energy levels will be presented.

Two hexylthiophene-conjugated BODIPYs with benzo[1,3,2]-oxazaborinine rings (370 and 371; Fig. 87) were developed for BHJSC's photosensitizing additive application by the group of Kubo and industrial collaborators from the Mitsubishi Chemical Group Science and Technology Research Center.²¹² By adding only 5 wt% of the NIR absorbing BODIPY dyes in the

blend ratio of a P3HT/indene-C₇₀ bisadduct (IC₇₀BA) bulk heterojunction structure, an increase from 3.7 to 4.0% of PCE was observed for 371 and up to 4.3% for 370 (see Fig. 87) (entries 1 and 2, Table 1). For the latter additive, it represents an increase of about 15% in the overall conversion efficiency. In addition to photovoltaic experiments, a complete photophysical and electrochemical characterization was presented, along with the DFT studies. These promising results confirm that well-defined NIR absorbing BODIPY derivative dyes do have the potential to be used as light-harvesting sensitizers in polymeric solar cells, probably in a manner depicted in Fig. 5. However, the authors mentioned that their focus for future work would be put toward structural optimization of the BODIPY-based

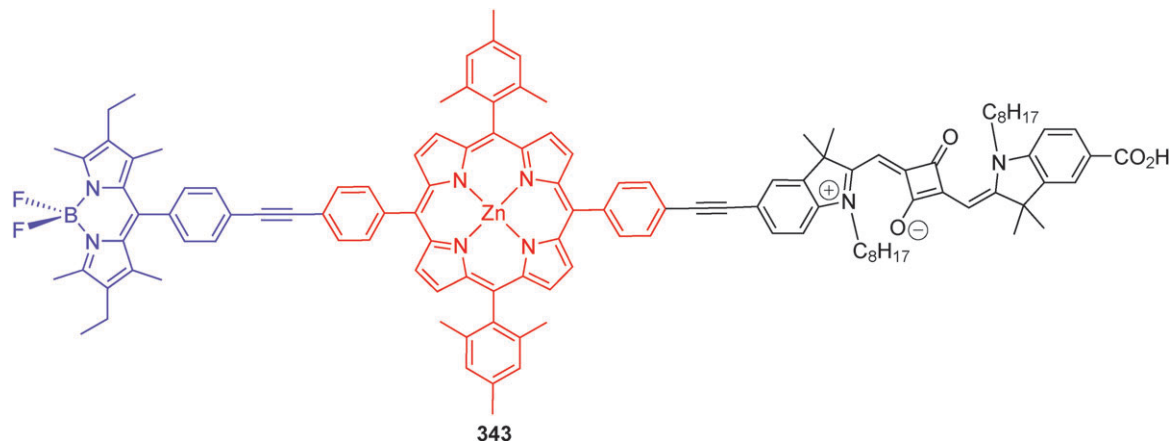


Fig. 77 Panchromatic trichromophoric sensitizer for DSSC using antenna effect.²⁰¹

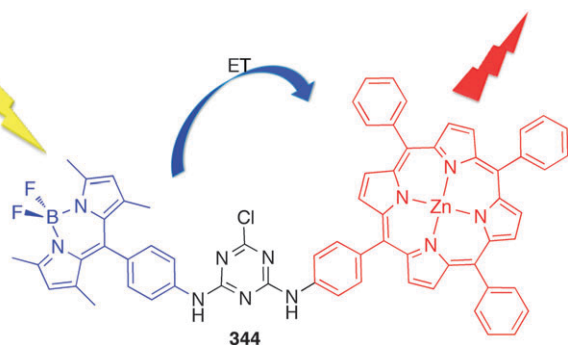


Fig. 78 BODIPY-Zn^{II} porphyrin dyad presenting photoinduced energy transfer.²⁰²

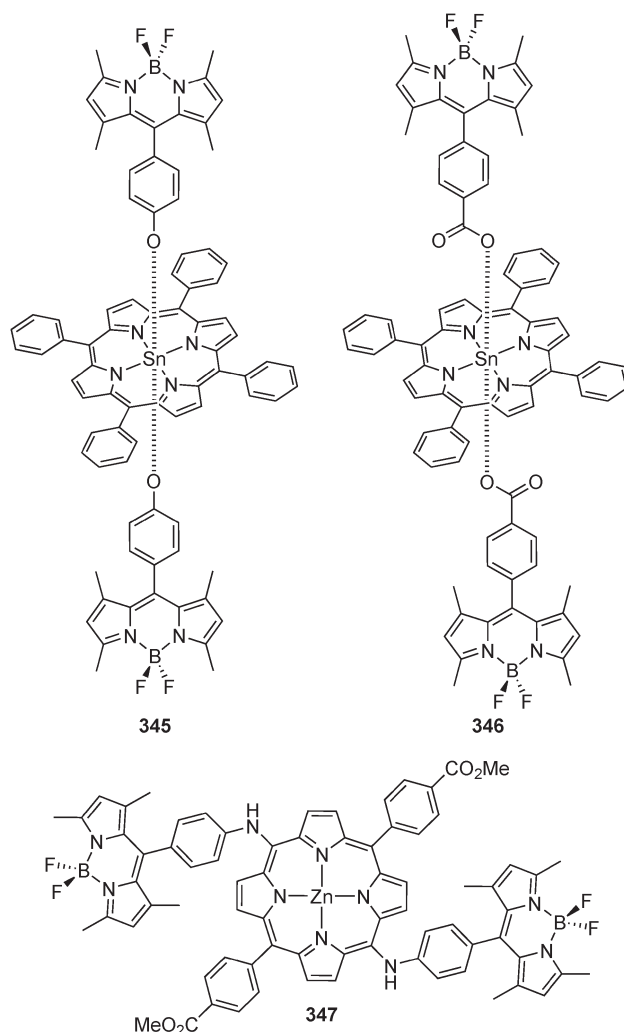


Fig. 79 BODIPY-porphyrin dyads bridged axially and peripherally.^{203,204}

sensitizers and on further investigation of mechanisms behind its LH effects.

BODIPY derivatives as donor materials are under constant investigation by the group of Ziessel and his collaborators. In 2010, they published the tailored hybrid BODIPY-oligothiophene donor **373** for BHJSC with improved performances (Fig. 88).²¹⁴ In fact, they related that the fixation of a 5-hexyl-2,2'-bithienyl (BT) unit on the BODIPY **372** increased the PCE of the resulting BHJSC from 1.3 to 2.2%, mainly due to a large increase of current density (entries 3 and 4, Table 1).²¹³ A complete photophysical and electrochemical characterization of the two compounds was also furnished. All those data led them to conclude that structural changes had little effect on the energy levels and light-harvesting properties of the D, but improved its charge transport properties. Therefore, they mentioned that further work is needed to determine the impact of the structural variation made on interfacial morphology, diffusion length or charge recombination parameters. Fabrication of new cells with PC₇₁BM as the A was also planned along with synthesis of other BODIPY-oligothiophene hybrid systems.

Ziessel *et al.* further reported the regioselective synthesis of 5-monostyryl and 2-tetracyanobutadiene π -extended BODIPY dyes (**374**–**377**; Fig. 88) in the perspective of integrating those molecular dyads and triads into solar cells.²²⁰ The

unsymmetrical 2,5-disubstituted BODIPY derivatives were obtained from 2-substituted precursors (iodo, ethynylaryl) using a regioselective Knoevenagel condensation reaction with dimethylaminobenzaldehyde. A [2+2] cycloaddition reaction

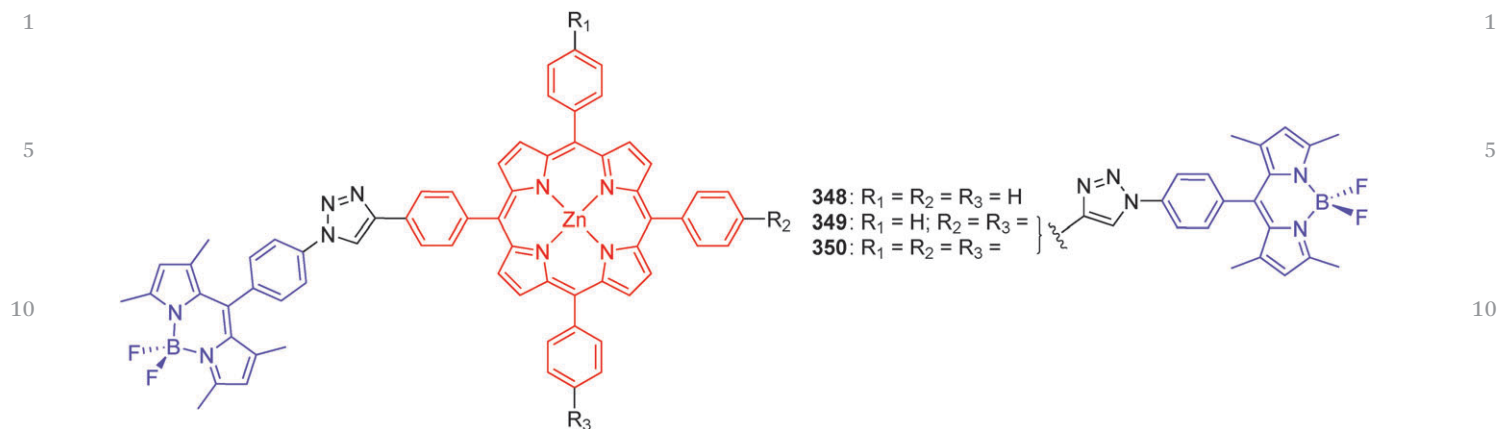


Fig. 80 BODIPY–ZnTPP dyad, tetrad and pentad with 1,2,3-triazole linkages.²⁰⁵

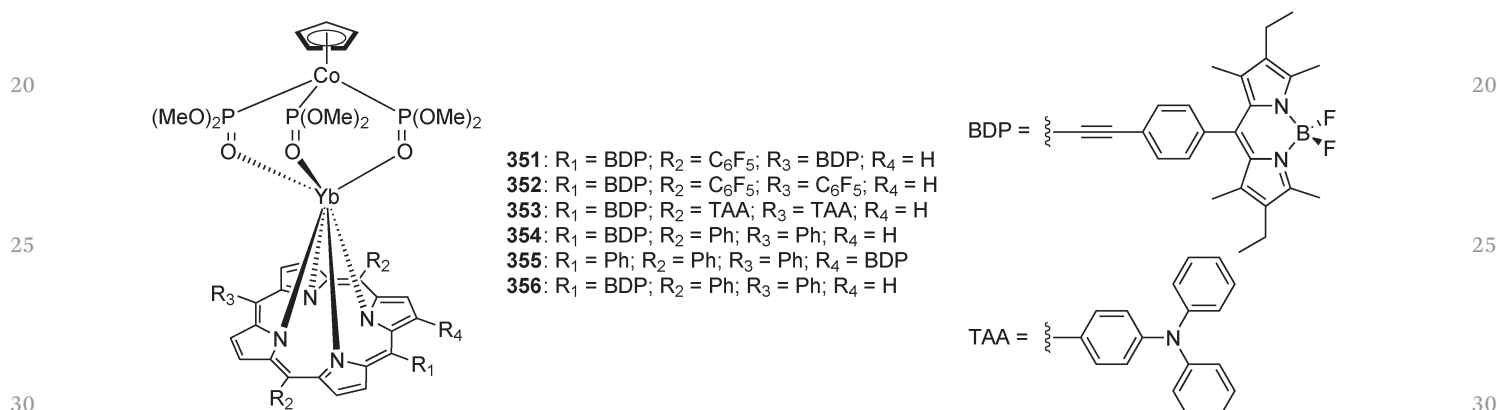


Fig. 81 Light-harvesting Yb^{III} –porphyrinate–BODIPY conjugates.²⁰⁶

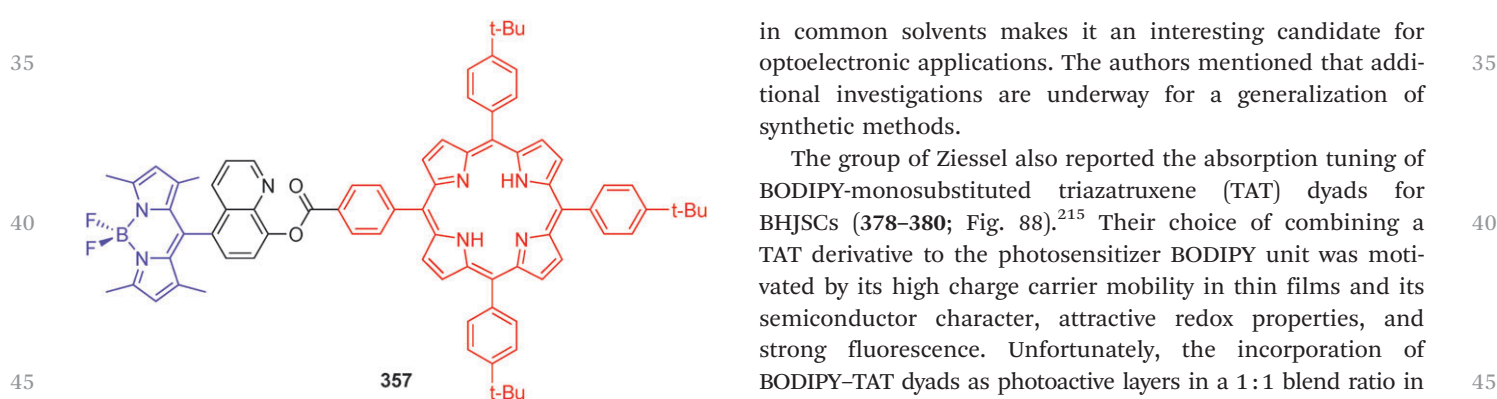


Fig. 82 FRET ratiometric sensor for Hg^{II} and Fe^{II} ions based on a BODIPY–porphyrin dyad.²⁰⁷

with tetracyanoethylene was carried out on the unsaturated 2-ethynyl-5-styryl-BODIPY **375** to obtain the 1,1,4,4-tetracyanobuta-1,3-diene (TCBD) derivative **377**. This last TCBD/BODIPY derivative **377** presented rich redox activity, an important feature for stable solar cells over time. Its strong charge transfer absorption band in the 500 to 700 nm range (even reaching up to 800 nm) combined with a good solubility

in common solvents makes it an interesting candidate for optoelectronic applications. The authors mentioned that additional investigations are underway for a generalization of synthetic methods.

The group of Ziesel also reported the absorption tuning of BODIPY-monomethylated triazatruxene (TAT) dyads for BHJSCs (**378–380**; Fig. 88).²¹⁵ Their choice of combining a TAT derivative to the photosensitizer BODIPY unit was motivated by its high charge carrier mobility in thin films and its semiconductor character, attractive redox properties, and strong fluorescence. Unfortunately, the incorporation of BODIPY–TAT dyads as photoactive layers in a 1 : 1 blend ratio in weight with PC_{61}BM gave rise in the best case to a modest PCE of 0.90% (entries 5–8, Table 1). The J – V curves for **379** indicated that the charge carrier extraction was not adequate, even with the acceptable hole mobility measured in the pure material. Interestingly, additional chromophore for more complex polyad systems appears achievable by a simple cross-coupling strategy with the remaining iodine at the *meso*-phenyl position. According to the authors, further work is in progress to improve active layer morphology and charge carrier mobility in the blend.

Finally, Ziesel *et al.* lately reached a PCE of up to 4.7% in BHJSC and observed an ambipolar behavior as organic field

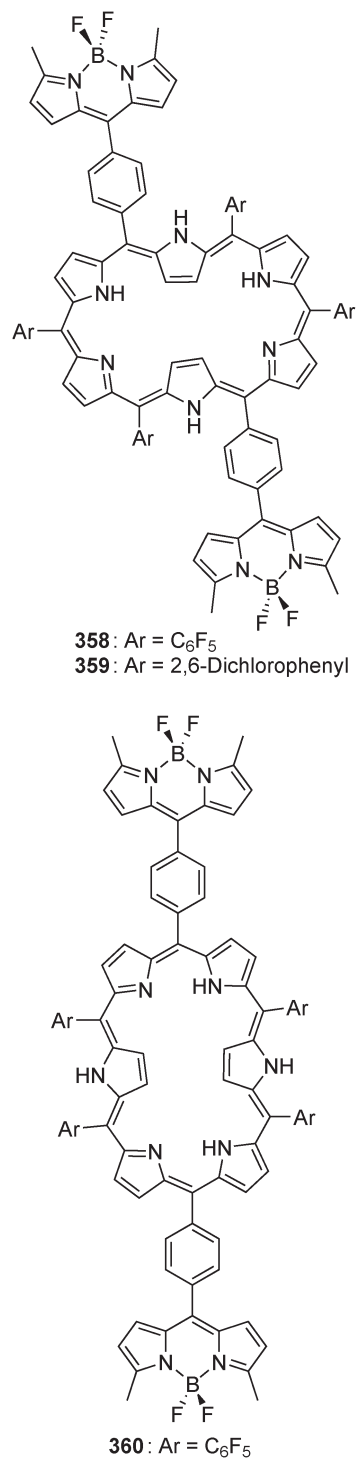


Fig. 83 Hexaphyrin–BODIPY hybrids.²⁰⁸

effect transistors (OFET) with thienyl-BODIPY scaffolding.²¹⁶ Their new green-absorbing DPM dyes engineered from bis-vinyl-thienyl modules (**381–384**; Fig. 88) proved to be planar by X-ray, exhibited strong absorption in the 713–724 nm range and displayed comparable electron and hole mobilities in thin films (up to $1 \times 10^{-3} \text{ cm}^2 \text{ V}^{-1} \text{ s}^{-1}$). Once assembled as BHJSC by a solution process in a low ratio with PC₆₁BM, the derivative

382 provided a PCE of up to 4.7% with a J_{SC} of 14.2 mA cm^{-2} , a V_{OC} of 0.7 V (entry 9, Table 1) and a broad external quantum efficiency (EQE) reaching 60% at its maximum value in the range from 350 to 920 nm (Fig. 89). These very promising results seem to arise from the planarity in the solid state of the thienyl-BODIPY derivatives, which favor short contact distances between neighboring molecules and exhibit high charge mobility. The authors mentioned that challenging studies are now in progress to collect the photons more efficiently in the 500–620 nm range in order to further improve device efficiency.

A first study testing the incorporation of ADPMs in OPV was reported in 2011 by the group of Ma.²¹⁷ Inspired by their exceptional NIR and solubility properties, the authors used solution processable tetraphenyl-ADPM **385** and its BF_2^+ and B–O chelated versions (**386** and **387**, respectively) as electron donors to prepare efficient planar heterojunction organic solar cells (Fig. 90). A vapor deposited layer of C₆₀ acceptor was added to the spin-coated layer of the ADPM donor and power efficiency of 0.6, 0.7 and 2.5% was obtained for **385**, **386** and **387**, respectively, under AM 1.5G simulated sun solar illumination (entries 10–12, Table 1). Attractively, the highest V_{OC} ($\sim 0.8 \text{ V}$) reported up to now for organic solar cells was obtained for the **387**/C₆₀ device, with photocurrent generation in the NIR region beyond 1.5 eV (see Fig. 91). Such results appear to be of great interest to sustain further research with small ADPM derivatives for OPV devices.

A second paper published in 2012 by members of Heliatek GmbH looked at the use of tetra-phenyl aza-BODIPY **386** and the previously reported benzannulated difluoro-bora-bis-(1-phenyl-indoyl)-azamethine **388** as donor materials again in PHJSC (entries 13–15, Table 1) (Fig. 90).^{218,221} They observed that upon benzannulation of the pyrrole of **386**, giving **388**, the thin film absorption maximum is red-shifted by about 70 nm up to 773 nm. Integrating those two materials in solar cells with a MIP-architecture (metal intrinsic p-doped) (Fig. 92), they were able to reach a higher V_{OC} value (0.96 V with BPADF as the hole transport layer) for **386** than the 0.8 V obtained by Ma *et al.* They were able to reach $\eta = 1.2\%$ with such a high V_{OC} , almost the double in efficiency compared to the 0.69% previously reported. On its side, the device based on **388** reached a mismatch corrected efficiency of 1.1% due to a V_{OC} of 0.65 V, a fill factor of 65% and an external quantum efficiency extending up to 860 nm. The authors were encouraged by the considerable contribution of far red and NIR absorption brought about by that family of chromophores. These simple ADPM NIR chromophores should be suitable for integration as photosensitizer additives in BHJSC to see to which extent they would be able to increase the PCE.

Based on the few examples of BODIPY oligomers or polyads integrated in BHJSCs, a few papers inspired us for the development of potential new donor materials. For instance, the versatile synthetic methodology published by Ziessel for the engineering of thiophene-substituted BODIPY dyes appears interesting in the context of integrating well-known optoelectronic active thiophene derivatives to fine-tune the properties of resulting polyads.²²³ They further push this idea of

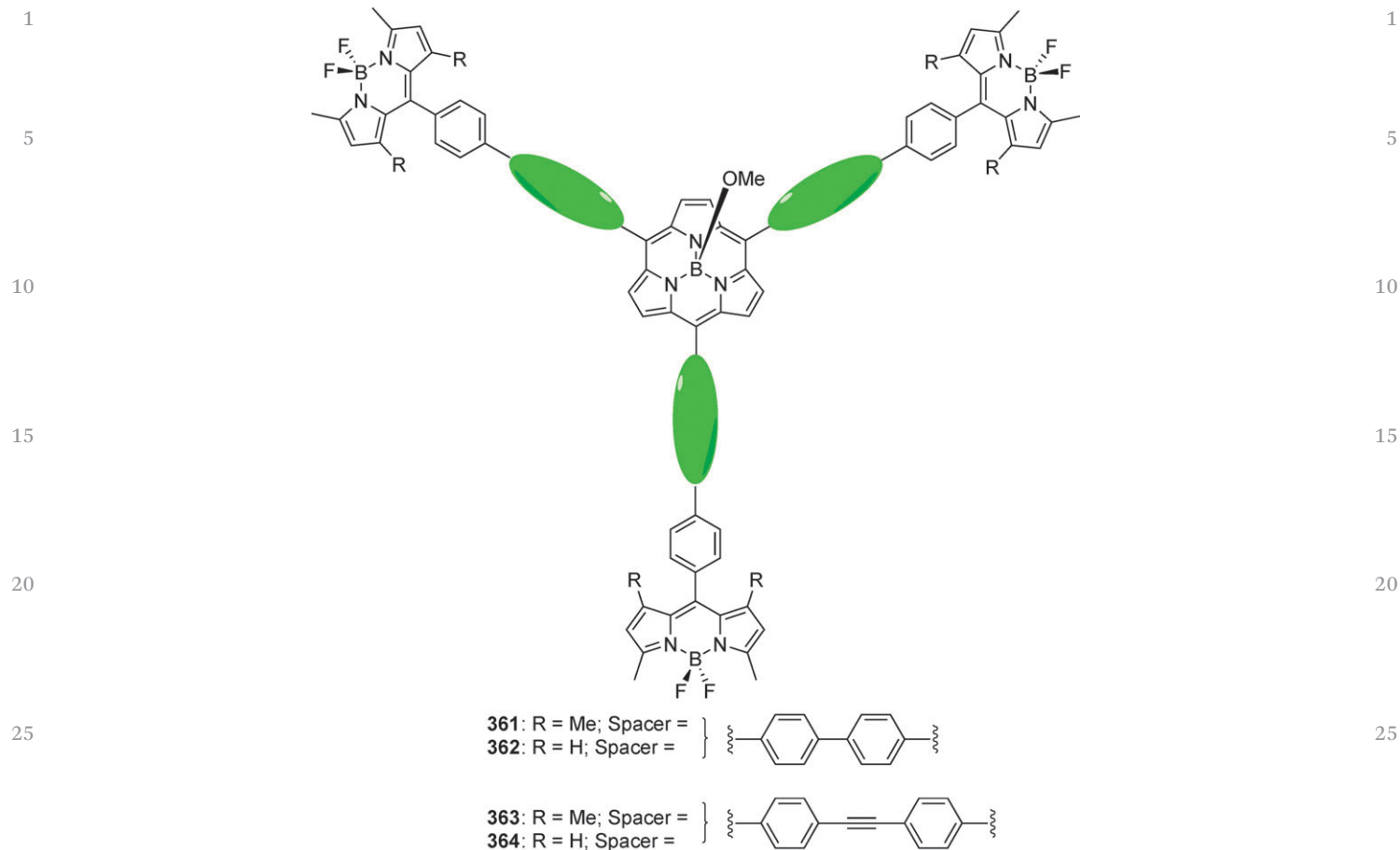


Fig. 84 BODIPY-subporphyrin hybrids bridged by a 1,4-biphenylene or 1,4-diphenylethynylene spacer.²⁰⁹

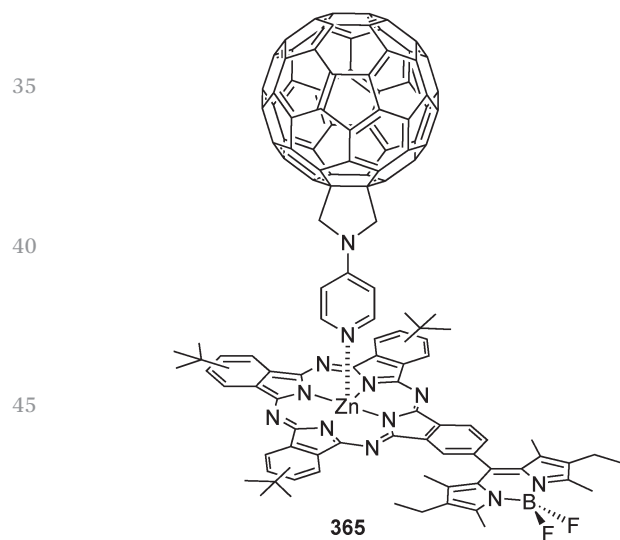


Fig. 85 Supramolecular C₆₀-based D-A assembly from a peripherally substituted BODIPY-ZnPc dyad.²¹⁰

Examples of potentially interesting thiophene-substituted BODIPY dyes (**389–395**) from those two papers are shown in Fig. 93. They exhibit π -extended conjugation along with solubilizing chains and/or place for further chemical modification at the *meso*-position. Another interesting chromophoric unit to incorporate for OPV application is the well-known fluorene. Nice examples of two different BODIPYs appended to a fluorene platform were reported, again by the group of Ziesel (**396** and **397**; Fig. 93).²²⁵ Interestingly, they thought about incorporating bipyridine groups in the architecture of **397** for further coordination to transition metals. This is paving the way for additional applications in artificial light-harvesting systems, such as H₂ production or DSSC.

Replacing the fluorene platform by a carbazole one may also provide an interesting avenue, as polymeric solar cells based on that moiety have proved their efficiency.¹² Ooyama *et al.* reported one example lately when they looked at the photovoltaic performance of DSSC based on D- π -A type BODIPY dye **398** bearing two electron-withdrawing pyridyl groups in 3,5-positions and an electron donor carbazole-diphenylamine moiety at the 8-position (Fig. 93).²²⁶ They observed a good LH efficiency in the red and NIR region. DSSC testing led to an incident photon-to-current conversion of $\sim 10\%$ over the range of 500 to 700 nm, with an onset at 800 nm. Such a chromophore

incorporating thiophene on a BODIPY core as they reported lately the preparation of unsymmetrical 3,5-dioligothienyl-BODIPYs exhibiting red and NIR emitting properties.²²⁴

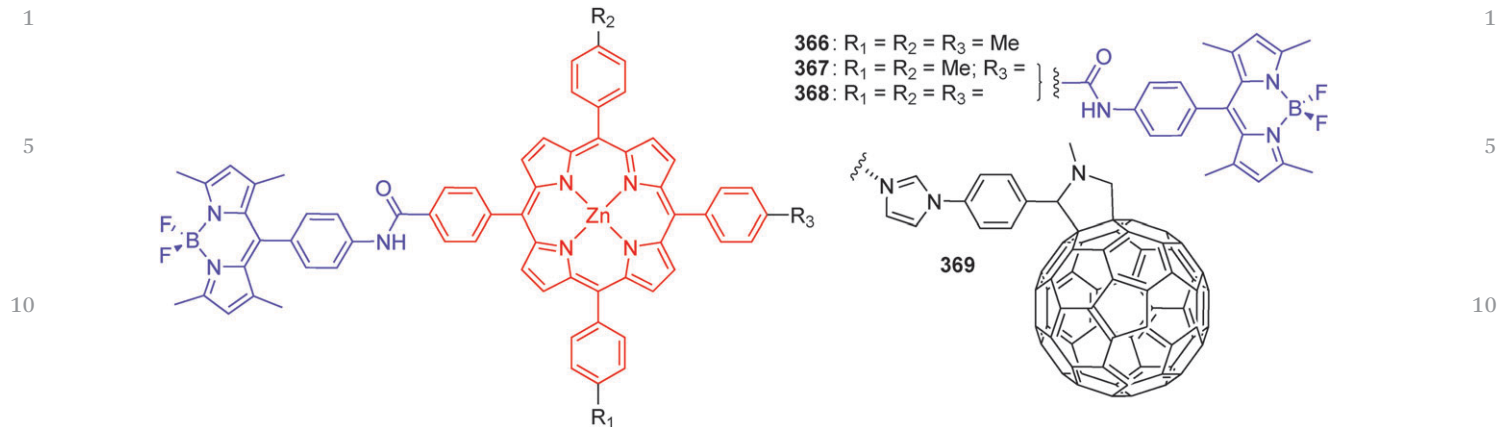


Fig. 86 Multi BODIPY–zinc porphyrin dyads accommodating fullerene as the photosynthetic composite of the antenna–reaction center.²¹¹

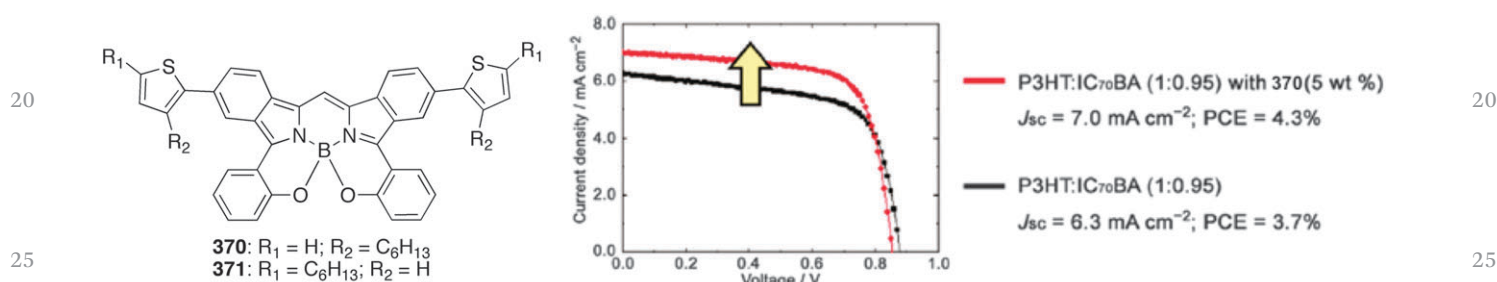


Fig. 87 Hexylthiophene-conjugated BODIPY with benzo[1,3,2]oxazaborinine rings for BHJSC's photosensitizing additive application.²¹² (Adapted with permission from *Org. Lett.*, 2011, **13**(17), 4574–4577. Copyright © 2011 American Chemical Society.)

Table 1 Photovoltaic parameters of OPV solar cells incorporating DPM and ADPM based derivatives

Entry	Device structure	Light intensity (mW cm^{-2})	J_{sc} (mA cm^{-2})	V_{oc} (V)	FF	η (%)	Ref.
1	ITO/PEDOT:PSS/P3HT:IC ₇₀ BA with 5 wt% 370/Ca/Al	100	7.0	0.85	0.71	4.3	212
2	ITO/PEDOT:PSS/P3HT:IC ₇₀ BA with 5 wt% 371/Ca/Al	100	6.8	0.85	0.70	4.0	212
3	ITO/PEDOT:PSS/372:PCBM/Al	NA	4.1	0.75	0.44	1.3	213
4	ITO/PEDOT:PSS/373:PCBM/Al	NA	6.9	0.74	0.38	2.2	214
5	ITO/PEDOT:PSS/378:PCBM/Al	100	0.5	0.57	0.28	0.1	215
6	ITO/PEDOT:PSS/379:PCBM/Al	100	2.9	0.71	0.29	0.7	215
7	ITO/PEDOT:PSS/379:PCBM/Ca/Al	100	3.6	0.83	0.29	0.9	215
8	ITO/PEDOT:PSS/380:PCBM/Al	100	2.0	0.71	0.29	0.4	215
9	ITO/PEDOT:PSS/382:PCBM/Ca/Al	100	14.3	0.70	0.47	4.7	216
10	ITO/PEDOT:PSS/385:C ₆₀ /bathocuproine/Ag	100	5.5	0.21	0.49	0.6	217
11	ITO/PEDOT:PSS/386:C ₆₀ /bathocuproine/Ag	100	3.1	0.47	0.48	0.7	217
12	ITO/PEDOT:PSS/387:C ₆₀ /bathocuproine/Ag	100	5.9	0.80	0.56	2.5	217
13	ITO/C ₆₀ /386/BPAPF/PV-TPD/ZnPc/Au	121	3.0	0.92	0.33	0.8	218
14	ITO/C ₆₀ /386/PV-TPD/BPAPF/ZnPc/Au	122	3.2	0.96	0.48	1.2	218
15	ITO/C ₆₀ /388/PV-TPD/ZnPc/Au	91	2.4	0.65	0.65	1.1	218
16	ITO/PEDOT:PSS/433:PCBM/Al	100	4.0	0.76	0.43	1.3	219
17	ITO/PEDOT:PSS/436:PCBM/Al	100	4.8	0.80	0.51	2.0	219

definitely appears to be a suitable candidate for integration into OPV devices.

Three different chromophoric units have also been incorporated with the BODIPY to achieve sensing. Their photostability in various conditions, *i.e.* wide pH and/or redox range, led us to think that they might be interesting for designing a new generation of long-lived OPV materials. The group of You reported a molecular dyad with a tetrathiafulvalene (TTF)

moiety (399; Fig. 93).²²⁷ A BODIPY–coumarin conjugate was also constructed on a monostyryl BODIPY platform by Lin and coworkers (400 and 401; Fig. 91).²²⁸ Interestingly, Yang *et al.* also reported lately BODIPY–coumarin derivatives linked through the *meso*-position.²²⁹ Finally, the group of Kim prepared a dyad with a 2-dicyanomethylene-3-cyano-2,5-dihydrofuran (DCDHF) group linked through pyrrolic position (402, Fig. 93).

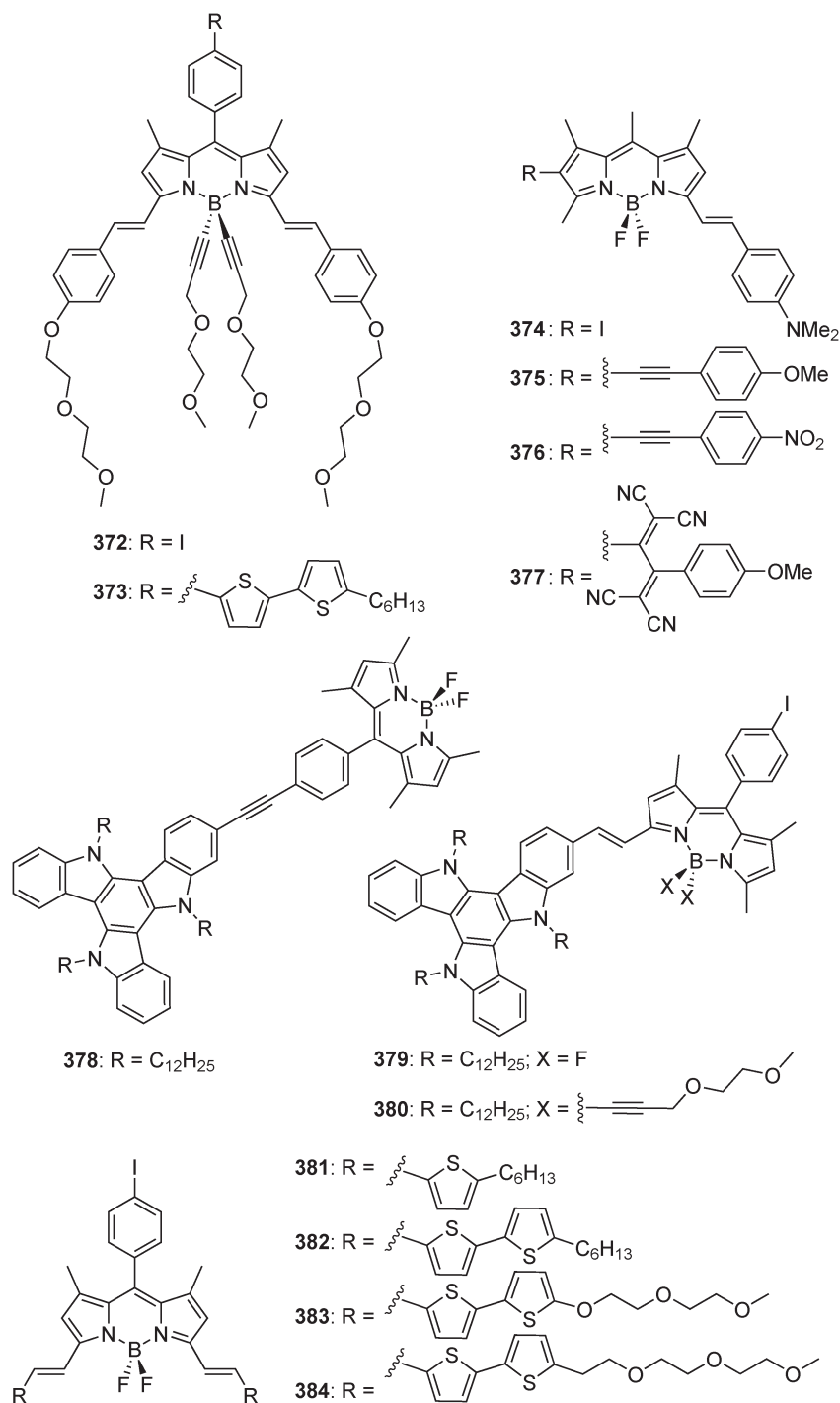


Fig. 88 BODIPY derivatives for photoactive donor materials in BHJSC.^{214–216,220}

Following the same idea of redox stability in the dyad, Ravikanth and coworkers reported four BODIPY–ferrocene conjugates (**403–406**; Fig. 93).²³⁰ The absorption studies indicated the presence of the CT band in BODIPY–ferrocene conjugates where the ferrocene(s) were directly connected to the BODIPY framework at the α -position, but not at the *meso*-position. However, all conjugates were non-fluorescent due to good electron transfer from the ferrocene to BODIPY unit. The

fluorescence was reactivated when an oxidizing agent oxidized ferrocene to ferrocenium ion. Zhu *et al.* reported another example of a ferrocene–BODIPY conjugate, linked in that case through vinylic bridges at α -positions, and looked at its electrochromic properties based on the charge transfer process (**407**; Fig. 93).²³¹ Further examples of BODIPY–ferrocene conjugates were recently reported by Misra *et al.* aiming to improve the electronic communication between the D and A moieties.^{232,233}

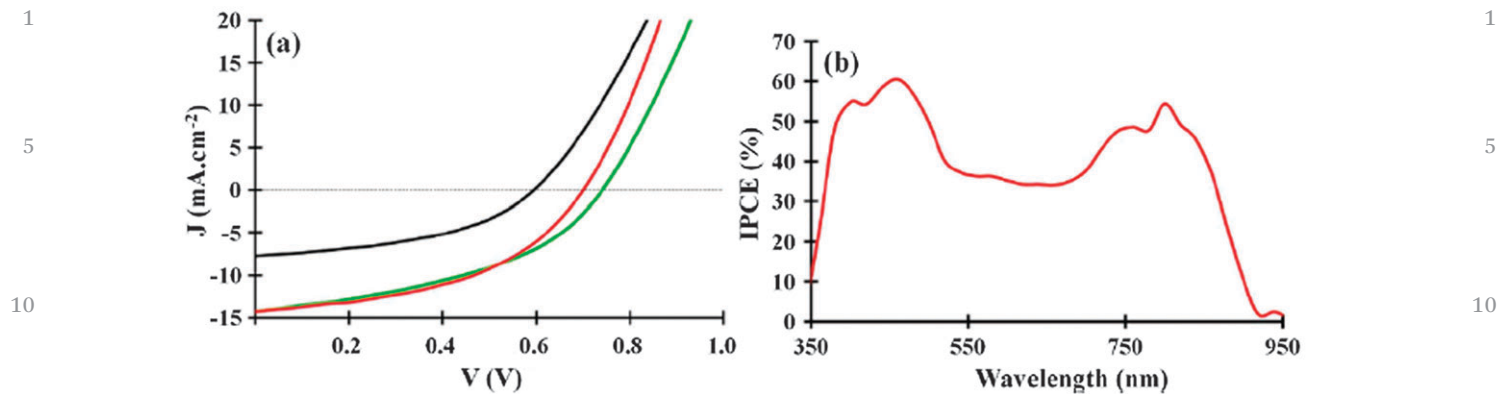


Fig. 89 Photovoltaic characterization (J - V curves and IPCE spectrum) of the best green-absorbing DPM dye 382.²¹⁶ (Reproduced with permission from *J. Am. Chem. Soc.*, 2012, **134**(42), 17404–17407. Copyright© 2012 American Chemical Society.)

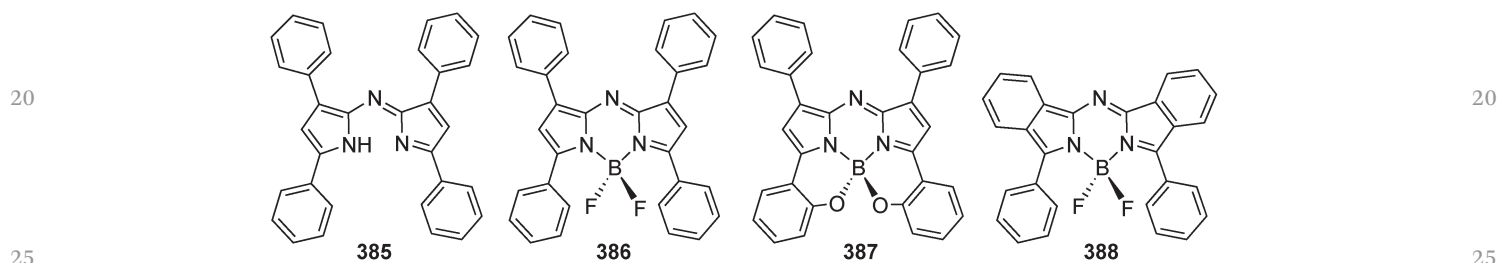


Fig. 90 ADPM-based derivatives tested in OPV.^{217,218}

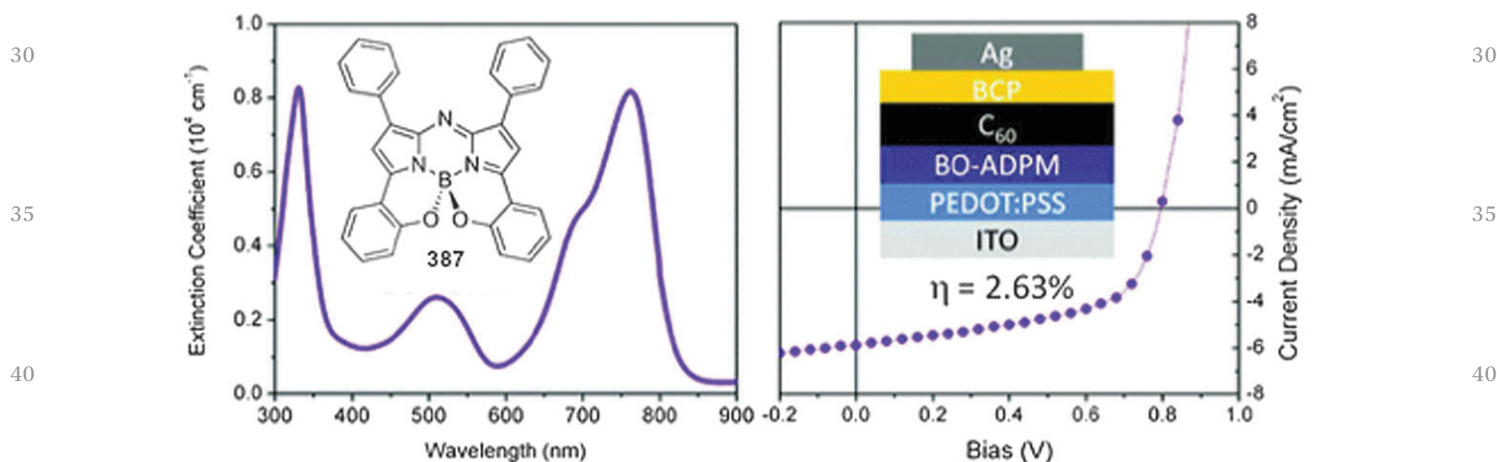


Fig. 91 Absorption spectrum and current density–voltage (J - V) characteristics for the BO-ADPM 387 in the given cell architecture.²¹⁷ (Adapted with permission from *ACS Appl. Mater. Interfaces*, 2011, **3**(11), 4469–4474. Copyright© 2011 American Chemical Society.)

The group of Ng reported the preparation of very interesting push-pull BODIPY derivatives (**408–411**; Fig. 94), which they used for second-order nonlinear optical applications.²³⁴ We strongly believe that such BODIPY derivatives bearing both an electron-donating 4-(dimethylamino)phenyl-ethynyl group and an electron withdrawing 4-nitrophenylethynyl group in the opposite 2- and 6-positions represent attractive candidates for OPV applications as well. However, the irreversibility of the first oxidation as observed by electrochemistry might hinder the lifetime of solar cells based on such compounds.

To conclude this section on BODIPY-based oligomers and polyads, a paper from Akkaya and collaborators reported in 2011 really expresses the idea of using D–A chromophoric groups to expand the absorption spectrum toward NIR and rationally fine-tune the energetic levels of the resulting dye.²³⁵ In fact, this paper optimized distyryl-BODIPY chromophores (**412–418**; Fig. 94) for efficient panchromatic sensitization in DSSC, but the basic principles are applicable to the design of OPV materials. Interestingly, compound **418** was prepared only to study the effect of excitation energy transfer (mostly through

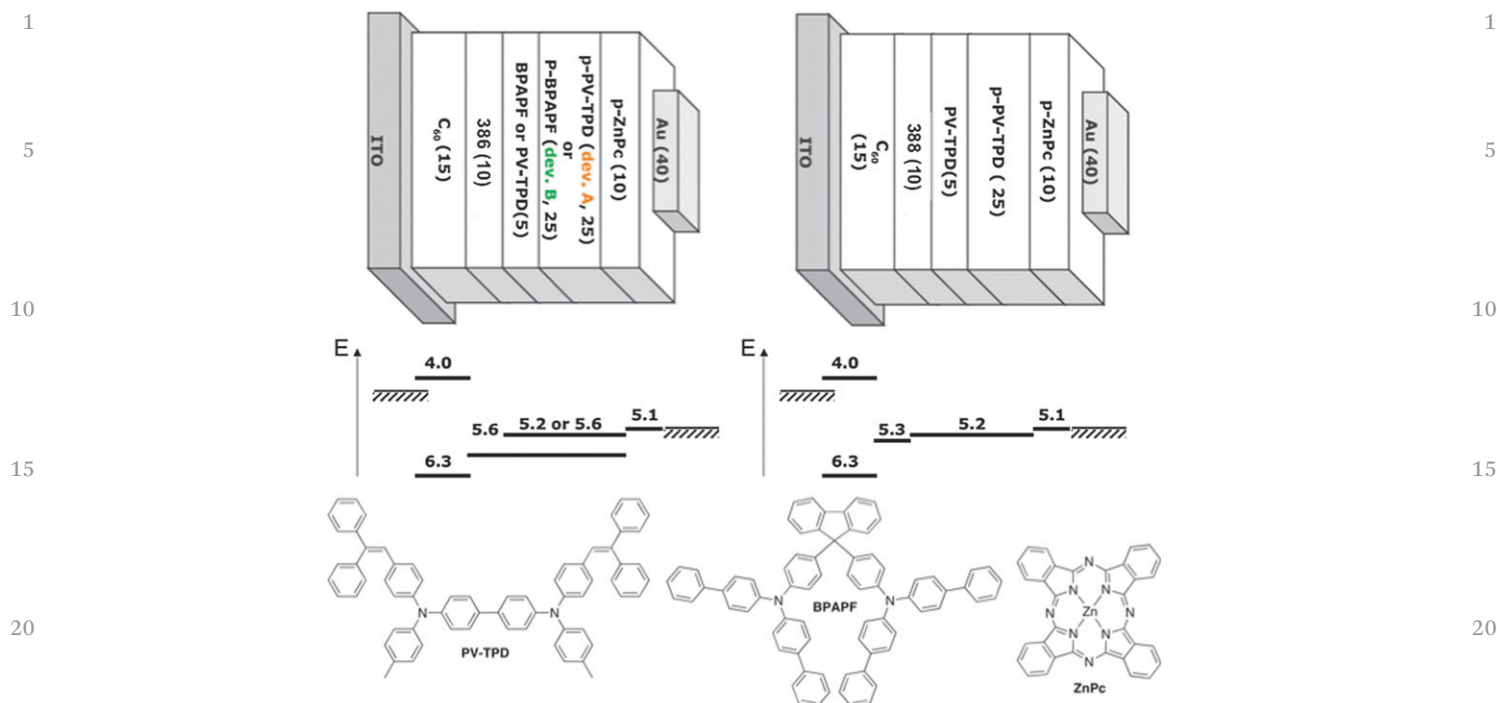


Fig. 92 Solar cell architectures and energy levels for aza-BODIPYs 386 (left) and 388 (right). Thicknesses in nm are given in parentheses.^{218,222}

space) in a photosensitizer. Photophysical studies proved efficient energy transfer from the peripheral BODIPY units, therefore a donor, toward the acceptor distyryl-BODIPY core lying lower in energy (NIR absorber). Also, the electrochemical characterization of **412** to **418** compounds revealed that **413** should be interesting for OPV based on a LUMO lying at 3.79 eV and a band gap of 1.38 eV (see Fig. 10). Overall, this type of systematic optimization approach appears suitable for the screening and rational design of new OPV materials based on DPM or ADPM dyes.

2.3. Polymers incorporating DPM

Many examples of integrating BODIPY derivatives into polymeric materials have appeared in the last five years, a few of them concerning OPV application. In fact, they were mainly prepared for their fluorescence and/or light-harvesting properties. We will here present some of them to outline the various ways to incorporate BODIPY in such polymers and to evaluate how suitable materials can be prepared for interesting photoactive layers in BHJSCs.

2.3.1 DPM in main-chain polymers. About fifteen examples of main-chain polymers containing BODIPY have been reported in the last five years. One of the first of interest published back in 2008 by Chujo *et al.* reported three highly luminescent BODIPY-based organoboron polymers (**420–422**; Fig. 95) obtained through Sonogashira coupling of the monomer **419** with different types of aryl diynes, namely 1,4-diethynylbenzene, 1,4-diethynyl-2,5-bis(trifluoromethyl)benzene and 2,7-diethynyl-9,9-dihexyl-9H-fluorene.²³⁶ Interestingly, the incorporation into the polymer is made through the boron center. These new polymers exhibited supramolecular self-assembled structures such as particles,

fibers and networks. Such behavior is interesting for the control of morphology in OPV application, one of the main issues that need to be addressed. The group of Chujo published another type of main-chain polymer containing BODIPY in 2010.²³⁷ The preparation of three aromatic ring-fused BODIPY-based conjugated polymers was presented (**426–428**; Fig. 96) with the full package of structural and property characterization necessary for this kind of material, along with density-functional theory (DFT) calculations. The synthetic route was again using a Pd-catalyzed Sonogashira coupling approach from the corresponding monomers (**423–425**; Fig. 96). The authors noted that intercalation in the *p*-phenylene-ethynylene main chain of BODIPY monomers induced a red-shift in the UV-absorption and photoluminescence (PL) spectra compared to BODIPY alone, which is reasoned as a consequence of the extended π -conjugation. From that also arise an intensely emitting behavior of the three copolymers in the range from the deep-red to NIR region ($\Phi_F = 33–49\%$). According to them, further studies are underway to design NIR luminescent conjugated polymers that will include aza-BODIPY monomers, in reason of the longer wavelength of the NIR emission.

The group of Liu reported two papers in 2009 in which they polymerized BODIPY monomers either as homopolymers or with fluorene, dialkyloxybenzene and thiophene derivatives by cross-coupling strategies (**429–433**; Fig. 96).^{238,239} In the first paper, they took advantage of the Pd-catalyzed Suzuki coupling approach to connect directly 9,9-dihexylfluorene to the β -position of three BODIPY monomers variously substituted in *meso* (**429–431**; Fig. 96).²³⁸ Through this strategy, they were able to tune the emission color of the significantly enhanced π -conjugated polyfluorenes obtained. The copolymers showed

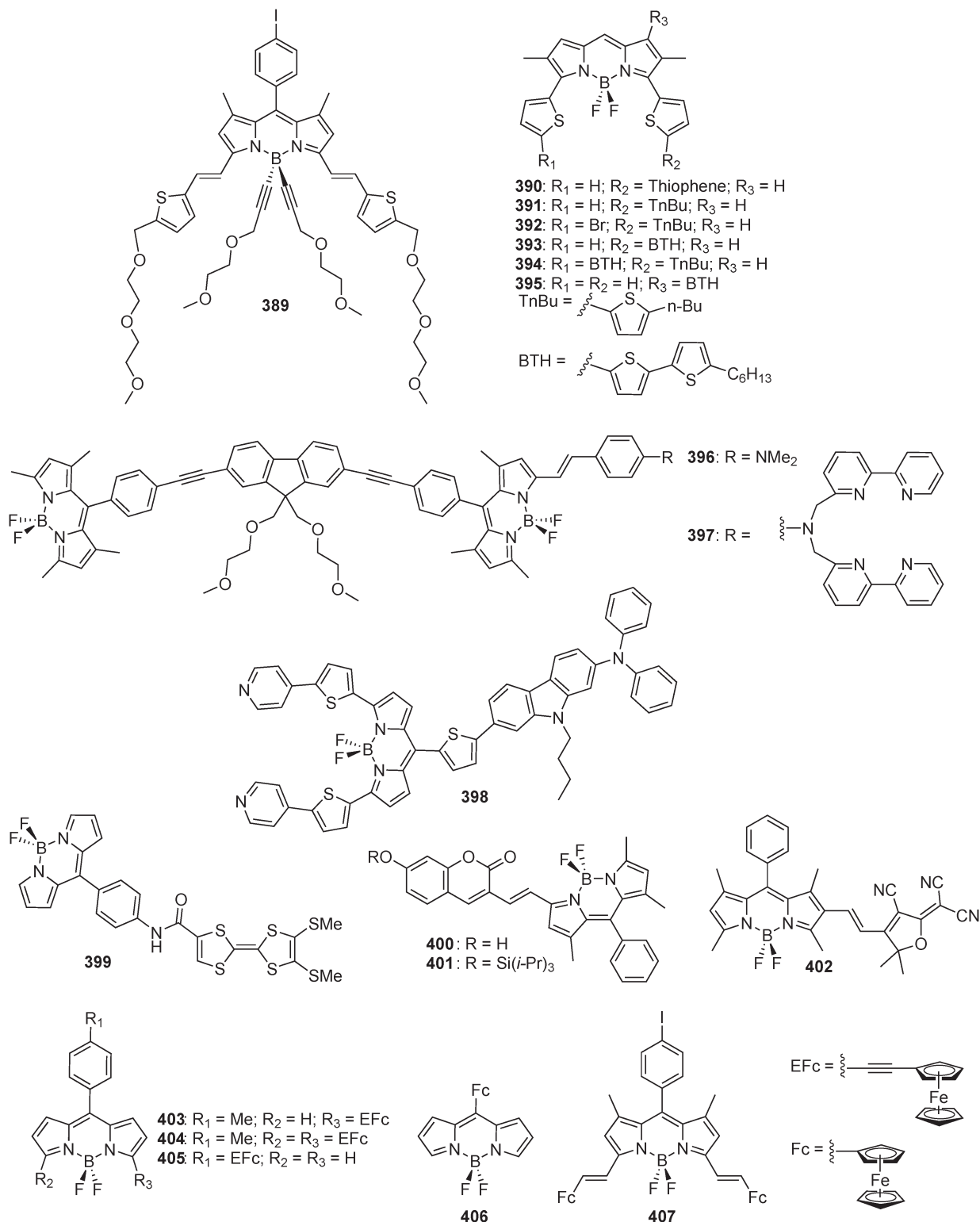


Fig. 93 Examples of interesting BODIPY dyes for OPV application.^{223–228,230,231}

absorption between 547 and 557 nm along with high molecular weight and good solubility in common organic solvents such as THF, DCM, chloroform and toluene. These properties are very encouraging for their incorporation in OPV devices. The second paper used the Pd-catalyzed Sonogashira polymerization

strategy to couple various 2,6-diethynyl-functionalized BODIPY monomers with either the corresponding 2,6-diiodo-functionalized BODIPY or 9,9-bis(6'-(hexylthio)hexyl)-2,7-diiodo-9H-fluorene, 1,4-diiodo-2,5-didecyloxybenzene and 2,5-diiodo-3-decylthiophenene (432–436; Fig. 96).²³⁹ In this case,

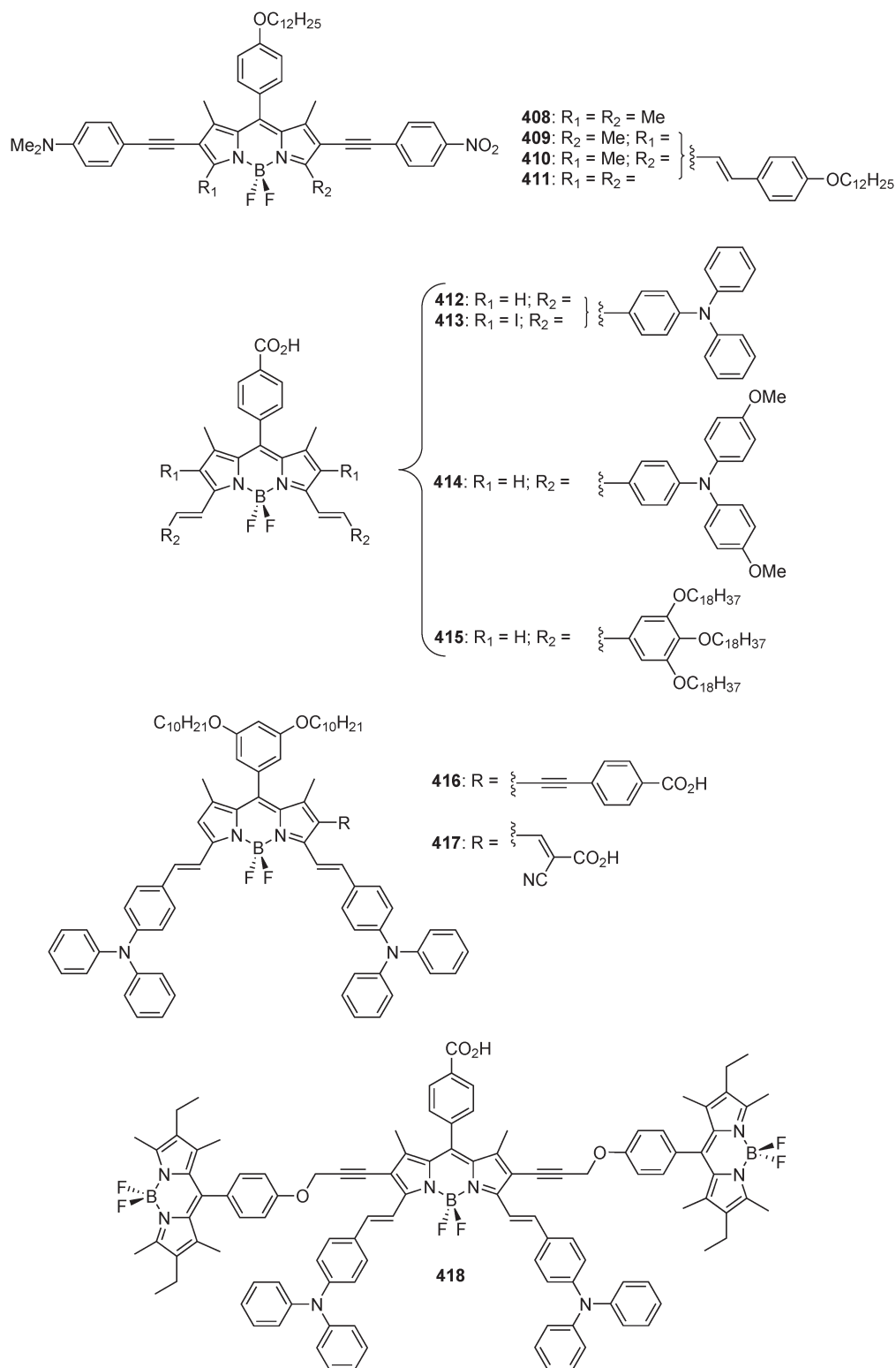


Fig. 94 Push-pull BODIPY derivatives.^{234,235}

absorption of the polymers was between 606 and 665 nm (**434** and **433**, respectively), pushed toward the NIR as compared to the first examples reported. In fact, polymers **433** and **436** were incorporated into OPV devices in collaboration with the group

of Fréchet to test them as electron donor materials.²¹⁹ The two polymers, presenting high absorption coefficients and low bandgaps of ~ 1.6 eV, were combined with the PCBM acceptor in solution-processed BHJSC (entries 16 and 17, Table 1). For

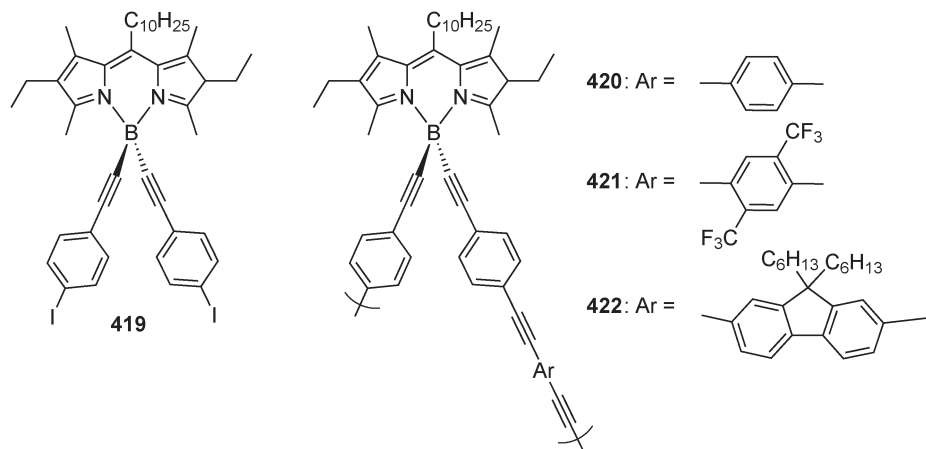


Fig. 95 Highly luminescent BODIPY-based organoboron polymers and their corresponding monomers.²³⁶

polymer **436**, a power conversion of 2.0% was achieved with $V_{OC} = 0.80$ V and $J_{SC} = 4.8$ mA cm⁻². With such bandgaps and LUMO levels around 3.70 eV, the polymers should theoretically be able to reach up to 7–8% of PCE (see Fig. 10). However, the authors pointed out that while the efficiency of 2.0% was at the time among the highest reported for dye-based materials, improvements in morphology control as well as structural modification were still needed to draw full benefit from this type of polymers.

Li and collaborators reported in 2008 a series of poly(aryleneethynylene)s containing BODIPY also obtained from the Sonogashira cross-coupling strategy (**437–440**; Fig. 96).²⁴⁰ While these polymers were synthesized and characterized for their nonlinear optical properties, their photophysical and electrochemical properties were assessed. Very interestingly, absorption maxima in the red region (between 535 and 640 nm) and low band-gaps were obtained (between 1.51 and 1.78 eV). These characteristics also make such polymers good candidates for their use as OPV materials.

Herrmann *et al.* reported in 2009 other examples of polymeric dyes bearing the BODIPY chromophore within the main chain.²⁴¹ They started from a diiodonated BODIPY monomer to prepare efficiently homo- and copolymers with a fully conjugated backbone *via* transition-metal-catalyzed polycondensation reactions (**441–443**; Fig. 96). The photophysical properties of the resulting polymeric materials were investigated in bulk and at the single molecule level. It was found by the authors that absorption and emission properties of BODIPY homopolymer **441** were similar to those of the parent BODIPY chromophore. In contrast, the copolymers made of 1,4-diethynylbenzene (**442**) and benzene (**443**) exhibited absorption and emission spectra that were shifted hypsochromically and bathochromically, respectively, in relation to the homopolymer. According to the authors, this behavior allows for easy color tuning by the appropriate choice of comonomers and encouraged them to direct efforts toward employing polymeric BODIPY dyes in organic electronic devices.

Zhu *et al.* reported lately the preparation *via* Sonogashira polymerization of four chiral NIR emissive polymers

incorporating styryl BODIPY derivatives and (*S*)-binaphthyl (**444–447**; Fig. 97).²⁴² Characterization by GPC, ¹H NMR and UV/Vis spectroscopy, cyclic voltammetry and circular dichroism was reported. In addition, they studied their derivatives by DFT calculations. The chiral polymers presented moderate molecular weights with high solubility in common solvents and stable chiroptical conformation. The four polymers also exhibited NIR emission and good anisotropic fluorescence, behavior expected to be useful in biological measurements and cellular imaging.

Hewavitharanage and collaborators reported another example of polymerization through the boron position.²⁴³ Their aim was to produce a D–A polymeric system where an organoboron quinolate acts as the D and the *E*-BODIPY moiety as the A (**448**; Fig. 98). Interestingly, the D part can absorb light at 264 nm and the BODIPY unit reemit at 525 nm the energy absorbed, giving rise to a 261 nm Stokes shift.

On the their hand, Skabara *et al.* presented in 2009 a redox stable low band gap conjugated polymer based on an EDOT–BODIPY–EDOT repeating unit (EDOT = 3,4-ethylene-dioxythiophene) connected at the α -position of the BODIPY.²⁴⁴ Interestingly, the preparation of this homopolymer has been made by electropolymerization from the EDOT–BODIPY–EDOT repeating unit (**449**; Fig. 99). A band gap of 0.8 eV, which is quite low and suitable for optoelectronic applications, was obtained with fully reversible n- and p-doping processes. The group of Algi also published two papers on copolymers incorporating EDOT as the comonomer of BODIPY derivatives through the β -position, with or without thiophene spacers (**450** and **451**; Fig. 99).^{245,246} Electropolymerization was again used to prepare environmentally robust electroactive materials bearing high stability, well-defined quasi-reversible redox couple and fast response time between redox states. All these properties clearly suggest that they would be suitable for OPV applications.

Bard and collaborators published another type of homopolymerisation synthetic route for the integration of BODIPY in the main chain. Instead of electropolymerisation, they used in that case anhydrous FeCl₃ in dichloromethane at room temperature to achieve the desired polymer exhibiting low MW

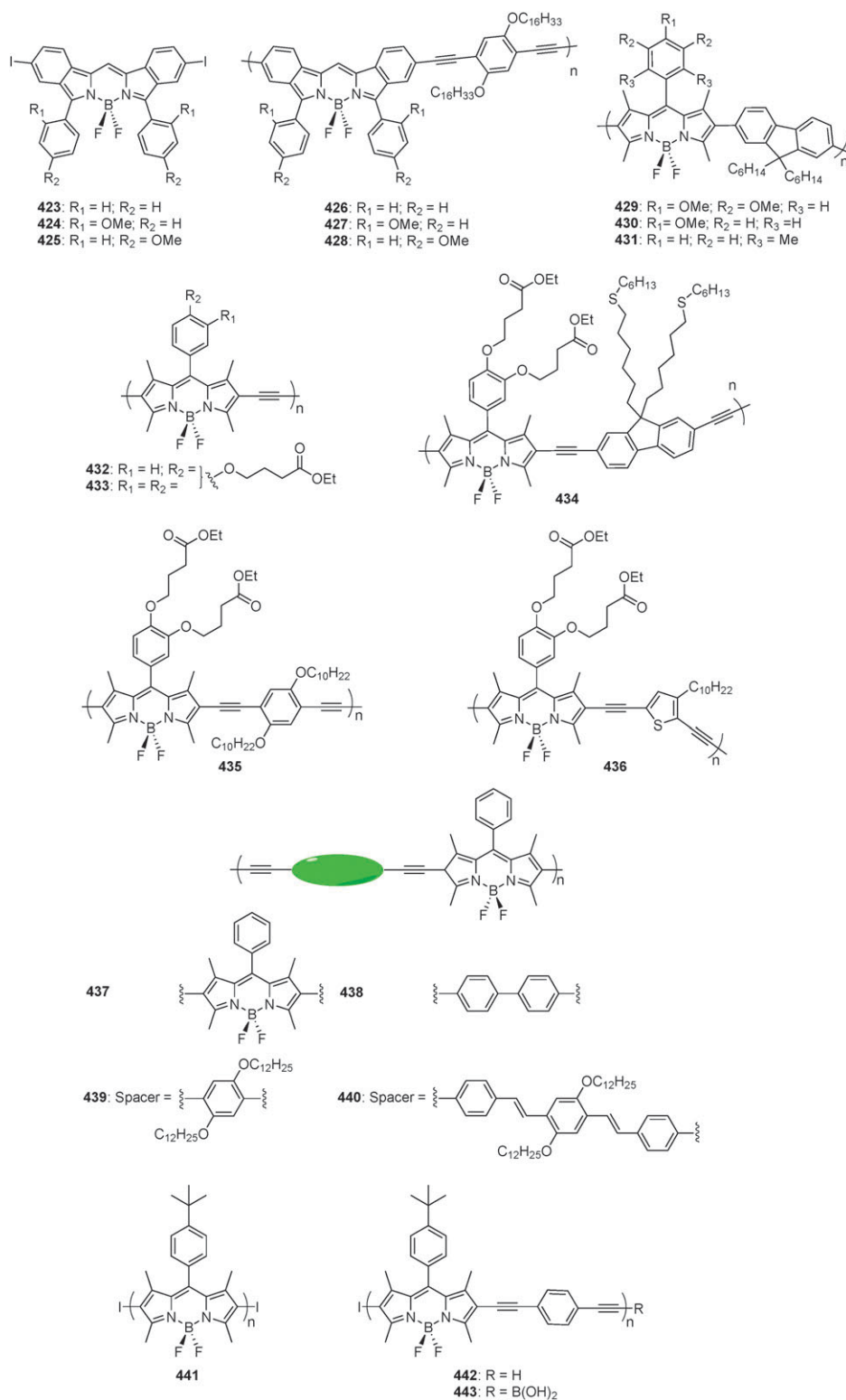


Fig. 96 BODIPY-based conjugated polymers.^{219,237–241}

along with dimers and trimers (452–456; Fig. 100).²⁴⁷ Noteworthy, another paper from Bard's group used a similar chemical approach combined with electrochemistry to afford dimers through the α - instead of the β -position (see Section 2.2.1).¹⁴¹

Other BODIPY-based alternating copolymers were reported lately taking advantage of the push-pull motif and clearly give hope for new BODIPY-based materials that can be useful in OPV applications. Thayumanavan and collaborators presented

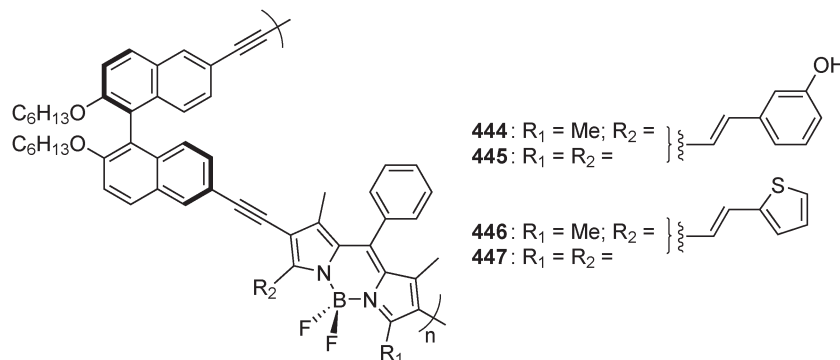


Fig. 97 Chiral NIR emissive polymers incorporating BODIPY derivatives and (*S*)-binaphthyl.²⁴²

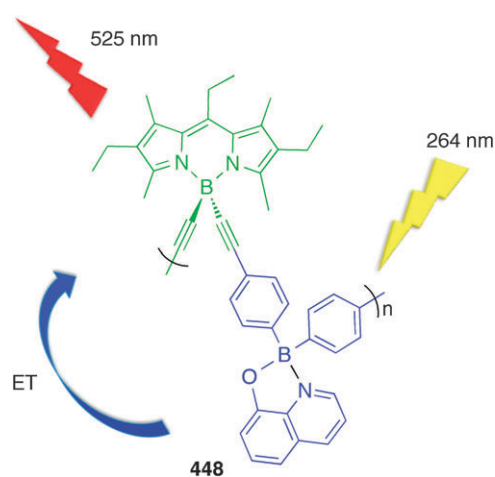


Fig. 98 *E*-BODIPY based fluorescent copolymer containing organoboron quinolate units.²⁴³

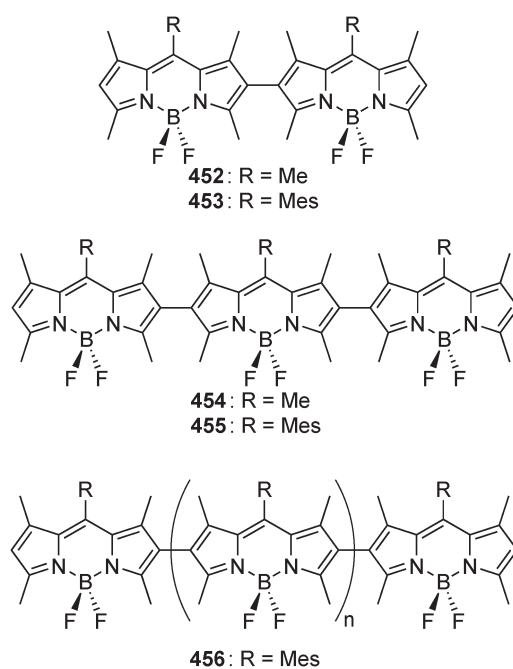


Fig. 100 BODIPY oligomers and homopolymer obtained by electrochemical polymerization with FeCl_3 .²⁴⁷

four novel π -conjugated alternating copolymers incorporating the BODIPY core as the donor and quinoxaline (Qx), 2,1,3-benzothiadiazole (BzT), *N,N'*-di(2'-ethyl)hexyl-3,4,7,8-naphthalene-tetracarboxylic diimide (NDI) and *N,N'*-di(2'-ethyl)hexyl-3,4,9,10-perylenetetracarboxylic diimide (PDI) as acceptors (**457–460**; Fig. 101).²⁴⁸ These new copolymers were synthesized *via* Pd-catalyzed Sonogashira polymerization and characterized by ^1H NMR, GPC, UV/visible spectroscopy and cyclic voltammetry techniques. DFT calculations were also performed on polymer repeat units and HOMO/LUMO energy levels obtained *in silico*

were compared to electrochemical results. The study revealed that copolymers with Qx and BzT possessed HOMO and LUMO energy levels comparable to those of the BODIPY homopolymer, while PDI stabilized both the HOMO and LUMO levels.

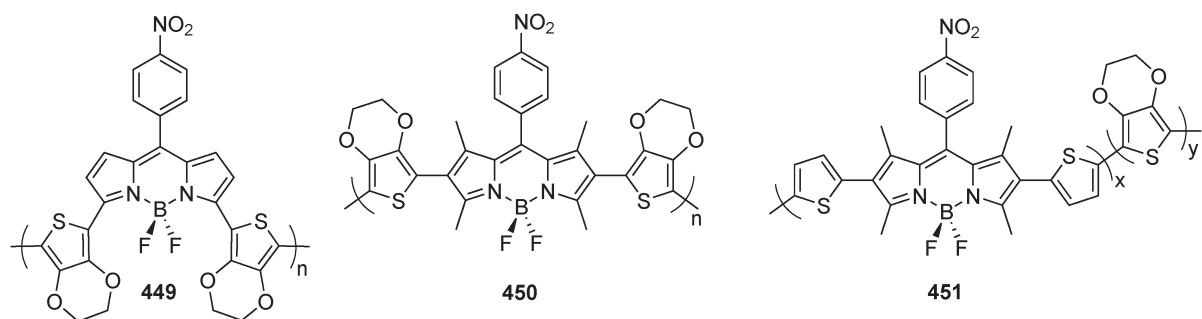


Fig. 99 EDOT-BODIPY copolymers obtained by electropolymerization.^{244–246}

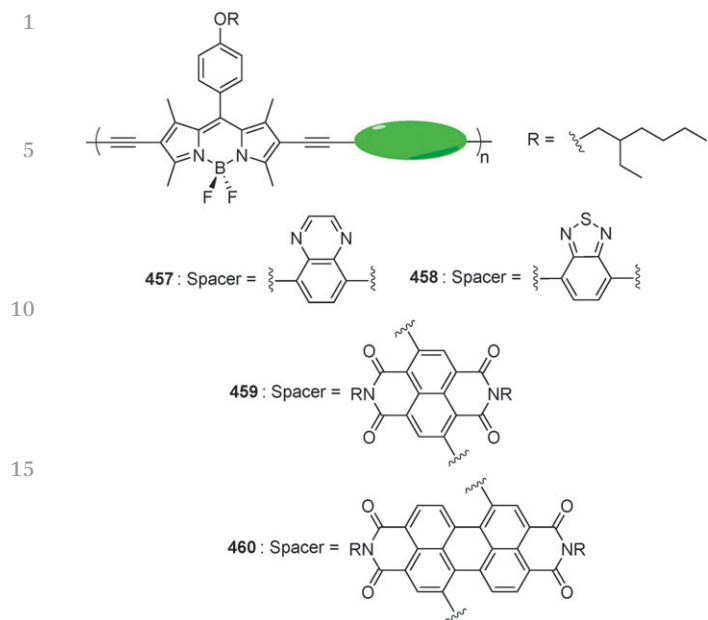


Fig. 101 BODIPY-based D–A π -conjugated alternating copolymers.²⁴⁸

Semiconductor behavior was studied in organic thin-film transistors (OTFT) and revealed that the homopolymer and Qz- and BzT-based copolymers showed only p-type behavior. On the other hand, copolymers with PDI and NDI exhibited only n-type behavior. Such polymers are definitely excellent candidates to be tested in OPV application as they present panchromatic absorption in the visible spectrum, low band-gaps and good charge transport properties.

2.3.2 DPM in side-chain polymers. Chujo and coworkers have also reported in 2010 water-soluble copolymers containing BODIPY dye.²⁴⁹ In this case, the hydrophobic BODIPY-based methyl methacrylate monomer **461** is integrated as a side-chain component *via* a reversible addition-fragmentation chain transfer (RAFT) copolymerization with the hydrophilic (2-dimethylamino)-ethyl methacrylate (DMAEMA) monomer in different ratios to give a copolymer of general structure **462** (Fig. 102). While these copolymers are not basically intended for optoelectronic applications, they have the interesting feature of being water-soluble. The authors have shown the high sensitivity of such copolymers toward the hydrophobic–hydrophilic balance. This is represented

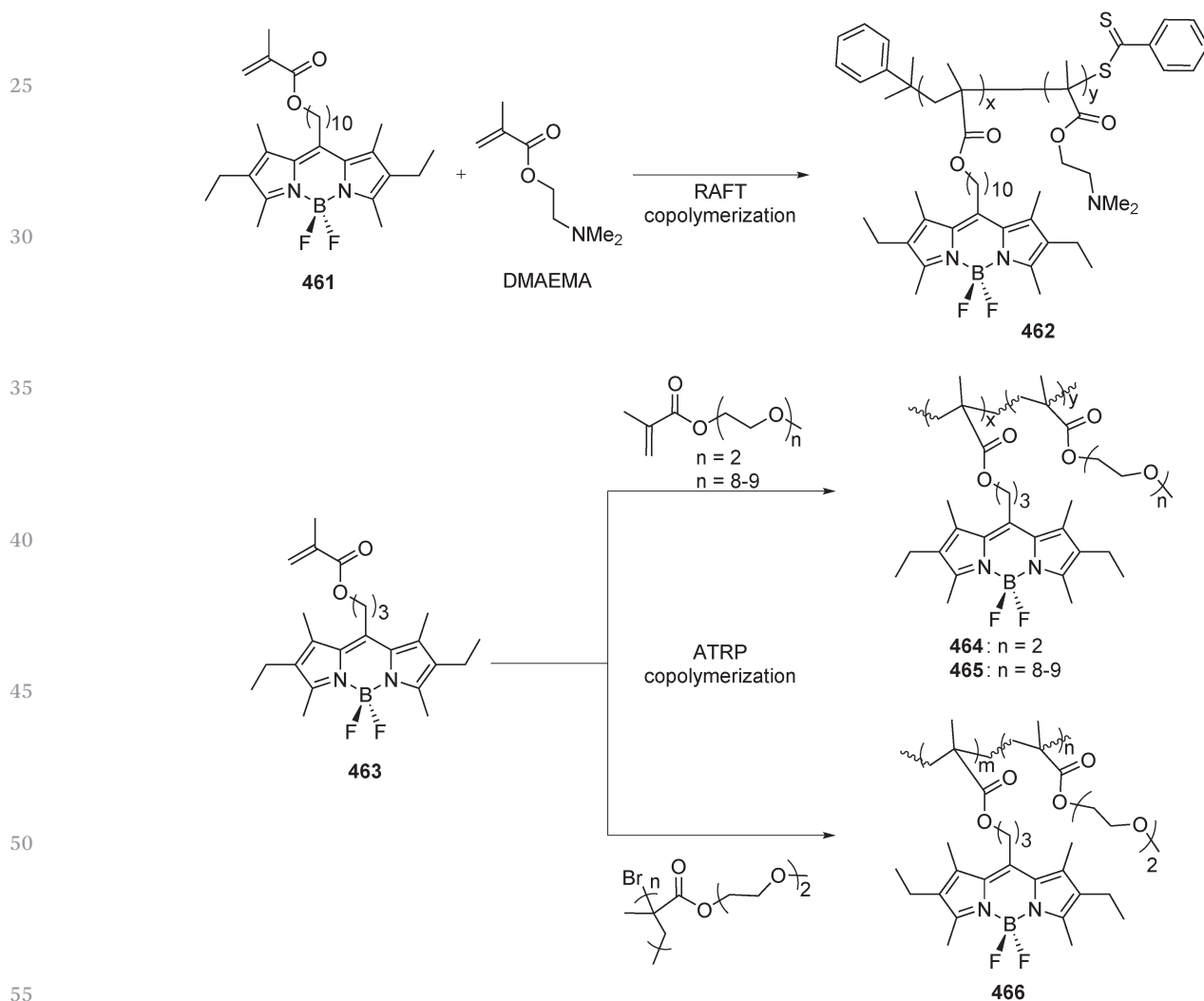


Fig. 102 BODIPY-based methyl methacrylate monomers used in RAFT and ATRP polymerizations along with their corresponding copolymers.^{249,250}

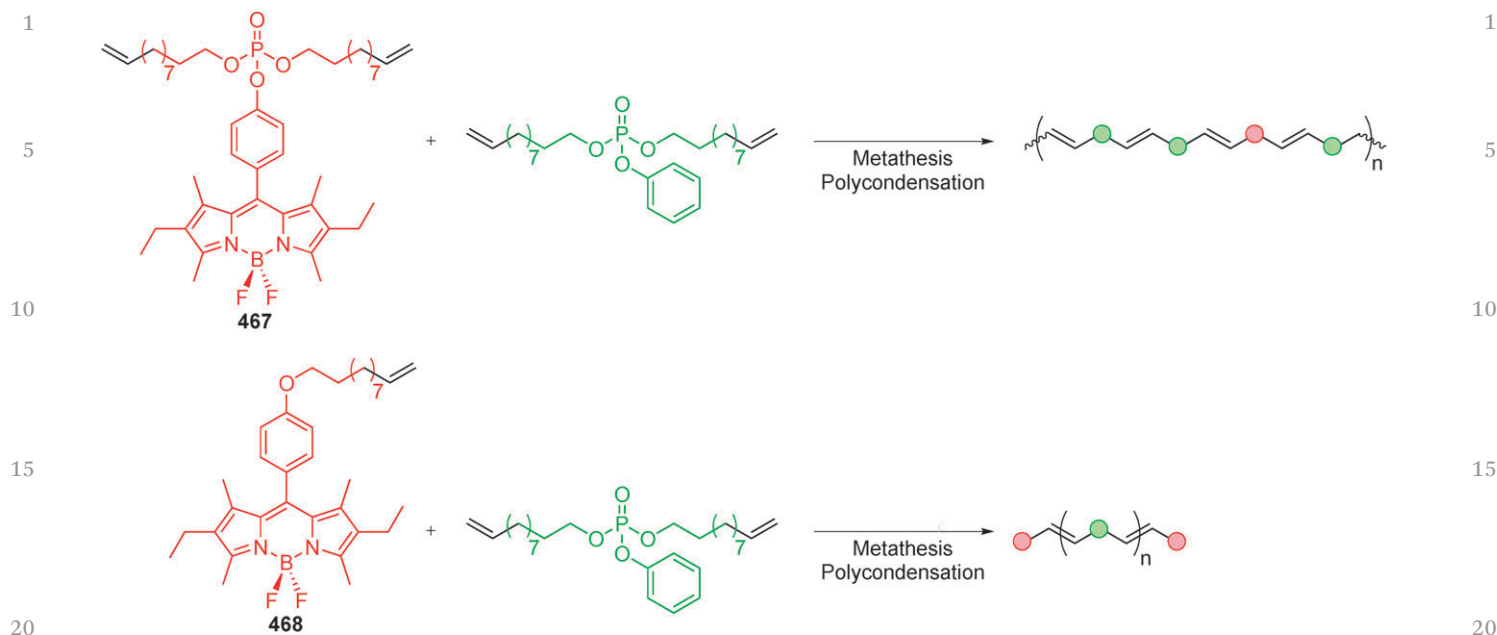


Fig. 103 Polyolefins integrating BODIPY chromophores as monomers and chain stoppers.²⁵¹

by the phase-separation occurring at lower temperature, *i.e.* lower critical solution temperature (LCST), when hydrophobic BODIPY content is increased. In fact, a ratio of only 1% or less of the BODIPY-containing monomer has led to water-soluble polymers. Also, they have called attention to the effective decrease/increase of emission intensity on heating and cooling in water causing the formation/inhibition of H-aggregation between two BODIPY planes in the LCST-type copolymers. This last assumption was supported by UV-visible absorption, PL and dynamic light-scattering (DLS) experiments. Their future plans for this kind of compounds are to develop BODIPY-based copolymers and hydrogels exhibiting color tuning of fluorescence by LCST.

Liras and coworkers reported BODIPY-conjugated thermo-sensitive fluorescent polymers based on 2-(2-methoxyethoxy)ethyl methacrylate (**464–466**; Fig. 102).²⁵⁰ Their synthetic

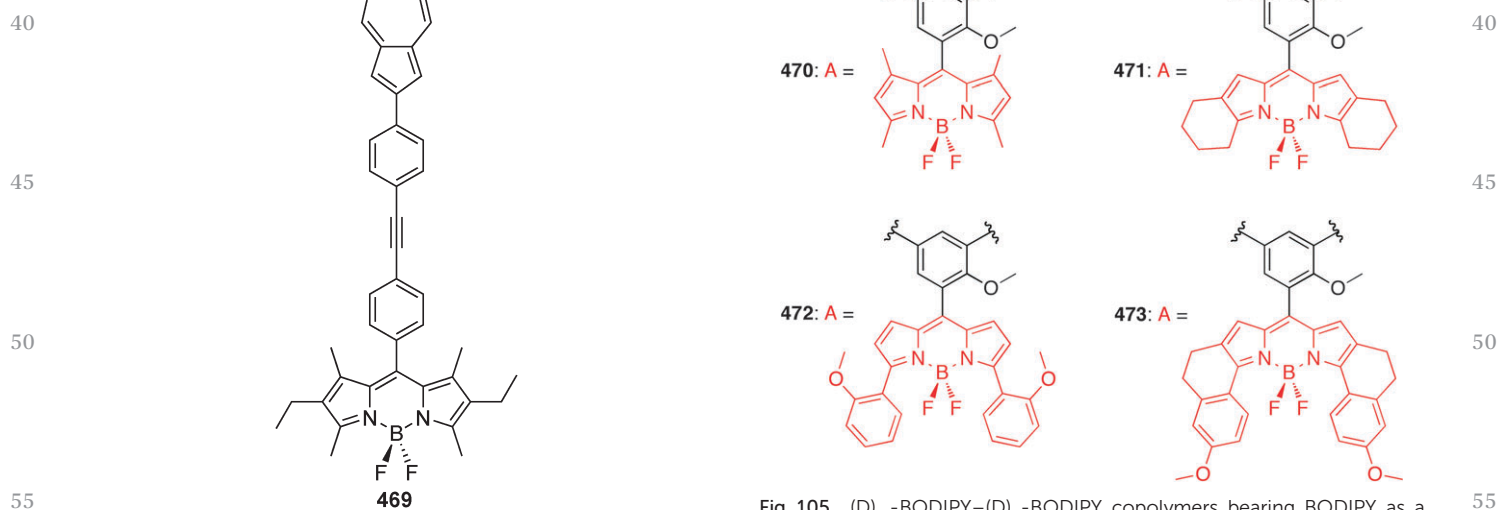


Fig. 104 Azulene dyad incorporating a BODIPY chromophore.²⁵²

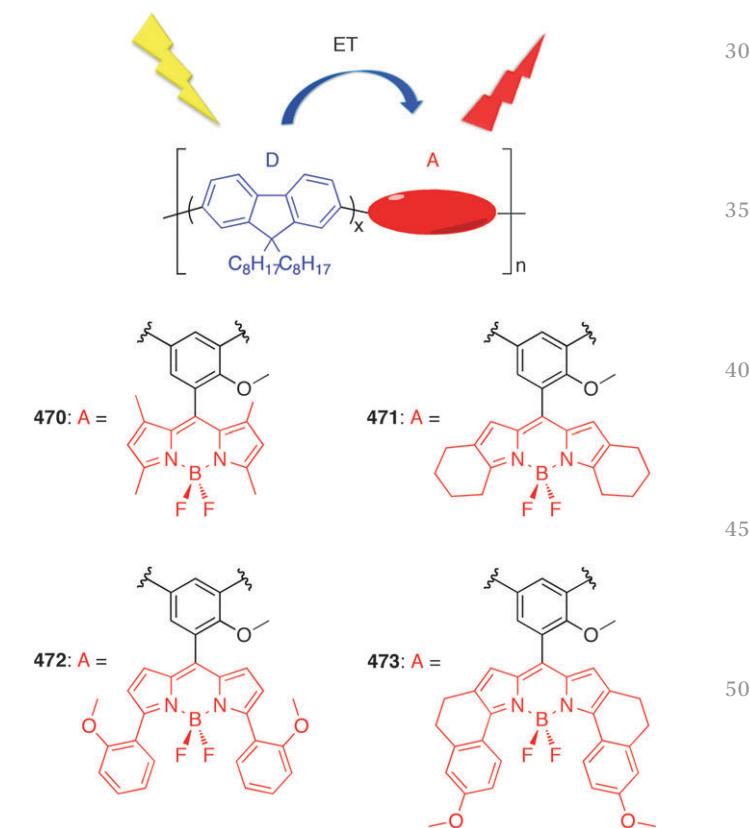


Fig. 105 $(D)_m$ -BODIPY- $(D)_n$ -BODIPY copolymers bearing BODIPY as a side chain.²⁵³

1 methodology was based on a methacrylic monomer containing
the BODIPY dye **463** that was incorporated by atom transfer
5 radical polymerization (ATRP) in three different thermo-

sensitive families of polymers based on 2-(2-methoxy-
ethoxy)ethyl methacrylate (MEO₂MA). The first one was con-
stituted of linear random terpolymers of general structure **464**

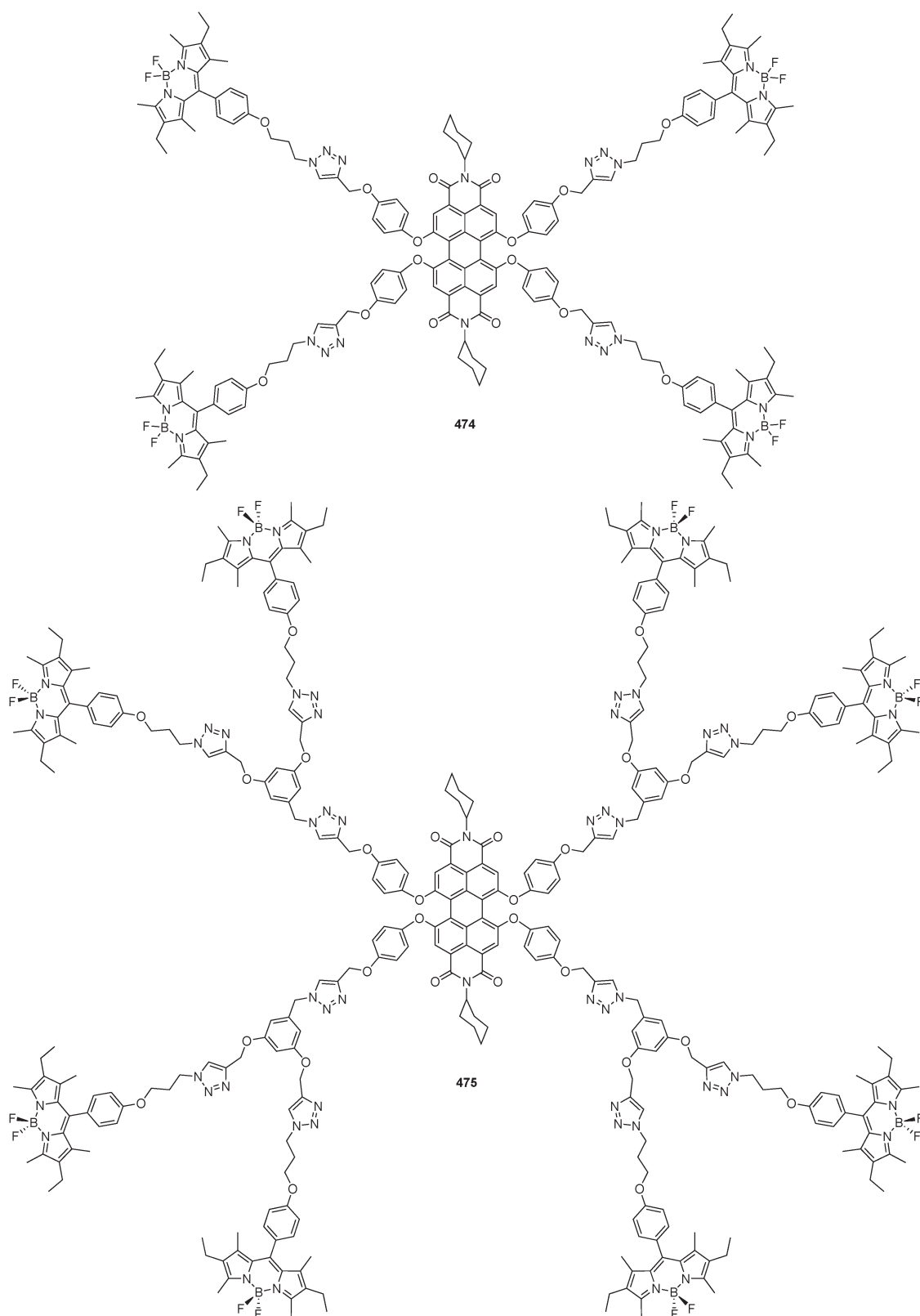


Fig. 106 Dendrimeric structures containing BODIPY and PDI units.²⁵⁵

and **465**. The second family was made of diblock copolymers **466** and the third one was a MEO₂MA-BODIPY based hydrogel (not shown).

Lately, Wurm *et al.* prepared polyolefins integrating BODIPY chromophore **467** as a monomer and **468** as a chain stopper (Fig. 103).²⁵¹ These chromophores were integrated by metathesis polycondensation with phenyl-di-(10-undecenyloxy)-phosphate comonomer using Grubbs' first-generation catalyst to give the resulting polymers. This method constitutes an interesting general method that can be used to design new polymers suitable for OPV application.

Nöll *et al.* reported another example of polymer incorporating a BODIPY as a side chain in 2011. In this case, a BODIPY chromophore was attached to an azulene to obtain a dyad (**469**; Fig. 104). Absorption spectra of the dyad showed a strong absorption band in the visible range dominated by the BODIPY. Fluorometric studies revealed that after excitation of the BODIPY subchromophoric unit, the azulene moiety efficiently quenched the system mainly through energy transfer, whereas charge transfer interactions play only a

minor role. They further electropolymerized the dyad at the surface of the electrode, but mentioned that further characterization of the product is a subject of further studies.

Finally, Burgess reported other examples using BODIPYs as side chains in polymeric structures.²⁵³ Four donor-acceptor systems were prepared to investigate the optical properties of copolymers comprised of polyfluorene doped with BODIPY-based fluors (**470–473**; Fig. 105). Their underlying hypothesis was energy harvested *via* the strong absorptivity of the major component, fluorene, would be primarily emitted from the BODIPY parts at much longer wavelength. The synthetic approach used was the Suzuki cross-coupling polymerization, yielding molecular weight ranging from 7 to 15 kDa. The authors mentioned that their system has several donors per acceptor part and therefore offers potential for fluorescent probe design, OLEDs and lasing materials. We also believe that simple replacement of the fluorene comonomer by 2,7-carbazole derivatives might lead to interesting OPV materials, in a similar fashion to PCDTBT.²⁵⁴

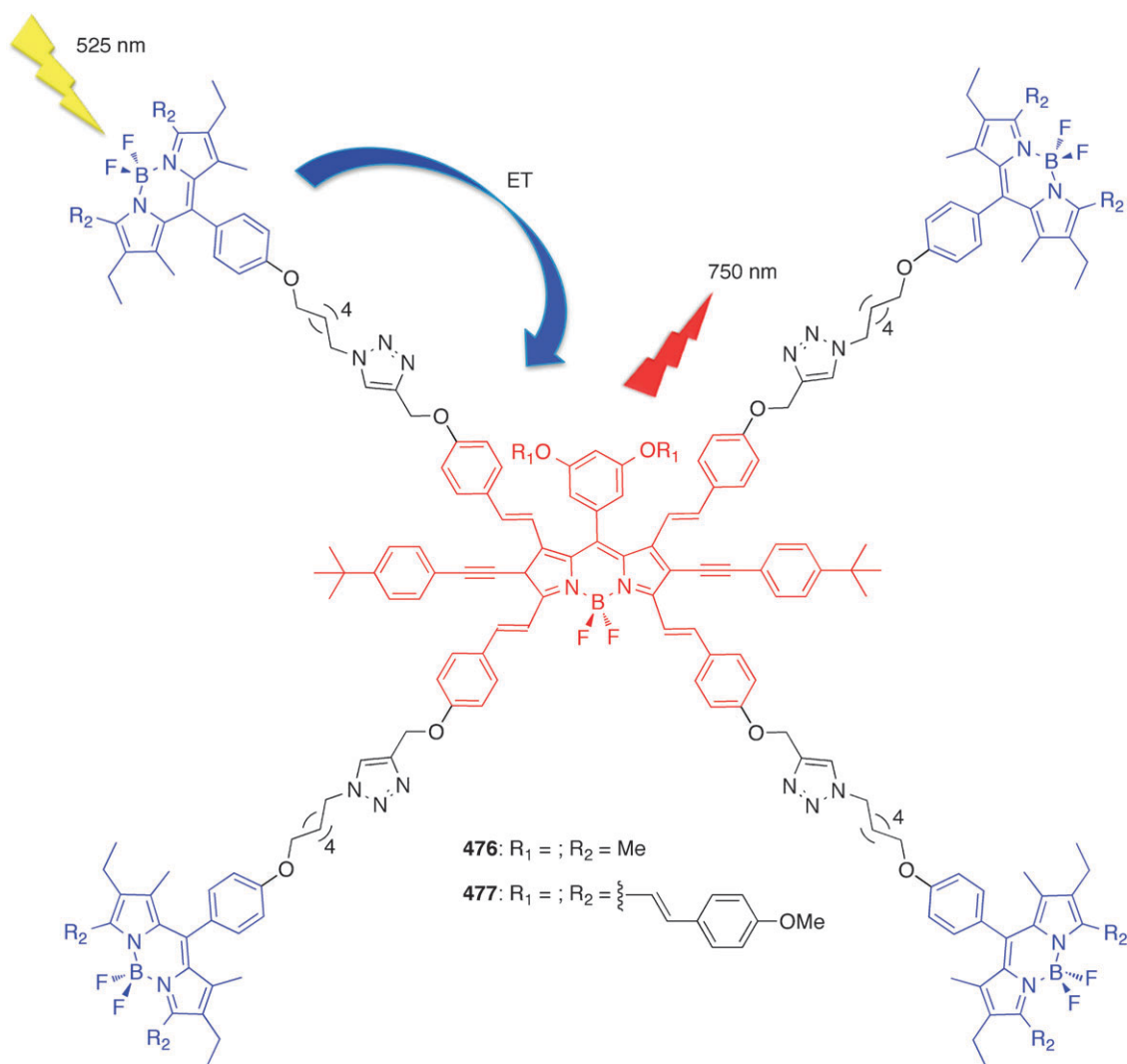


Fig. 107 Tetrastryl-BODIPY-based light-harvesting dendritic system.²⁵⁶

2.3.3 DPM and ADPM in dendritic polymers and MOFs.

The last BODIPY-containing macromolecular materials to be

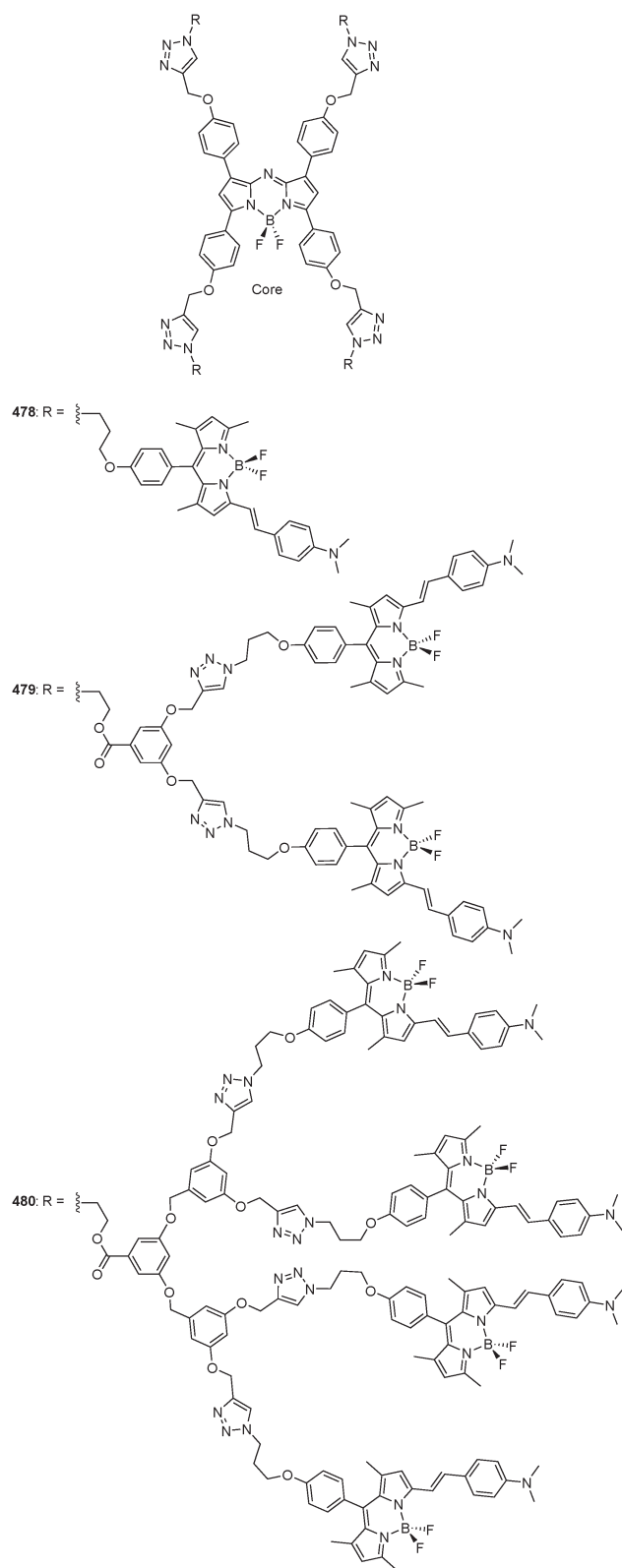


Fig. 108 Structure of dendritic light-harvesting systems containing an aza-BODIPY acceptor surrounded by BODIPY donors.²⁵⁷

presented in this review concern dendrimeric assemblies and metal–organic frameworks (MOFs). Akkaya and co-workers published in 2010 the convergent synthesis of dendritic BODIPY appended perylene-diimide dyes and the study of their light-harvesting properties.²⁵⁵ Two dendrimers were obtained, one with 4 and the other with 8 BODIPY units at the periphery with a perylene-diimide (PDI) dye at the core (474 and 475, respectively; Fig. 106). As mentioned, the synthetic approach combines a convergent one along with click-chemistry between azides and terminal alkynes (Huisgen reaction). The great potential of this system is demonstrated since light is effectively collected as a result of the large absorption cross-section of the dendrimer and efficiently channeled to the core PDI unit. Overall, the system functions like an antenna, mimicking natural light harvesting. The authors exposed the advantage of their judicious design to encounter the general rule of decreasing efficiency of energy transfer when the cross-section is enlarged, even with the increase of absorption that it generates. This design is based on the great spectral overlap between the energy donor chromophores, BODIPY, and the core PDI energy acceptor. Akkaya and his team arrived at the conclusion that BODIPY and PDI are a good match for that kind of a system and that the versatility of chemistry allowed by BODIPY derivatives will lead in the future to light-harvesting systems with a strong directional energy transfer. They recently published a second paper on a tetrasteryl-BODIPY-based dendritic light harvester (477; Fig. 107) and estimated the energy transfer efficiency of such a system by comparison with its related methyl-substituted derivative 476.²⁵⁶ The authors transformed versatile BODIPY dyes into bright NIR-emitting fluorophores by quadruple styryl substitutions and proved that an efficient synthesis of a light harvester is possible when clickable functionalities on the styryl moieties are inserted.

In 2009, Li prepared dendritic systems working in an antenna fashion.²⁵⁷ Interestingly, they used an aza-BODIPY as the core unit and energy transfer acceptor, while multi-donor BODIPY chromophores were integrated in the periphery (478–480; Fig. 108). Synthesis of these macromolecular assemblies was achieved by an efficient “click-chemistry” by Cu^I-catalyzed 1,3-dipolar cycloaddition. This antenna system allowed the migration of the excited-state energy of BODIPY units in the periphery toward the core unit by fluorescence resonance energy transfer. In fact, selective excitation of the donor gave a high ET, in the order of >90% efficiency. Amplified emission also occurs in the process. The authors pointed out that such a facile approach for extending the functionalization of aza-BODIPYs should open the way for development of novel NIR dyes for numerous applications in optical devices.

Reiser and collaborators combined a covalent and a non-covalent immobilization strategy as a new general method for the synthesis of multifunctional carbon nanomaterials (481 and 482; Fig. 108).²⁵⁸ Highly magnetic carbon-coated cobalt nanoparticles (Co/C) served as a scaffold for noncovalent functionalization of pyrene-tagged BODIPY fluorescent dye through π – π stacking interactions. Next to the reversibly immobilized pyrene-tagged dye, fully covalent functionalization of the

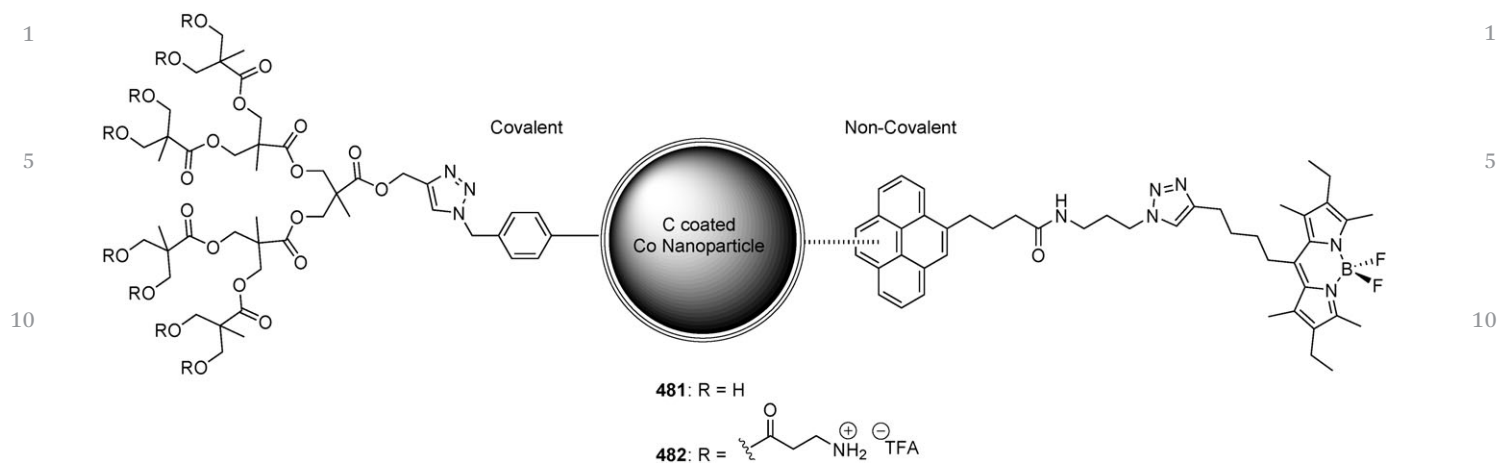


Fig. 109 Combined covalent and noncovalent functionalization of cobalt/carbon nanoparticles with dendrimers and BODIPY fluorescent dye.²⁵⁸

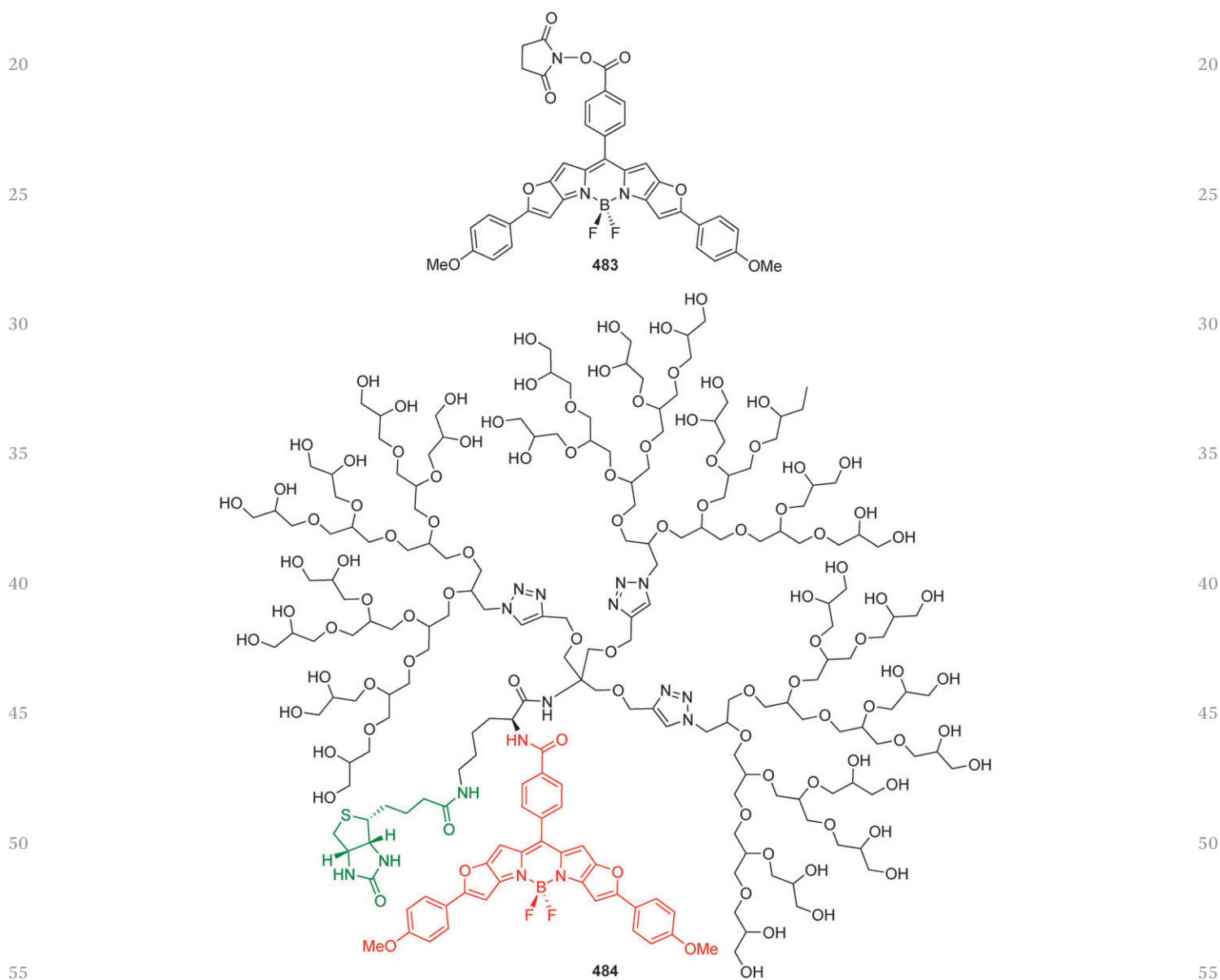


Fig. 110 Water-soluble biotinylated PGD-BODIPY and its precursor.²⁵⁹

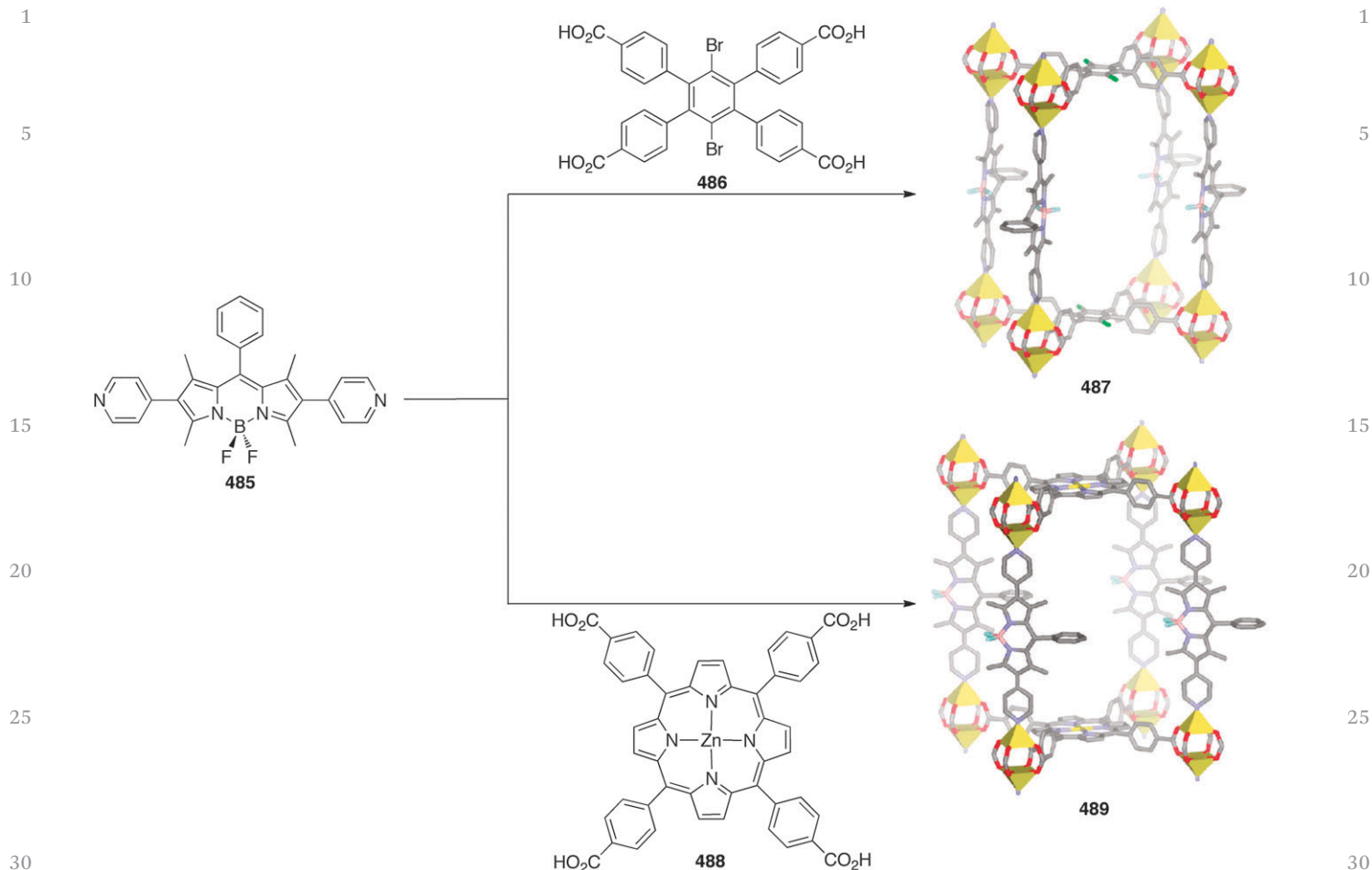


Fig. 111 MOFs incorporating BODIPY in the assembly.²⁶⁰ (Adapted with permission from *J. Am. Chem. Soc.*, 2011, **133**(40), 15858–15861. Copyright© 2011 American Chemical Society.)

magnetic core-shell nanoparticles was accomplished by grafting dendrimers *via* “click chemistry”. Alternatively, the nanoparticle surface could be covalently functionalized with a BODIPY dye following the same procedure.

On their side, Zimmerman *et al.* published the dendritic single-molecule fluorescent probe **484** that is monovalent, photostable and minimally blinking based on the BODIPY derivative **483** (Fig. 109).²⁵⁹ This probe, based on a ring-fused BODIPY core that is conjugated to a polyglycerol dendrimer (PGD), makes the hydrophobic fluorophore **483** water-soluble. The dendrimer emits in the far-red region (705 nm) in a long and stable fashion, without the necessity for an anti-fading agent such as Trolox. These interesting properties were reported to greatly simplify the use of the fluorophore for imagery applications (Fig. 110).

Finally, a nice example integrating BODIPY in light-harvesting MOFs was reported in 2011 by Hupp and collaborators.²⁶⁰ They prepared two different assemblies from BODIPY ligand **485**, one isostructural (**487**) and the other one with a pillared-paddlewheel type structure (**489**) featuring both BODIPY and Zn^{II}-porphyrine **488** (Fig. 111). Due to a well-organized D–A assembly, the nearly black crystals of **489** present essentially quantitative structure-to-structure energy transfer (*i.e.* **485**-to-**488**; antenna effect) and are

capable of panchromatic light-harvesting. The authors pointed out that while this energy transfer is efficient and rapid, the effectiveness of pillared-paddlewheel materials similar to **489** in moving excitons between proximal, well-aligned, and chemically identical structures/chromophores still needs to be established. From our point of view, such a system might be very interesting in the context of OPV materials if the directionality of the generated charges and processability issues can be addressed. Actually, other examples of light-harvesting hybrid assemblies have been recently reviewed by George *et al.* and might provide interested readers insights into the subject.²⁶¹ Also, the integration of small BODIPY molecules into MOF's structure might be an easy way to access new interesting photophysical properties, as proved lately by Manzano *et al.*, by obtaining dual absorption in the UV-vis when confining a BODIPY dye in LTL zeolite nanochannels.²⁶²

Outlook and concluding remarks

This review article intended to present the most recent developments in the use of materials based on dipyrromethenes and some of their structurally related azadipyrromethenes for

1 organic photovoltaic applications. As these materials are fairly
 new in the already well-known domain of converting light into
 electrical current, a survey of the recent research was done. We
 presented and discussed the variety of relevant design, syn-
 5 thetic methodologies and photophysical studies showing the
 more promising results for the improvement of conversion
 efficiency of both small-molecule and macromolecular based
 organic solar cells that incorporate DPM in their architecture.
 Many inherent advantages of DPM derivatives led us to believe
 10 in their strong potential for OPV applications in the forth-
 coming years. First, their great optical properties, *i.e.* high
 molar extinction coefficients and absorption/emission in the
 NIR, make them competitive with porphyrinoids and other NIR
 chromophores. Second, they offer abundant leverage possibi-
 15 lities for fine-tuning the photophysical properties by variation
 of the substituents. Finally, they present greater versatility of
 metal coordination geometries allowed by a bidentate motif
 compared to the more rigid square planar one of the parent
 porphyrinoid family. This is definitively of great interest in the
 20 perspective of developing new OPV materials taking advantage
 of the metallic center as a way to coarsely tune energy levels.
 Overall, DPM based materials appear to fulfill the requirements
 of reliability, versatility and ease of preparation needed for the
 design of OPV materials at low cost that will be able to convert a
 25 part of the tremendous 3×10^{24} J provided to our planet each
 year by the Sun.

List of abbreviations

A	Acceptor
ADPM	Azadipyromethene
ATRP	Atom transfer radical polymerization
BAEB	Bis(arylethynyl)benzene
35 BHJ	Bulk-heterojunctions
BHJSC	Bulk-heterojunction solar cells
Bpy	Bipyridine
BzT	2,1,3-Benzothiadiazole
C _{xx}	Fullerene derivative containing XX carbons
40 CuAAC	Cu ^I -catalyzed azide-alkyne cycloaddition
Cys	Cysteine
D	Donor
D–A	Donor–acceptor
DFT	Density-functional theory
45 DMAEMA	(2-Dimethylamino)ethyl methacrylate
DPM	Dipyromethene
DSSC	Dye-sensitized solar cells
<i>E</i>	Energy
<i>E_d</i>	Energy of the downhill driving force
50 <i>E_g</i>	Band-gap energy
ECL	Electrogenerated chemiluminescence
EDOT	3,4-Ethylene-dioxythiophene
EQE	External quantum efficiency
ET	Energy transfer
55 EET	Electronic energy transfer
ETA	Extremely thin absorber

eV	Electron volt	1
FF	Fill factor	
FRET	Fluorescence resonance energy transfer	
GSH	Glutathione	
Hcy	Homocysteine	5
HOMO	Highest occupied molecular orbital	
ICT	Intramolecular charge transfer	
IC ₇₀ BA	Indene-C ₇₀ bisadduct	
ITO	Indium tin oxide	
IL	Intra-ligand	10
<i>J_L</i>	Light-generated current	
<i>J_{MP}</i>	Current of the maximum power output	
<i>J_{SC}</i>	Short-circuit current density	
<i>J–V</i>	Current–voltage curve	
L	Ligands	15
LCST	Lower critical solution temperature	
LED	Light emitting diode	
LH	Light-harvesting	
LUMO	Lowest unoccupied molecular orbital	
MLCT	Metal-to-ligand charge transfer	20
MOF	Metal–organic framework	
NBS	<i>N</i> -Bromosuccinimide	
NDI	<i>N,N'</i> -Di(2'-ethyl)hexyl-3,4,7,8- naphthalenetetracarboxylicdiimide	
NIR	Near infrared	25
OLED	Organic light emitting diode	
OPV	Organic photovoltaic	
OSC	Organic solar cell	
OTFT	Organic thin film transistor	
<i>P_{in}</i>	Power input	30
<i>P_{out}</i>	Power output	
PCBM	[6,6]-Phenyl-C ₆₁ -butyric acid methyl ester	
PCE (<i>η</i>)	Power conversion efficiency	
PDI	Perylenediimide	
PEDOT:PSS	Poly(3,4-ethylene- dioxothiophene):poly(styrenesulfonate)	35
PHJSC	Planar-heterojunction solar cells	
PL	Photoluminescence	
PMMA	Poly(methyl methacrylate)	
PSC	Polymeric solar cells	40
PTZ	Phenothiazine	
Qx	Quinoxaline	
RAFT	Reversible addition-fragmentation chain transfer	
S	Spacer	
S _E Ar	Electrophilic aromatic substitution	45
S _N	Nucleophilic substitution	
S _N Ar	Nucleophilic aromatic substitution	
SWNT	Single wall carbon nanotube	
TAEB	Tetrakis(arylethynyl)benzene	
TAEP	Tetrakis(arylethynyl)-1,4-pyrazine	50
TAT	Triazatruxene	
TCBD	1,1,4,4-Tetracyanobuta-1,3-dione	
TD-DFT	Time-dependent density-functional theory	
TTA	Triplet–triplet annihilation	
TTF	Tetrathiafulvalene	55
UV	Ultraviolet	

1	V_B	Built-in potential
	V_{MP}	Voltage of the maximum power output
	V_{OC}	Open-circuit voltage
	ZnPc	Zn ^{II} -phthalocyanine
5	ZnTPP	Zn ^{II} -tetraphenylporphyrin
	λ_{ab}	Absorption wavelength
	λ_{em}	Emission wavelength
	Φ_F	Quantum yield of fluorescence (excited at λ_{ab})
	Φ_T	Quantum yield for the triplet generation
10	$\Phi(^1O)$	Quantum yield for the singlet oxygen generation

Acknowledgements

15 GSH thanks the Natural Sciences and Engineering Research Council of Canada (NSERC), the Centre for Self-Assembled Chemical Structures and the Direction des Relations Internationales (Université de Montréal, UdeM) for financial support. AB is thankful to NSERC, Fonds de recherche du Québec – Nature et technologies (FRQNT) and Saint-Jean Photochemicals Inc. (sjpc.com) for a BMP-Innovation grant and to UdeM for an excellence grant. The authors also thank Anne-Catherine Bédard for her help in the revision process of the manuscript along with Dr Denis Désilets and Francis Bélanger for useful scientific discussions.

Notes and references

- 1 M. Z. Jacobson and M. A. Delucchi, *Sci. Am.*, 2009, **301**, 58–65.
- 2 M. Gratzel, *Nature*, 2001, **414**, 338–344.
- 3 N. Armaroli and V. Balzani, *Energy Environ. Sci.*, 2011, **4**, 3193–3222.
- 4 **Q18** *Nat. Mater.*, 2012, **11**, 173.
- 5 *Nat. Mater.*, 2012, **11**, 178–179.
- 6 M. A. Green, K. Emery, Y. Hishikawa, W. Warta and E. D. Dunlop, *Prog. Photovoltaics*, 2012, **20**, 12–20.
- 7 G. Dennler, M. C. Scharber and C. J. Brabec, *Adv. Mater.*, 2009, **21**, 1323–1338.
- 8 Polyera Corporation, *Polyera Achieves World-Record Organic Solar Cell Performance*, 2013, Retrieved from: <http://www.polyera.com/newsflash/polyera-achieves-world-record-organic-solar-cell-performance>.
- 9 Sumitomo Chemical Corporation, *Material from Sumitomo Chemical Employed in UCLA's Tandem Polymer Photovoltaic Cell Achieving Power Conversion Efficiency of 10.6%*, 2012, Retrieved from: <http://www.sumitomo-chem.co.jp/english/newsreleases/docs/20120214e.pdf>.
- 10 Heliatek GmbH, *Heliatek achieves new world record for organic solar cells with certified 9.8% cell efficiency*, 2011, Retrieved from: http://www.heliatek.com/newscenter/latest_news/heliatek-erzielt-mit-98-zertifizierter-zelleffizienz-neuen-weltrekord-fur-organische-solarzellen/?lang=en#.
- 11 Y. Sun, G. C. Welch, W. L. Leong, C. J. Takacs, G. C. Bazan and A. J. Heeger, *Nat. Mater.*, 2012, **11**, 44–48.
- 12 D. Gendron and M. Leclerc, *Energy Environ. Sci.*, 2011, **4**, 1225–1237.
- 13 G. D. Scholes, G. R. Fleming, A. Olaya-Castro and R. van Grondelle, *Nat. Chem.*, 2011, **3**, 763–774.
- 14 I. Radivojevic, A. Varotto, C. Farley and C. M. Drain, *Energy Environ. Sci.*, 2010, **3**, 1897–1909.
- 15 M. V. Martinez-Diaz, G. de la Torre and T. Torres, *Chem. Commun.*, 2010, **46**, 7090–7108.
- 16 M. G. Walter, A. B. Rudine and C. C. Wamser, *J. Porphyrins Phthalocyanines*, 2010, **14**, 759–792.
- 17 H. Lemmetyinen, N. V. Tkachenko, A. Efimov and M. Niemi, *Phys. Chem. Chem. Phys.*, 2011, **13**, 397–412.
- 18 C. W. Tang and A. C. Albrecht, *J. Chem. Phys.*, 1975, **62**, 2139–2149.
- 19 M. Grätzel, *Acc. Chem. Res.*, 2009, **42**, 1788–1798.
- 20 G. C. Vougioukalakis, A. I. Philippopoulos, T. Stergiopoulos and P. Falaras, *Coord. Chem. Rev.*, 2011, **255**, 2602–2621.
- 21 Y.-J. Cheng, S.-H. Yang and C.-S. Hsu, *Chem. Rev.*, 2009, **109**, 5868–5923.
- 22 M. C. Scharber, D. Mühlbacher, M. Koppe, P. Denk, C. Waldauf, A. J. Heeger and C. J. Brabec, *Adv. Mater.*, 2006, **18**, 789–794.
- 23 C. Jiao, K.-W. Huang, J. Luo, K. Zhang, C. Chi and J. Wu, *Org. Lett.*, 2009, **11**, 4508–4511.
- 24 A. Mishra and P. Bäuerle, *Angew. Chem., Int. Ed.*, 2012, **51**, 2020–2067.
- 25 H. Dau and I. Zaharieva, *Acc. Chem. Res.*, 2009, **42**, 1861–1870.
- 26 Y. Li, *Acc. Chem. Res.*, 2012, **45**, 723–733.
- 27 F. Fabregat-Santiago, G. Garcia-Belmonte, I. Mora-Sero and J. Bisquert, *Phys. Chem. Chem. Phys.*, 2011, **13**, 9083–9118.
- 28 Z.-G. Zhang and J. Wang, *J. Mater. Chem.*, 2012, **22**, 4178–4187.
- 29 L. Pandey, C. Risko, J. E. Norton and J.-L. Brédas, *Macromolecules*, 2012, **45**, 6405–6414.
- 30 P. M. Beaujuge and J. M. J. Fréchet, *J. Am. Chem. Soc.*, 2011, **133**, 20009–20029.
- 31 K. Maturová, S. S. van Bavel, M. M. Wienk, R. A. J. Janssen and M. Kemerink, *Adv. Funct. Mater.*, 2011, **21**, 261–269.
- 32 Citation report from Web of Science on september 16th 2013 for the search: “Organic Photovoltaic”.
- 33 M. Jørgensen, K. Norrman, S. A. Gevorgyan, T. Tromholt, B. Andreasen and F. C. Krebs, *Adv. Mater.*, 2012, **24**, 580–612.
- 34 N. Espinosa, M. Hosel, D. Angmo and F. C. Krebs, *Energy Environ. Sci.*, 2012, **5**, 5117–5132.
- 35 Citation report from Web of Science on september 16th 2013 for the search: “Organic Photovoltaic”.
- 36 Citation report from Web of Science on september 16th 2013 for the search: “Organic Photovoltaic”.
- 37 J. M. Lupton, *ChemPhysChem*, 2011, **13**, 901–907.
- 38 I. Hwang and G. D. Scholes, *Chem. Mater.*, 2010, **23**, 610–620.
- 39 Y. Sun, Q. Wu and G. Shi, *Energy Environ. Sci.*, 2011, **4**, 1113–1132.
- 40 P. Sonar, J. P. Fong Lim and K. L. Chan, *Energy Environ. Sci.*, 2011, **4**, 1558–1574.

- 1 41 J. D. Servaites, M. A. Ratner and T. J. Marks, *Energy Environ. Sci.*, 2011, **4**, 4410–4422.
- 42 T. Ameri, G. Dennler, C. Lungenschmied and C. J. Brabec, *Energy Environ. Sci.*, 2009, **2**, 347–363.
- 5 43 S. Sista, Z. Hong, L.-M. Chen and Y. Yang, *Energy Environ. Sci.*, 2011, **4**, 1606–1620.
- 44 T. Xu and Q. Qiao, *Energy Environ. Sci.*, 2011, **4**, 2700–2720.
- 45 L. Yang, H. Zhou, S. C. Price and W. You, *J. Am. Chem. Soc.*, 2012, **134**, 5432–5435.
- 10 46 W.-Y. Wong, *J. Organomet. Chem.*, 2009, **694**, 2644–2647.
- 47 A. Loudet and K. Burgess, *Chem. Rev.*, 2007, **107**, 4891–4932.
- 48 G. Ulrich, R. Ziessel and A. Harriman, *Angew. Chem., Int. Ed.*, 2008, **47**, 1184–1201.
- 15 49 T. E. Wood and A. Thompson, *Chem. Rev.*, 2007, **107**, 1831–1861.
- 50 N. Boens, V. Leen and W. Dehaen, *Chem. Soc. Rev.*, 2012, **41**, 1130–1172.
- 51 L. Yuan, W. Lin, K. Zheng, L. He and W. Huang, *Chem. Soc. Rev.*, 2013, **42**, 622–661.
- 20 52 S. G. Awuah and Y. You, *RSC Adv.*, 2012, **2**, 11169–11183.
- 53 K. Tanaka and Y. Chujo, *Macromol. Rapid Commun.*, 2012, **33**, 1235–1255.
- 54 M. Benstead, G. H. Mehl and R. W. Boyle, *Tetrahedron*, 2011, **67**, 3573–3601.
- 25 55 R. Ziessel and A. Harriman, *Chem. Commun.*, 2011, **47**, 611–631.
- 56 L. Zeng, C. Jiao, X. Huang, K.-W. Huang, W.-S. Chin and J. Wu, *Org. Lett.*, 2011, **13**, 6026–6029.
- 30 57 A. Wakamiya, T. Murakami and S. Yamaguchi, *Chem. Sci.*, 2013, **4**, 1002–1007.
- 58 L. Jiao, C. Yu, M. Liu, Y. Wu, K. Cong, T. Meng, Y. Wang and E. Hao, *J. Org. Chem.*, 2010, **75**, 6035–6038.
- 59 T. Uppal, X. Hu, F. R. Fronczek, S. Maschek, P. Bobadova-Parvanova and M. G. H. Vicente, *Chem.–Eur. J.*, 2012, **18**, 3893–3905.
- 35 60 Y. Hayashi, N. Obata, M. Tamaru, S. Yamaguchi, Y. Matsuo, A. Saeki, S. Seki, Y. Kureishi, S. Saito, S. Yamaguchi and H. Shinokubo, *Org. Lett.*, 2012, **14**, 866–869.
- 40 61 T. Sakida, S. Yamaguchi and H. Shinokubo, *Angew. Chem., Int. Ed.*, 2011, **50**, 2280–2283.
- 62 T. Ito, Y. Hayashi, S. Shimizu, J.-Y. Shin, N. Kobayashi and H. Shinokubo, *Angew. Chem., Int. Ed.*, 2012, **51**, 8542–8545.
- 45 63 D. Sakow, B. Böker, K. Brandhorst, O. Burghaus and M. Bröring, *Angew. Chem., Int. Ed.*, 2013, **52**, 4912–4915.
- 64 C. Jiao, L. Zhu and J. Wu, *Chem.–Eur. J.*, 2011, **17**, 6610–6614.
- 65 C. Jiao, K.-W. Huang and J. Wu, *Org. Lett.*, 2011, **13**, 632–635.
- 50 66 M. Ishida, Y. Naruta and F. Tani, *Angew. Chem., Int. Ed.*, 2010, **49**, 91–94.
- 67 N. Boens, V. Leen, W. Dehaen, L. Wang, K. Robeyns, W. Qin, X. Tang, D. Beljonne, C. Tonnelé, J. M. Paredes, M. J. Ruedas-Rama, A. Orte, L. Crovetto, E. M. Talavera and J. M. Alvarez-Pez, *J. Phys. Chem. A*, 2012, **116**, 9621–9631.
- 68 T. Kowada, S. Yamaguchi and K. Ohe, *Org. Lett.*, 2010, **12**, 296–299.
- 69 S. G. Awuah, J. Polreis, V. Biradar and Y. You, *Org. Lett.*, 2011, **13**, 3884–3887.
- 70 K. Tanaka, H. Yamane, R. Yoshii and Y. Chujo, *Bioorg. Med. Chem.*, 2013, **21**, 2715–2719.
- 71 S. G. Awuah, S. K. Das, F. D'Souza and Y. You, *Chem.–Asian J.*, 2013, **8**, 3123–3132.
- 72 K. Krumova and G. Cosa, *J. Am. Chem. Soc.*, 2010, **132**, 17560–17569.
- 10 73 V. Lakshmi and M. Ravikanth, *J. Org. Chem.*, 2011, **76**, 8466–8471.
- 74 V. Lakshmi and M. Ravikanth, *Chem. Phys. Lett.*, 2013, **564**, 93–97.
- 75 J. Li, B. Hu, G. Hu, X. Li, P. Lu and Y. Wang, *Org. Biomol. Chem.*, 2012, **10**, 8848–8859.
- 76 Y. Chen, J. Zhao, H. Guo and L. Xie, *J. Org. Chem.*, 2012, **77**, 2192–2206.
- 77 X. Liu, Z. Xu and J. M. Cole, *J. Phys. Chem. C*, 2013, **117**, 16584–16595.
- 20 78 Y. Marfin, E. Romyantsev, Y. Fadeev and E. Antina, *Russ. J. Phys. Chem. A*, 2012, **86**, 1068–1072.
- 79 M. Y. Choi, J. A. Pollard, M. A. Webb and J. L. McHale, *J. Am. Chem. Soc.*, 2002, **125**, 810–820.
- 80 R. Hu, C. F. A. Gomez-Duran, J. W. Y. Lam, J. L. Belmonte-Vazquez, C. Deng, S. Chen, R. Ye, E. Pena-Cabrera, Y. Zhong, K. S. Wong and B. Z. Tang, *Chem. Commun.*, 2012, **48**, 10099–10101.
- 25 81 T. T. Vu, M. Y. Dvorko, E. Y. Schmidt, J.-F. Audibert, P. Retailleau, B. A. Trofimov, R. B. Pansu, G. Clavier and R. Meallet-Renault, *J. Phys. Chem. C*, 2013.
- 30 82 Q. Wang, H. Lu, L. Gai, W. Chen, G. Lai and Z. Li, *Dyes Pigm.*, **94**, 183–186. Q19
- 83 J. Lu, H. Fu, Y. Zhang, Z. J. Jakubek, Y. Tao and S. Wang, *Angew. Chem., Int. Ed.*, 2011, **50**, 11658–11662.
- 35 84 D. Cho, M. Fujitsuka, J. Ryu, M. Lee, H. Kim, T. Majima and C. Im, *Chem. Commun.*, 2012, **48**, 3347–3349.
- 85 S. Banfi, E. Caruso, S. Zaza, M. Mancini, M. B. Gariboldi and E. Monti, *J. Photochem. Photobiol., B*, 2012, **114**, 52–60. Q20
- 40 86 J. C. Er, M. K. Tang, C. G. Chia, H. Liew, M. Vendrell and Y.-T. Chang, *Chem. Sci.*, 2013, **4**, 2168–2176.
- 87 B. Verbelen, V. Leen, L. Wang, N. Boens and W. Dehaen, *Chem. Commun.*, 2012, **48**, 9129–9131.
- 45 88 L.-Y. Niu, Y.-S. Guan, Y.-Z. Chen, L.-Z. Wu, C.-H. Tung and Q.-Z. Yang, *J. Am. Chem. Soc.*, 2012, **134**, 18928–18931.
- 89 G. Ulrich, R. Ziessel and A. Haefele, *J. Org. Chem.*, 2012, **77**, 4298–4311.
- 90 L. Wang, B. Verbelen, C. Tonnele, D. Beljonne, R. Lazzaroni, V. Leen, W. Dehaen and N. Boens, *Photochem. Photobiol. Sci.*, 2013, **12**, 835–847.
- 50 91 V. Leen, M. Van der Auweraer, N. Boens and W. Dehaen, *Org. Lett.*, 2011, **13**, 1470–1473.
- 92 T. V. Goud, A. Tutar and J.-F. Biellmann, *Tetrahedron*, 2006, **62**, 5084–5091.
- 55

- 1 93 E. Pena-Cabrera, A. Aguilar-Aguilar, M. Gonzalez-Dominguez, E. Lager, R. Zamudio-Vazquez, J. Godoy-Vargas and F. Villanueva-Garcia, *Org. Lett.*, 2007, **9**, 3985–3988.
- 5 94 L. N. Sobenina, A. M. Vasil'tsov, O. V. Petrova, K. B. Petrushenko, I. A. Ushakov, G. Clavier, R. Meallet-Renault, A. I. Mikhaleva and B. A. Trofimov, *Org. Lett.*, 2011, **13**, 2524–2527.
- Q21 95 I. Esnal, A. Urias-Benavides, C. F. A. Gómez-Durán, C. A. Osorio-Martínez, I. García-Moreno, A. Costela, J. Bañuelos, N. Epelde, I. López Arbeloa, R. Hu, B. Zhong Tang and E. Peña-Cabrera, *Chem.-Asian J.*, 2013, **8**, 2691–2700.
- 10 96 C. Goze, G. Ulrich, L. J. Mallon, B. D. Allen, A. Harriman and R. Ziessel, *J. Am. Chem. Soc.*, 2006, **128**, 10231–10239.
- 15 97 C. Tahtaoui, C. Thomas, F. Rohmer, P. Klotz, G. Duportail, Y. Mély, D. Bonnet and M. Hibert, *J. Org. Chem.*, 2007, **72**, 269–272.
- 98 P. Didier, G. Ulrich, Y. Mely and R. Ziessel, *Org. Biomol. Chem.*, 2009, **7**, 3639–3642.
- 20 99 V. Leen, D. Miscoria, S. Yin, A. Filarowski, J. Molisho Ngongo, M. Van der Auweraer, N. Boens and W. Dehaen, *J. Org. Chem.*, 2011, **76**, 8168–8176.
- 100 T. Bura, P. Retailleau, G. Ulrich and R. Ziessel, *J. Org. Chem.*, 2011, **76**, 1109–1117.
- 25 101 G. Ulrich, A. Haefele, P. Retailleau and R. Ziessel, *J. Org. Chem.*, 2012, **77**, 5036–5048.
- 102 C. Yu, L. Jiao, X. Tan, J. Wang, Y. Xu, Y. Wu, G. Yang, Z. Wang and E. Hao, *Angew. Chem., Int. Ed.*, 2012, **51**, 7688–7691.
- 30 103 C. Yu, Y. Xu, L. Jiao, J. Zhou, Z. Wang and E. Hao, *Chem.-Eur. J.*, 2012, **18**, 6437–6442.
- 104 M. Zhang, E. Hao, Y. Xu, S. Zhang, H. Zhu, Q. Wang, C. Yu and L. Jiao, *RSC Adv.*, 2012, **2**, 11215–11218.
- 105 V. Lakshmi, M. Shaikh and M. Ravikanth, *J. Fluoresc.*, 2013, **23**, 519–525.
- 35 106 L. Jiao, W. Pang, J. Zhou, Y. Wei, X. Mu, G. Bai and E. Hao, *J. Org. Chem.*, 2011, **76**, 9988–9996.
- 107 X.-F. Zhang and X. Yang, *J. Phys. Chem. B*, 2013, **117**, 5533–5539.
- 40 108 X.-F. Zhang and X. Yang, *J. Phys. Chem. B*, 2013, **117**, 9050–9055.
- 109 M. J. Ortiz, A. R. Agarrabeitia, G. Duran-Sampedro, J. Bañuelos Prieto, T. A. Lopez, W. A. Massad, H. A. Montejano, N. A. García and I. Lopez Arbeloa, *Tetrahedron*, 2012, **68**, 1153–1162.
- 45 110 W. Li, L. Li, H. Xiao, R. Qi, Y. Huang, Z. Xie, X. Jing and H. Zhang, *RSC Adv.*, 2013, **3**, 13417–13421.
- 111 V. Leen, P. Yuan, L. Wang, N. Boens and W. Dehaen, *Org. Lett.*, 2012, **14**, 6150–6153.
- 50 112 S. Madhu, R. Gonnade and M. Ravikanth, *J. Org. Chem.*, 2013, **78**, 5056–5060.
- 113 N. Shivran, S. Mula, T. K. Ghanty and S. Chattopadhyay, *Org. Lett.*, 2011, **13**, 5870–5873.
- 114 E. Palao, A. R. Agarrabeitia, J. Banuelos-Prieto, T. A. Lopez, I. Lopez-Arbeloa, D. Armesto and M. J. Ortiz, *Org. Lett.*, 2013, **15**, 4454–4457.
- 115 J. A. Jacobsen, J. R. Stork, D. Magde and S. M. Cohen, *Dalton Trans.*, 2010, **39**, 957–962.
- 116 G. Ulrich, S. Goeb, A. De Nicola, P. Retailleau and R. Ziessel, *J. Org. Chem.*, 2011, **76**, 4489–4505.
- 117 J.-H. Olivier, A. Haefele, P. Retailleau and R. Ziessel, *Org. Lett.*, 2010, **12**, 408–411.
- 118 A. Haefele, C. Zedde, P. Retailleau, G. Ulrich and R. Ziessel, *Org. Lett.*, 2010, **12**, 1672–1675.
- 119 X.-D. Jiang, J. Zhang, T. Furuyama and W. Zhao, *Org. Lett.*, 2011, **14**, 248–251.
- 120 S. L. Niu, G. Ulrich, R. Ziessel, A. Kiss, P.-Y. Renard and A. Romieu, *Org. Lett.*, 2009, **11**, 2049–2052.
- 121 J.-S. Lu, S.-B. Ko, N. R. Walters and S. Wang, *Org. Lett.*, 2012, **14**, 5660–5663.
- 122 T. Lundrigan, S. M. Crawford, T. S. Cameron and A. Thompson, *Chem. Commun.*, 2012, **48**, 1003–1005.
- 123 C. Bonnier, W. E. Piers, A. Al-Sheikh Ali, A. Thompson and M. Parvez, *Organometallics*, 2009, **28**, 4845–4851.
- 124 D. A. Smithen, A. E. G. Baker, M. Offman, S. M. Crawford, T. S. Cameron and A. Thompson, *J. Org. Chem.*, 2012, **77**, 3439–3453.
- 125 S. M. Crawford and A. Thompson, *Org. Lett.*, 2010, **12**, 1424–1427.
- 126 Y. Cakmak and E. U. Akkaya, *Org. Lett.*, 2008, **11**, 85–88.
- 127 A. C. Benniston, G. Copley, A. Harriman, D. Howgego, R. W. Harrington and W. Clegg, *J. Org. Chem.*, 2010, **75**, 2018–2027.
- 128 M. A. H. Alamiry, A. C. Benniston, G. Copley, A. Harriman and D. Howgego, *J. Phys. Chem. A*, 2011, **115**, 12111–12119.
- 129 A. C. Benniston, G. Copley, H. Lemmetyinen and N. V. Tkachenko, *Eur. J. Org. Chem.*, 2010, 2867–2877.
- 130 A. C. Benniston, S. Clift, J. Hagon, H. Lemmetyinen, N. V. Tkachenko, W. Clegg and R. W. Harrington, *Chem-PhysChem*, 2012, **13**, 3672–3681.
- 131 D. Bai, A. C. Benniston, J. Hagon, H. Lemmetyinen, N. V. Tkachenko and R. W. Harrington, *Phys. Chem. Chem. Phys.*, 2013, **15**, 9854–9861.
- 132 B. Wang, P. Li, F. Yu, P. Song, X. Sun, S. Yang, Z. Lou and K.-L. Han, *Chem. Commun.*, 2013, **49**, 1014–1016.
- 133 S.-R. Liu and S.-P. Wu, *Org. Lett.*, 2013, **15**, 878–881.
- 134 L. Gai, J. Mack, H. Liu, Z. Xu, H. Lu and Z. Li, *Sens. Actuators, B*, 2013, **182**, 1–6.
- 135 C. Dumas-Verdes, F. Miomandre, E. Lepicier, O. Galangau, T. T. Vu, G. Clavier, R. Meallet-Renault and P. Audebert, *Eur. J. Org. Chem.*, 2010, 2525–2535.
- 136 J. C. T. Carlson, L. G. Meimetis, S. A. Hilderbrand and R. Weissleder, *Angew. Chem., Int. Ed.*, 2013, **52**, 6917–6920.
- 137 C. A. Swamy P, S. Mukherjee and P. Thilagar, *Chem. Commun.*, 2013, **49**, 993–995.
- 138 A. B. Nepomnyashchii, M. Broring, J. Ahrens, R. Kruger and A. J. Bard, *J. Phys. Chem. C*, 2010, **114**, 14453–14460.
- 139 J. Rosenthal, A. B. Nepomnyashchii, J. Kozhukh, A. J. Bard and S. J. Lippard, *J. Phys. Chem. C*, 2011, **115**, 17993–18001.
- 140 A. B. Nepomnyashchii, G. Kolesov and B. A. Parkinson, *ACS Appl. Mater. Interfaces*, 2013, **5**, 5931–5936.

- 1 141 A. B. Nepomnyashchii, M. Bröring, J. Ahrens and A. J. Bard, *J. Am. Chem. Soc.*, 2011, **133**, 19498–19504.
- 142 I.-S. Shin, S. W. Bae, H. Kim and J.-I. Hong, *Anal. Chem.*, 2010, **82**, 8259–8265.
- 5 143 A. B. Nepomnyashchii and A. J. Bard, *Acc. Chem. Res.*, 2012, **45**, 1844–1853.
- 144 D. T. Chase, B. S. Young and M. M. Haley, *J. Org. Chem.*, 2011, **76**, 4043–4051.
- 145 B. Hu, Q. Su, P. Lu and Y. Wang, *Sens. Actuators, B*, 2012, **168**, 310–317.
- 10 146 Y. Ueno, J. Jose, A. Loudet, C. Pérez-Bolivar, P. Anzenbacher and K. Burgess, *J. Am. Chem. Soc.*, 2011, **133**, 51–55.
- 147 A. Harriman, L. J. Mallon, K. J. Elliot, A. Haefele, G. Ulrich and R. Ziessel, *J. Am. Chem. Soc.*, 2009, **131**, 13375–13386.
- 15 148 M. A. H. Alamiry, J. P. Hagon, A. Harriman, T. Bura and R. Ziessel, *Chem. Sci.*, 2012, **3**, 1041–1048.
- 149 A. Nierth, A. Y. Kobitski, G. U. Nienhaus and A. Jaschke, *J. Am. Chem. Soc.*, 2010, **132**, 2646–2654.
- 20 150 R. Ziessel, G. Ulrich, A. Haefele and A. Harriman, *J. Am. Chem. Soc.*, 2013, **135**, 11330–11344.
- 151 R. Ziessel, M. A. H. Alamiry, K. J. Elliott and A. Harriman, *Angew. Chem., Int. Ed.*, 2009, **48**, 2772–2776.
- 152 A. Harriman and R. Ziessel, *Photochem. Photobiol. Sci.*, 2010, **9**, 960–967.
- 25 153 S. Caprasecca, C. Curutchet and B. Mennucci, *Photochem. Photobiol. Sci.*, 2011, **10**, 1602–1609.
- 154 D. Hablot, R. Ziessel, M. A. H. Alamiry, E. Bahraidah and A. Harriman, *Chem. Sci.*, 2013, **4**, 444–453.
- 30 155 A. Harriman, M. A. H. Alamiry, J. P. Hagon, D. Hablot and R. Ziessel, *Angew. Chem., Int. Ed.*, 2013, **52**, 6611–6615.
- 156 J. Godoy, G. Vives and J. M. Tour, *Org. Lett.*, 2010, **12**, 1464–1467.
- 157 P.-L. E. Chu, L.-Y. Wang, S. Khatua, A. B. Kolomeisky, S. Link and J. M. Tour, *ACS Nano*, 2012.
- Q22 158 J. Massue, D. Frath, G. Ulrich, P. Retailleau and R. Ziessel, *Org. Lett.*, 2012, **14**, 230–233.
- 159 A. Nano, R. Ziessel, P. Stachelek and A. Harriman, *Chem.–Eur. J.*, 2013, **19**, 13528–13537.
- 40 160 D. Frath, J. E. Yarnell, G. Ulrich, F. N. Castellano and R. Ziessel, *ChemPhysChem*, 2013, **14**, 3348–3354.
- 161 J. Iehl, J.-F. Nierengarten, A. Harriman, T. Bura and R. Ziessel, *J. Am. Chem. Soc.*, 2012, **134**, 988–998.
- 162 P. Yang, W. Wu, J. Zhao, D. Huang and X. Yi, *J. Mater. Chem.*, 2012, **22**, 20273–20283.
- 45 163 D. Huang, J. Zhao, W. Wu, X. Yi, P. Yang and J. Ma, *Asian J. Org. Chem.*, 2012, **1**, 264–273.
- 164 W. Wu, H. Guo, W. Wu, S. Ji and J. Zhao, *J. Org. Chem.*, 2011, **76**, 7056–7064.
- 50 165 P. Yang, J. Zhao, W. Wu, X. Yu and Y. Liu, *J. Org. Chem.*, 2012, **77**, 6166–6178.
- 166 C. Zhang, J. Zhao, S. Wu, Z. Wang, W. Wu, J. Ma, S. Guo and L. Huang, *J. Am. Chem. Soc.*, 2013, **135**, 10566–10578.
- 55 167 W. Wu, J. Zhao, H. Guo, J. Sun, S. Ji and Z. Wang, *Chem.–Eur. J.*, 2012, **18**, 1961–1968.
- 168 T. Lazarides, T. M. McCormick, K. C. Wilson, S. Lee, D. W. McCamant and R. Eisenberg, *J. Am. Chem. Soc.*, 2010, **133**, 350–364.
- 169 A. M. Lifschitz, C. M. Shade, A. M. Spokoiny, J. Mendez-Arroyo, C. L. Stern, A. A. Sarjeant and C. A. Mirkin, *Inorg. Chem.*, 2013, **52**, 5484–5492.
- 170 Z. Zhang and D. Dolphin, *Inorg. Chem.*, 2010, **49**, 11550–11555.
- 171 H. Maeda, T. Nishimura, R. Akuta, K. Takaishi, M. Uchiyama and A. Muranaka, *Chem. Sci.*, 2013, **4**, 1204–1211.
- 172 K. Servaty, E. Cauet, F. Thomas, J. Lambermont, P. Gerbaux, J. De Winter, M. Ovaere, L. Volker, N. Vaeck, L. Van Meervelt, W. Dehaen, C. Moucheron and A. Kirsch-De Mesmaeker, *Dalton Trans.*, 2013, **42**, 14188–14199.
- 15 173 X. Qu, C. Li, H. Chen, J. Mack, Z. Guo and Z. Shen, *Chem. Commun.*, 2013, **49**, 7510–7512.
- 174 K. Nakano, K. Kobayashi and K. Nozaki, *J. Am. Chem. Soc.*, 2011, **133**, 10720–10723.
- 175 A. Kochem, L. Chiang, B. Baptiste, C. Philouze, N. Leconte, O. Jarjayes, T. Storr and F. Thomas, *Chem.–Eur. J.*, 2012, **18**, 14590–14593.
- 176 S. Rausaria, A. Kamadulski, N. P. Rath, L. Bryant, Z. Chen, D. Salvemini and W. L. Neumann, *J. Am. Chem. Soc.*, 2011, **133**, 4200–4203.
- 25 177 E. R. King, G. T. Sazama and T. A. Betley, *J. Am. Chem. Soc.*, 2012, **134**, 17858–17861.
- 178 M. Yadav, A. K. Singh and D. S. Pandey, *Organometallics*, 2009, **28**, 4713–4723.
- 179 M. Yadav, A. K. Singh, B. Maiti and D. S. Pandey, *Inorg. Chem.*, 2009, **48**, 7593–7603.
- 30 180 T. M. McLean, J. L. Moody, M. R. Waterland and S. G. Telfer, *Inorg. Chem.*, 2012, **51**, 446–455.
- 181 J. D. Hall, T. M. McLean, S. J. Smalley, M. R. Waterland and S. G. Telfer, *Dalton Trans.*, 2010, **39**, 437–445.
- 35 182 Q.-X. Zhou, W.-H. Lei, Y.-J. Hou, Y.-J. Chen, C. Li, B. Zhang and X. Wang, *Dalton Trans.*, 2013, **42**, 2786–2791.
- 183 W. Wu, J. Sun, X. Cui and J. Zhao, *J. Mater. Chem. C*, 2013, **1**, 4577–4589.
- 184 A. A. Rachford, R. Ziessel, T. Bura, P. Retailleau and F. N. Castellano, *Inorg. Chem.*, 2010, **49**, 3730–3736.
- 185 S. Diring, B. Ventura, A. Barbieri and R. Ziessel, *Dalton Trans.*, 2012, **41**, 13090–13096.
- 186 G. Pistolis, A. Kaloudi Chantzzea, N. Karakostas, F. Pitterl, C. Raptopoulou and N. Glezos, *Chem. Commun.*, 2012, **48**, 12213–12215.
- 45 187 S. Kusaka, R. Sakamoto, Y. Kitagawa, M. Okumura and H. Nishihara, *Chem.–Asian J.*, 2012, **7**, 907–910.
- 188 R. Sakamoto, S. Kusaka, Y. Kitagawa, M.-a. Kishida, M. Hayashi, Y. Takara, M. Tsuchiya, J. Kakinuma, T. Takeda, K. Hirata, T. Ogino, K. Kawahara, T. Yagi, S. Ikehira, T. Nakamura, M. Isomura, M. Toyama, S. Ichikawa, M. Okumura and H. Nishihara, *Dalton Trans.*, 2012, **41**, 14035–14037.
- 50 189 M. E. El-Khouly, A. N. Amin, M. E. Zandler, S. Fukuzumi and F. D'Souza, *Chem.–Eur. J.*, 2012, **18**, 5239–5247.
- 55

- 1 190 V. Bandi, K. Ohkubo, S. Fukuzumi and F. D'Souza, *Chem. Commun.*, 2013, **49**, 2867–2869.
- 191 W.-J. Shi, M. E. El-Khouly, K. Ohkubo, S. Fukuzumi and D. K. P. Ng, *Chem.-Eur. J.*, 2013, **19**, 11332–11341.
- 5 192 M. T. Whited, P. I. Djurovich, S. T. Roberts, A. C. Durrell, C. W. Schlenker, S. E. Bradforth and M. E. Thompson, *J. Am. Chem. Soc.*, 2011, **133**, 88–96.
- 193 T. K. Khan and M. Ravikanth, *Tetrahedron*, 2011, **67**, 5816–5824.
- 10 194 E. A. Medlycott and G. S. Hanan, *Coord. Chem. Rev.*, 2006, **250**, 1763–1782.
- 195 E. A. Medlycott and G. S. Hanan, *Chem. Soc. Rev.*, 2005, **34**, 133–142.
- 196 T. K. Khan and M. Ravikanth, *Eur. J. Org. Chem.*, 2011, 7011–7022.
- 15 197 T. K. Khan and M. Ravikanth, *Tetrahedron*, 2012, **68**, 830–840.
- 198 J.-Y. Liu, Y. Huang, R. Menting, B. Roder, E. A. Ermilov and D. K. P. Ng, *Chem. Commun.*, 2013, **49**, 2998–3000.
- 20 199 R. Menting, J.-Y. Liu, Y.-S. Huang, D. K. P. Ng, B. Roder and E. A. Ermilov, *Phys. Chem. Chem. Phys.*, 2013, **15**, 6912–6919.
- 200 B. Brizet, A. Eggenspieler, C. P. Gros, J.-M. Barbe, C. Goze, F. Denat and P. D. Harvey, *J. Org. Chem.*, 2012, **77**, 3646–3650.
- 25 201 J. Warnan, F. Buchet, Y. Pellegrin, E. Blart and F. Odobel, *Org. Lett.*, 2011, **13**, 3944–3947.
- 202 T. Lazarides, G. Charalambidis, A. Vuillamy, M. Réglie, E. Klontzas, G. Froudakis, S. Kuhri, D. M. Guldi and A. G. Coutsolelos, *Inorg. Chem.*, 2011, **50**, 8926–8936.
- 30 203 T. Lazarides, S. Kuhri, G. Charalambidis, M. K. Panda, D. M. Guldi and A. G. Coutsolelos, *Inorg. Chem.*, 2012, **51**, 4193–4204.
- 204 K. Ladomenou, T. Lazarides, M. K. Panda, G. Charalambidis, D. Daphnomili and A. G. Coutsolelos, *Inorg. Chem.*, 2012, **51**, 10548–10556.
- 35 205 M. J. Leonardi, M. R. Topka and P. H. Dinolfo, *Inorg. Chem.*, 2012, **51**, 13114–13122.
- 206 T. Zhang, X. Zhu, W.-K. Wong, H.-L. Tam and W.-Y. Wong, *Chem.-Eur. J.*, 2013, **19**, 739–748.
- 40 207 Y. Chen, L. Wan, X. Yu, W. Li, Y. Bian and J. Jiang, *Org. Lett.*, 2011, **13**, 5774–5777.
- 208 J.-Y. Shin, T. Tanaka, A. Osuka, Q. Miao and D. Dolphin, *Chem.-Eur. J.*, 2009, **15**, 12955–12959.
- 209 H. Sugimoto, M. Muto, T. Tanaka and A. Osuka, *Eur. J. Org. Chem.*, 2011, 71–77.
- 45 210 Y. Rio, W. Seitz, A. Gouloumis, P. Vazquez, J. L. Sessler, D. M. Guldi and T. Torres, *Chem.-Eur. J.*, 2010, **16**, 1929–1940.
- 211 E. Maligaspe, T. Kumpulainen, N. K. Subbaiyan, M. E. Zandler, H. Lemmetyinen, N. V. Tkachenko and F. D'Souza, *Phys. Chem. Chem. Phys.*, 2010, **12**, 7434–7444.
- 50 212 Y. Kubo, K. Watanabe, R. Nishiyabu, R. Hata, A. Murakami, T. Shoda and H. Ota, *Org. Lett.*, 2011, **13**, 4574–4577.
- 55 213 T. Rousseau, A. Cravino, T. Bura, G. Ulrich, R. Ziessel and J. Roncali, *Chem. Commun.*, 2009, 1673–1675.
- 214 T. Rousseau, A. Cravino, E. Ripaud, P. Leriche, S. Rihn, A. De Nicola, R. Ziessel and J. Roncali, *Chem. Commun.*, 2010, **46**, 5082–5084.
- 215 T. Bura, N. Leclerc, S. Fall, P. Lévêque, T. Heiser and R. Ziessel, *Org. Lett.*, 2011, **13**, 6030–6033. 5
- 216 T. Bura, N. Leclerc, S. Fall, P. Lévêque, T. Heiser, P. Retailleau, S. Rihn, A. Mirloup and R. Ziessel, *J. Am. Chem. Soc.*, 2012, **134**, 17404–17407.
- 217 S. Y. Leblebici, L. Catane, D. E. Barclay, T. Olson, T. L. Chen and B. Ma, *ACS Appl. Mater. Interfaces*, 2011, **3**, 4469–4474. 10
- 218 T. Mueller, R. Gresser, K. Leo and M. Riede, *Sol. Energy Mater. Sol. Cells*, 2012, **99**, 176–181.
- 219 B. Kim, B. Ma, V. R. Donuru, H. Liu and J. M. J. Frechet, *Chem. Commun.*, 2010, **46**, 4148–4150. 15
- 220 S. Niu, G. Ulrich, P. Retailleau and R. Ziessel, *Org. Lett.*, 2011, **13**, 4996–4999.
- 221 R. Gresser, M. Hummert, H. Hartmann, K. Leo and M. Riede, *Chem.-Eur. J.*, 2011, **17**, 2939–2947.
- 222 T. Mueller, R. Gresser, K. Leo and M. Riede, Organic solar cells based on a novel infrared absorbing azabodipy dye, *Sol. Energy Mater. Sol. Cells*, 2012, **99**, 176–181, Copyright 2012, with permission from Elsevier. 20
- 223 S. Rihn, P. Retailleau, N. Bugsaliewicz, A. De Nicola and R. Ziessel, *Tetrahedron Lett.*, 2009, **50**, 7008–7013. 25
- 224 A. Poirel, A. De Nicola and R. Ziessel, *Org. Lett.*, 2012, **14**, 5696–5699.
- 225 T. Bura and R. Ziessel, *Tetrahedron Lett.*, 2010, **51**, 2875–2879.
- 226 Y. Ooyama, Y. Hagiwara, T. Mizumo, Y. Harima and J. Ohshita, *New J. Chem.*, 2013, **37**, 2479–2485. 30
- 227 J. Xiong, L. Sun, Y. Liao, G.-N. Li, J.-L. Zuo and X.-Z. You, *Tetrahedron Lett.*, 2011, **52**, 6157–6161.
- 228 X. Cao, W. Lin, Q. Yu and J. Wang, *Org. Lett.*, 2011, **13**, 6098–6101. 35
- 229 Z. Yang, Y. He, J.-H. Lee, N. Park, M. Suh, W.-S. Chae, J. Cao, X. Peng, H. Jung, C. Kang and J. S. Kim, *J. Am. Chem. Soc.*, 2013, **135**, 9181–9185.
- 230 M. R. Rao, K. V. P. Kumar and M. Ravikanth, *J. Organomet. Chem.*, 2010, **695**, 863–869. 40
- 231 X. Yin, Y. Li, Y. Li, Y. Zhu, X. Tang, H. Zheng and D. Zhu, *Tetrahedron*, 2009, **65**, 8373–8377.
- 232 R. Misra, B. Dhokale, T. Jadhav and S. M. Mobin, *Dalton Trans.*, 2013, **42**, 13658–13666.
- 233 B. Dhokale, P. Gautam, S. M. Mobin and R. Misra, *Dalton Trans.*, 2013, **42**, 1512–1518. 45
- 234 W.-J. Shi, P.-C. Lo, A. Singh, I. Ledoux-Rak and D. K. P. Ng, *Tetrahedron*, 2012, **68**, 8712–8718.
- 235 S. Kolemen, O. A. Bozdemir, Y. Cakmak, G. Barin, S. Erten-Ela, M. Marszalek, J.-H. Yum, S. M. Zakeeruddin, M. K. Nazeeruddin, M. Grätzel and E. U. Akkaya, *Chem. Sci.*, 2011, **2**, 949–954. 50
- 236 A. Nagai, J. Miyake, K. Kokado, Y. Nagata and Y. Chujo, *J. Am. Chem. Soc.*, 2008, **130**, 15276–15278.
- 237 A. Nagai and Y. Chujo, *Macromolecules*, 2010, **43**, 193–200. 55

- 1 238 V. R. Donuru, G. K. Vegesna, S. Velayudham, S. Green and H. Liu, *Chem. Mater.*, 2009, **21**, 2130–2138.
- 239 G. Meng, S. Velayudham, A. Smith, R. Luck and H. Liu, *Macromolecules*, 2009, **42**, 1995–2001.
- 5 240 M. Zhu, L. Jiang, M. Yuan, X. Liu, C. Ouyang, H. Zheng, X. Yin, Z. Zuo, H. Liu and Y. Li, *J. Polym. Sci., Part A: Polym. Chem.*, 2008, **46**, 7401–7410.
- 241 F. E. Alemdaroglu, S. C. Alexander, D. Ji, D. K. Prusty, M. Börsch and A. Herrmann, *Macromolecules*, 2009, **42**, 6529–6536.
- 10 242 Y. Wu, X. Mao, X. Ma, X. Huang, Y. Cheng and C. Zhu, *Macromol. Chem. Phys.*, 2012, **213**, 2238–2245.
- 243 P. Hewavitharanage, P. Nzeata and J. Wiggins, *Eur. J. Chem.*, 2012, **3**, 13–16.
- 15 244 J. C. Forgie, P. J. Skabara, I. Stibor, F. Vilela and Z. Vobecka, *Chem. Mater.*, 2009, **21**, 1784–1786.
- 245 A. Cihaner and F. Algi, *React. Funct. Polym.*, 2009, **69**, 62–67.
- 246 F. Algi and A. Cihaner, *Org. Electron.*, 2009, **10**, 453–458.
- 247 A. B. Nepomnyashchii, M. Bröring, J. Ahrens and A. J. Bard, *J. Am. Chem. Soc.*, 2011, **133**, 8633–8645.
- 20 248 B. C. Popere, A. M. Della Pelle and S. Thayumanavan, *Macromolecules*, 2011, **44**, 4767–4776.
- 249 A. Nagai, K. Kokado, J. Miyake and Y. Cyujo, *J. Polym. Sci., Part A: Polym. Chem.*, 2010, **48**, 627–634.
- 25 250 R. Paris, I. Quijada-Garrido, O. Garcia and M. Liras, *Macromolecules*, 2010, **44**, 80–86.
- 251 F. Marsico, A. Turshatov, K. Weber and F. R. Wurm, *Org. Lett.*, 2013, **15**, 3844–3847.
- 252 G. Nöll, J. Daub, M. Lutz and K. Rurack, *J. Org. Chem.*, 2011, **76**, 4859–4873.
- 253 C. Thivierge, A. Loudet and K. Burgess, *Macromolecules*, 2011, **44**, 4012–4015.
- 254 N. Blouin and M. Leclerc, *Acc. Chem. Res.*, 2008, **41**, 1110–1119.
- 255 O. A. Bozdemir, M. D. Yilmaz, O. Buyukcakilir, A. Siemiarczuk, M. Tutas and E. U. Akkaya, *New J. Chem.*, 2010, **34**, 151–155.
- 256 Z. Kostereli, T. Ozdemir, O. Buyukcakilir and E. U. Akkaya, *Org. Lett.*, 2012, **14**, 3636–3639.
- 257 M. Yuan, X. Yin, H. Zheng, C. Ouyang, Z. Zuo, H. Liu and Y. Li, *Chem.-Asian J.*, 2009, **4**, 707–713.
- 15 258 Q. M. Kainz, A. Schätz, A. Zöpfl, W. J. Stark and O. Reiser, *Chem. Mater.*, 2011, **23**, 3606–3613.
- 259 S. K. Yang, X. Shi, S. Park, T. Ha and S. C. Zimmerman, *Nat. Chem.*, 2013, **5**, 692–697.
- 260 C. Y. Lee, O. K. Farha, B. J. Hong, A. A. Sarjeant, S. T. Nguyen and J. T. Hupp, *J. Am. Chem. Soc.*, 2011, **133**, 15858–15861.
- 261 K. V. Rao, K. K. R. Datta, M. Eswaramoorthy and S. J. George, *Chem.-Eur. J.*, 2012, **18**, 2184–2194.
- 262 H. Manzano, L. Gartzia-Rivero, J. Banuelos and I. Lopez-Arbeloa, *J. Phys. Chem. C*, 2013, **117**, 13331–13336.

30

30

35

35

40

40

45

45

50

50

55

55